(NASA-CR-168173) THERMAL TRACTION CONTACT PERFORMANCE EVALUATION UNDER FULLY FLOODED AND STARVED CONDITIONS Interim Report (Transmission Research, Inc., Cleveland, Ohio.) 132 p HC A07/MF A01 CSCL 13I G3/37

N85-25848

Unclas 212[illegible]

NASA CR--168173

THERMAL TRACTION CONTACT PERFORMANCE EVALUATION UNDER FULLY FLOODED AND STARVED CONDITIONS

By:
Joseph L. Tevaarwerk
Transmission Research Inc.

May 1985

Prepared for:

NATIONAL AERONAUTICS AND SPACE ADMINISTRATION
Lewis Research Centre
Cleveland OH 44135
Under Contract DEN 3-35

THERMAL TRACTION CONTACT PERFORMANCE EVALUATION UNDER FULLY FLOODED AND STARVED CONDITIONS.

By:
Joseph L. Tevaarwerk
Transmission Research Inc.
May 1985.

Prepared for:
NATIONAL AERONAUTICS AND SPACE ADMINISTRATION
Lewis Research Centre
Cleveland, Ohio 44135

1. Report No: NASA CR-168173

2. Government Accession No:

3. Recipient's Catalog No:

4. Title and Subtitle:

THERMAL TRACTION CONTACT PERFORMANCE EVALUATION UNDER FULLY FLOODED AND STARVED CONDITIONS.

5. Report Date: May 1985.

6. Performing Organization Code:

7. Author(s):

J.L. Tevaarwerk, Applied Tribology
RR3 Stokes Lane , Shelburne, VT 05482

8. Performing Organization Report No:

9. Performing Organization Name and Address:

Transmission Research Inc.
10823 Magnolia Dr, Cleveland, OHIO 44106

10. Work Unit No:

11. Contract or Grant No: DEN 3-35

12. Sponsoring Agency Name and Address:

NASA Lewis Research Center.
Cleveland OH 44135

13. Type of Report and Period Covered: Contractor Report.

14. Sponsoring Agency Code:

15. Supplementary Notes:

Second Interim Report:
Project Manager, D.A. Rohn, Bearing Gearing and Transmission Section,
NASA Lewis Research Center, Cleveland, Ohio 44135.

16. Abstract

Ultra high speed traction tests were performed on two traction fluids commonly employed. Traction data on these fluids is required for purposes of traction drive design optimization techniques. To obtain the traction data, an existing twin disc traction test machine was employed. This machine was modified to accommodate the range of test variables. All the data reported was obtained under conditions of side slip, a technique whereby only low power levels are required to simulate real traction drive contacts.

The range of the tests variables were; contact pressure from 1 to 1.8 GPa, disc surface velocity from 50 to 120 m/sec, fluid inlet temperature from 50 to 120 °C , contact spin from 0 to 1.5% and inlet fluid supply from fully flooded to fully starved. The resulting traction curves were reduced to three constants by using the Johnson and Tevaarwerk isothermal traction model coupled to a thermal correction technique for large slip and spin results. Theoretical traction predictions were performed for a representative number of curves that showed the influence of rolling velocity, of contact pressure and of aspect ratio. To establish the accuracy of the thermal model the predictions were performed with increasing levels of independence of experimentally determined parameters. In the final resulting prediction only two non linear thermal parameters were used for the prediction of 15 different traction curves covering the entire range of variables as used in the investigation, with the exception of the influence of asperity traction. Comparison of these theoretical curves and corresponding experimental traces show very good agreement.

17. Key Words (Suggested by Author(s)):

Traction drives; Traction; Traction fluid;
Traction lubricant; Traction drive design;
High speed traction; Traction drive performance.

18. Distribution Statement:

Unclassified. Unlimited.
Star Category 37

19. Security Classif. (of this report)	20. Security Classif. (of this page)	21. No. of pages	22. Price*
Unclassified	Unclassified	VIII + 121 pp	

*For sale by the National Technical Information Service, Springfield, Virginia 22161

SUMMARY

Ultra high speed traction tests were performed on two traction fluids commonly employed. Traction data on these fluids is required for purposes of traction drive design optimization techniques. These techniques will allow for the best possible design of a given drive configuration. For adequate test data the entire range of operating conditions of the drives should be covered by the traction test program and this includes conditions of large slip and possible influences of fluid starvation.

To obtain the traction data, an existing twin disc traction test machine was employed. This machine was modified to accommodate the range of test variables. All the data reported was obtained under conditions of side slip, a technique whereby only low power levels are required to simulate real traction drive contacts. The range of the tests variables were: contact pressure from 1 to 1.8 GPa, disc surface velocity from 50 to 120 m/sec, fluid inlet temperature from 50 to 120 °C , contact spin from 0 to 1.5% and inlet fluid supply from fully flooded to fully starved. The resulting traction curves were reduced to three constants by using the Johnson and Tevaarwerk isothermal traction model coupled to a thermal correction technique for large slip and spin results. The three constants are the elastic shear modulus and two non linear thermal parameters.

Theoretical traction predictions were performed for a representative number of curves that showed the influence of rolling velocity, of contact pressure and of aspect ratio. To establish the accuracy of the thermal model the predictions were performed with increasing levels of independence of experimentally determined parameters. In the final resulting prediction only two non linear thermal parameters were used for the prediction of 15 different traction curves covering the entire range of variables as used in the investigation, with the exception of the influence of asperity traction. Comparison of these theoretical curves and corresponding experimental traces show very good agreement.

The influence of asperity traction was extracted from the experimental curves with starvation by predicting the traction under fully flooded conditions and using the difference to predict the asperity traction as a function of the number of asperities in contact. It was found that the amount of traction force per asperity in contact was pretty well independent of the traction contact conditions and also of the traction fluid. Comparison between theoretically predicted traction curves including the effect of asperity traction and experimental curves shows reasonable agreement.

TABLE OF CONTENTS

		page
	SUMMARY	i
	TABLE OF CONTENTS	ii
	NOMENCLEATURE	iv
	LIST OF FIGURES	vi
1-0	INTRODUCTION	1
1-1	Prior traction investigations	2
1-2	Traction data research program	3
2-0	EXPERIMENTS	4
2-1	Description of twin disc machines	4
2-2	Instrumentation of the traction tester	5
2-2-1	Measurement of the traction force	5
2-2-2	Measurement of side slip	5
2-2-3	Measurement of toroid surface temperature	6
2-2-4	Measurement of the disc speed	6
2-2-5	Contact ratio measurements	6
2-3	Traction measurements	7
2-3-1	Typical traction traces	7
2-4	The application of spin	9
3-0	THEORETICAL ANALYSIS	11
3-1	Isothermal traction analysis	12
3-2	Thermal traction analysis	13
4-0	CALCULATION OF THERMAL TRACTION CURVES	16
4-1	Influence of side slip	16
4-2	Influence of spin	16
4-2-1	Influence of spin under low slip	17
4-2-2	Influence of spin for large slip	18
4-2-3	Thermal influence of small spin	19
5-0	EXTRACTION OF THE TRACTION PARAMETERS	20
5-1	Extraction of the shear modulus	20
5-1-1	Shear modulus for constant properties	20
5-1-2	Shear modulus with simple compliance correction	21
5-1-3	Shear modulus with complex compliance correction	22
5-1-4	Complex correction with reduced pressure effects	23
5-2	Extraction of the large strain parameters	24
5-3	Analysis of the experimental results	25
5-3-1	Multiple traction curve regression	25

6-0 PREDICTION OF THE EXPERIMENTAL TRACTION CURVES 27
6-1 Prediction with individual constants 27
6-2 Prediction with multiple fitted constants 28
6-3 Theoretical traction prediction with asperity contact 28
6-3-1 Analysis of the asperity traction 29

7-0 CONCLUSION 33

8-0 REFERENCES 34

APPENDICES:

I-A Summary of traction test data on TDF88
I-B Summary of traction test data on SANTO50

II-A Summary of modulus analysis on TDF88
II-B Summary of modulus analysis on SANTO50

III-A Summary of thermal hyperbolic sine analysis on TDF88
III-B summary of thermal hyperbolic sine analysis on SANTO50

LIST OF FIGURES

PHOTOGRAPHS

2-1 Overview of the complete traction test system

2-2 Overview of the data acquisition system

2-3a Overview of the traction tester

2-3b Close-up of the traction tester. (RH side)

2-3c Overview of the traction tester. (LH side)

EXPERIMENTAL RESULTS

2-4 TDF88 Flooded results for increasing speed

2-5 ,, Starved ,, ,, ,,

2-6 SANTO50 Flooded results for increasing speed

2-7 ,, Starved ,, ,, ,,

2-8 TDF88 Flooded results for increasing pressure

2-9 ,, Starved ,, ,, ,,

2-10 SANTO50 Flooded results for increasing pressure

2-11 ,, Starved ,, ,, ,,

2-12 TDF88 Flooded results for increasing aspect ratio

2-13 ,, Starved ,, ,, ,, ,,

2-14 SANTO50 Flooded results for increasing aspect ratio

2-15 ,, Starved ,, ,, ,, ,,

2-16 TDF88 Spin traction curves

2-17 SANTO50 Spin traction curves

ANALYSIS OF THE RESULTS.

5-1 Regression line for individual thermal constants on TDF88 for increasing speed

5-2 Regression line for individual thermal constants on SANTO50 for increasing speed

5-3 Regression line for individual thermal constants on TDF88 for increasing pressure

5-4 Regression line for individual thermal constants on SANTO50 for increasing pressure

5-5 Regression line for individual thermal constants on TDF88 for increasing aspect ratio

5-6 Regression line for individual thermal constants on SANTO50 for increasing aspect ratio

5-7 Regression line for combined thermal constants on TDF88 for increasing speed

5-8 Regression line for combined thermal constants on SANTO50 for increasing speed

5-9 Regression line for combined thermal constants for TDF88 for increasing pressure

5-10 Regression line for combined thermal constants for SANTO50 for increasing pressure

5-11 Regression line for combined thermal constants for TDF88 for increasing aspect ratio

5-12 Regression line for combined thermal constants for SANTO50 for increasing aspect ratio

5-13 Regression line for combined thermal constants for TDF88 for various conditions of speed, pressure, aspect ratio and inlet temperature.

5-14 Regression line for combined thermal constants for SANTO50 for various conditions of speed, pressure, aspect ratio and inlet temperature.

COMPARISON WITH PREDICTED RESULTS

6-1 Experimental side slip traction curves for TDF88 at various pressures,temperatures, aspect ratios and rolling velocities.

6-2 Experimental side slip traction curves for SANTO50 at various pressures, temperatures, aspect ratios and rolling velocities.

6-3 Comparison of experimental with theoretically predicted traction curves for TDF88 based upon individually fitted thermal constants and shear modulus at various pressures, temperatures, rolling velocities and aspect ratios.

6-4 Comparison of experimental with theoretically predicted traction curves for SANTO50 based upon individually fitted thermal constants and shear modulus at various pressures, temperatures, rolling velocities and aspect ratios.

6-5 Comparison of experimental with theoretically predicted traction curves for TDF88 based upon individually fitted thermal constants at various pressures, temperatures, rolling velocities ,aspect ratios and spin.

6-6 Comparison of experimental with theoretically predicted traction curves for SANTO50 based upon individually fitted thermal constants at various pressures, temperatures, rolling velocities, aspect ratios and spin.

6-7 Comparison of experimental with theoretically predicted traction curves for TDF88 based upon multiple curve fitted thermal constants and shear modulus at various pressures, temperatures, rolling velocities and aspect ratios.

6-8 Comparison of experimental with theoretically predicted traction curves for SANTO50 based upon multiple curve fitted thermal constants and shear msodulus at various pressures, temperatures, rolling velocities and aspect ratios.

6-9 Comparison of experimental with theoretically predicted traction curves for TDF88 based upon multiple curve fitted thermal constants and shear modulus at various pressures, temperatures, rolling velocities, spin and aspect ratios.

6-10 Comparison of experimental with theoretically predicted traction curves for SANTO50 based upon multiple curve fitted thermal constants and shear modulus at various pressures, temperatures, rolling velocities, spin and aspect ratios.

6-11 Experimental traction curves for TDF88 under starved conditions at various pressures, temperatures, rolling velocities and aspect ratios.

6-12 Experimental traction curves for SANTO50 under starved conditions at various pressures, temperatures, rolling velocities and aspect ratios.

6-13 Comparison of experimental with theoretically predicted traction curves for TDF88 under starved conditions based upon individually fitted thermal constants and shear modulus at various pressures, temperatures, rolling velocities and aspect ratios.

6-14 Comparison of experimental with theoretically predicted traction curves for SANTO50 under starved conditions based upon individually fitted thermal constants and shear modulus at various pressures, temperatures, rolling velocities and aspect ratios.

6-15 Comparison of experimental with theoretically predicted traction curves for TDF88 under assumed fully flooded conditions based upon multiple curve fitted thermal constants and shear modulus at various pressures, temperatures, rolling velocities and aspect ratios.

6-16 Comparison of experimental with theoretically predicted traction curves for SANTO50 under assumed fully flooded conditions based upon multiple curve fitted thermal constants and shear modulus at various pressures, temperatures, rolling velocities and aspect ratios.

6-17 Comparison of experimental with theoretically predicted traction curves for TDF88 including asperity traction due to starved conditions based upon multiple curve fitted thermal constants and shear modulus at various pressures, temperatures, rolling velocities and aspect ratios.

6-18 Comparison of experimental with theoretically predicted traction curves for SANTO50 including asperity traction due to starved conditions based upon multiple curve fitted thermal constants and shear modulus at various pressures, temperatures, rolling velocities and aspect ratios.

6-19 Comparison of experimental with theoretically predicted traction curves for TDF88 including asperity traction due to starved conditions based upon multiple curve fitted thermal constants and shear modulus at various pressures, temperatures, rolling velocities, spin and aspect ratios.

6-20 Comparison of experimental with theoretically predicted traction curves for SANTO50 including asperity traction due to starved conditions based upon multiple curve fitted thermal constants and shear modulus at various pressures, temperatures, rolling velocities, spin and aspect ratios.

6-21 Variation of asperity traction with the voltage fraction.

6-22 Correlation between predicted and experimental asperity traction as a function of the contact fraction.

NOMENCLEATURE.

Below follows a list of the various symbols used in the text and their units.

Sym.	DESCRIPTION	Units
a,b	Semi Hertzian contact size in the x and y direction	[m]
A	Fluid viscosity temperature parameter	[°C]
B	Fluid viscosity pressure parameter	[°C/Pa]
C_s	Specific heat of the disc material	[J/kg.°C]
C	Shear stress temperature parameter for thermal model	[°C/Pa]
C_f	Contact fraction for asperities	[-]
C'	Elastically strained fraction of contact	[-]
D	Solidification temperature for the fluid	[°C]
De	Deborah number	[-]
e	Curvature offset from the rolling axis	[mm]
E	Viscosity constant for non linear thermal model	[Pa.sec]
E'	Composite elastic modulus for the disc material	[Pa]
$F(\tau)$	Dissipative function for traction model	[sec^{-1}]
F_x	Contact force in the x direction	[N]
F_y	Contact force in the y direction	[N]
F_z	Normal force on the contact	[N]
f	Number of asperities in contact	[-]
G	Fluid shear modulus (uncorrected)	[Pa]
G_c	Compliance corrected fluid shear modulus (simple)	[Pa]
G_j	Fully corrected fluid shear modulus	[Pa]
G_e	Johnson Elasticity parameter	[-]
G_s	Shear modulus of the disc material	[Pa]
h	Central film thickness in contact	[m]
J1	Dimensionless longitudinal slip variable	[-]
J2	Dimensionless side slip variable	[-]
J3	Dimensionless spin variable	[-]
J4	Dimensionless longitudinal traction variable	[-]
$J4_e$	Elastic stress portion of J4	[-]
$J4_p$	Plastic stress portion of J4	[-]
$J4_t$	Thermal dimensionless longitudinal traction	[-]
J5	Dimensionless side slip traction variable	[-]
J6	Dimensionless spin torque variable	[-]
k	Contact aspect ratio (b/a)	[-]
k_f	Thermal conductivity of fluid	[N/sec °C]
k_s	Thermal conductivity of disc material	[N/sec °C]
K	Calibration constant in side slip measurement	[m]
m	Initial slope of the zero spin traction curve	[-]
m'	Traction slope for dry discs	[-]
P	Pressure	[Pa]

P_o	Hertzian contact pressure	[Pa]
P_e	Psuedo Peclet number	[-]
P_r	Reduced Hertz pressure fraction	[-]
Q	Kalker coefficient	[-]
q	Thermal heat flux due to traction	[N/m sec]
R_x	Equivalent radius of curvature in x direction	[m]
R_y	Equivalent radius of curvature in y direction	[m]
R_e	Equivalent radius of curvature for discs	[-]
S	Auxiliary variable used in elastic/plastic model	[-]
t	time	[sec]
U	Rolling speed of the discs	[m/sec]
VF	Voltage fraction for asperities	[-]
V0	Viscosity parameter	[Pa.sec]
ΔV	Side slip velocity of the discs	[m/sec]
ΔU	Longitudinal slip velocity of the discs	[m/sec]
Δx	Small displacement of the displacement transducer	[m]
YI	Inlet shear heating factor	[-]

GREEK SYMBOLS.

α	Angle of tilt of the toroidal axis	[rad]
$\alpha(\theta)$	Pressure viscosity coefficient	[1/Pa]
β	Side slip angle	[rad]
ω	Angular spin velocity on the contact	[rad/sec]
θ	Temperature of the fluid	[°C]
θ_c	Shearplane temperature	[°C]
θ_o	Inlet temperature	[°C]
τ	Shear stress	[Pa]
τ_s	Non linear stress parameter for hyperbolic sine	[Pa]
τ_c	Limiting strength of fluid at shear plane temperature	[Pa]
τ_o	Limiting strength of fluid at inlet temperature	[Pa]
$\dot{\gamma}$	Shear strain rate (V/h)	[1/sec]
η	Viscosity	[Pa.sec]
μ	Traction coef. F_x/F_z or F_y/F_z	[-]
$\bar{\mu}$	Peak traction coefficient	[-]
ρ_s	Density of the disc material	[kg/m^{-3}]
ψ χ	Hertzian contact shape parameters	[-]

1-0 INTRODUCTION

Traction or friction plays a major role in today's technological society in that it holds one of the keys to reduce our overall energy consumption, and thereby the dependence on unreliable sources of this energy. Friction and traction indicate the resistance to relative motion of two 'contacting' bodies. The term traction and friction have the same meaning in a tribological sense, however friction is used when this resistance is undesirable and traction is used when it is desirable.

The mechanical components in which friction and traction are important are rolling element bearings, gears, cam and tappets and traction drives. Because these devices almost always operate in a wet or fluid lubricated environment, the traction or friction is mostly governed by the particular fluid that is used. In the first three devices friction is the key source of inefficiency and because of the multitude of bearings and gears in service, a small reduction in these losses can amount to phenomenal savings in energy. Rolling element bearings actually have rather interesting requirement for friction or traction in that at low to medium speeds friction should be low, but at high speeds traction should be high to ensure that the rolling elements operate at the correct velocities.

Traction drives on the other hand rely on the transmittal of tractive forces for power transmission purposes and they require high fluid traction at all times. With variable speed traction drives it is possible to allow prime movers to operate at their most efficient power point, almost independent of the load requirements. It is by these means that traction drives can indirectly be looked upon as potential energy savers. Fuel consumption reductions of 25 to 40 % are believed possible with the use of variable speed traction drives in automobiles. This report addresses itself to the phenomena of traction and is aimed at providing fluid traction data for two fluids operating under widely varying conditions, with particular emphasis on traction drives.

1-1 TRACTION DRIVE TECHNOLOGY.

Traction drives have been in existence for a long period of time. They are simple in concept and relatively easy to manufacture. However successful traction drives are few and the reason for this is that while simple in concept, the analytical tools required to develop a drive in direct competition with other transmissions have been sadly lacking in the past. This is rapidly being remedied however with recent developments and interest in this area of design. An excellent review article dealing with the historical aspects of traction drives and the related technology is presented by Loewenthal [1].

In simple terms the traction drives basic elements are two rollers, pressed into nominal contact, rolled about their respective axis and power is transmitted in the form of a shear stress across the contact area. A fluid is present to prevent initial surface scuffing damage and to provide for some form of cooling. The rolling motion of the discs draws this fluid into the contact zone and a thin layer of this fluid will separate the actual contact area. It is also in this region where the torque is transmitted from one roller to the next and it should not surprise one that the performance of a traction drive depends to a large extent upon the rheological properties of the fluid. Close examination of the fluid history as it passes through the contact gap reveals that it experiences a sudden pressure pulse from atmospheric to possibly several Giga Pascal in a time period of 1 to .1 m/sec. The shear stress that is transmitted from one disc to the other (about 10% of the normal stress) passes through this layer of fluid "trapped" in the contact and causes a shear. This in turn will lead to heat generation and from simple calculations, temperatures in the center of the film can easily reach several hundred degrees Centigrade.

To study the rheological properties of the fluid under these conditions precludes the use of most of the conventional instruments used for steady state measurements. In fact the only suitable type of instrument for the study is a disc machine where most of the conditions are the same or simi · to those in traction drives. From the resulting traction tests, certain models are inferred and it is in this area where there has been a lot of activity recently.

To the designer of traction drives, the traction behaviour of the fluid under the severe conditions is of utmost importance because of the direct influence that it has on the efficiency, size and life of a given drive. Besides a good rheological model for the fluid, he must have at his disposal pertinent rheological properties of the fluid that he proposes to use.

1-2 PRIOR TRACTION INVESTIGATIONS

As mentioned in the introduction, there has been a lot of activity in the area of traction research, both in the past and recently. Notable contributions have come from Clark et al [2], Hewko [3], Smith [4], Smith et al [5], Johnson and Cameron [6], Niemann and Stoessel [7], and more recently Johnson and Roberts [8] and Johnson and Tevaarwerk [9]. Some of these investigations were strictly experimental in nature, and aimed at obtaining traction drive design data, while others were aimed at understanding the traction phenomena so that rheological models could be formulated. This latter research is of course ultimately aimed at relating fluid molecular properties to traction properties. Research by Johnson and Tevaarwerk [9], Daniels [10], Hirst and Moore [11] and Alsaad et al [12] is directed specifically towards this purpose. The reader is referred to an excellent review by Johnson [13] for further aspects of this topic.

Many of the rheological models derived so far have been isothermal in nature. This is not so much due to the level of understanding of traction but rather because of the degree of complexity that thermal analysis introduces. This is not to say however that thermal effects are not important, a simple method is required however to include them in the analysis.

Current understanding of traction has led to traction models that describe the fluid shear behaviour in terms of an elastic and a dissipative element. For purposes of mathematical tractability this dissipative element is taken to be plastic like in nature. This gives an adequate description of the fluid behaviour at conditions such as those encountered in traction drives. An analysis of traction drive performance using such a model was done by Tevaarwerk [14]. It showed that under certain conditions the prediction technique by Magi [15] can be used. This work has now been further expanded by developing a simple method to correct for thermal effects due to spin, Tevaarwerk [16], and an overall thermal traction study, Tevaarwerk [17].

As with all models however, their usefulness is severely restricted if inadequate input traction data is available to the designer. This is especially so if new high traction fluids are used that were not tested previously for use under conditions that exist in modern highly advanced traction drives.

1-2 TRACTION DATA RESEARCH PROGRAM

Several novel and new forms of traction drives have recently been developed and tested by Loewenthal et al [18] and Kemper [19] and McCoin et al. [20]. For purposes of design of these drives, adequate fluid rheological data is needed under the operating speeds, pressures and temperatures encountered. Besides the above it is desirable to investigate the influence of contact area, aspect ratio, spin and side slip on the traction behaviour. Additionally, the data could be tested against an existing traction model to investigate how well it predicts the observed traction. The first part of this investigation concerned itself with the isothermal aspect of traction and the results are reported in Tevaarwerk [21], the second part of this investigation, reported here, covers the thermal aspects of traction and the influence of asperity contact. This work was performed by Transmission Research Incorporated of Cleveland Ohio under contract to the NASA Lewis Research Center, Cleveland, Ohio. The NASA technical project manager was Mr. D. A. Rohn from the Bearing, Gearing and Transmission Section at the NASA Lewis Research Center.

2-0 EXPERIMENTS

The various traction experiments were carried out on an existing twin disc test facility, shown in figure 2-1, 2-2 and 2-3. This test facility was modified such that it would be capable of traction measurements for speeds up to 120 m/sec, and facilities were provided for the asperity contact measurement and fluid starvation. Traction curves were obtained by using the side slip technique; a technique whereby large traction transfer can be measured without the need for a large motor generator set.

2-1 DESCRIPTION OF TWIN DISC MACHINE.

For an extensive description of twin disc traction testers the reader is referred to the literature; Smith [4] and Johnson and Roberts [8]. Basically the machine consists of two discs, called the upper and lower disc. The lower disc is mounted in rolling element bearings through shafts and the only degree of freedom is one of rotation about this axis. The lower disc always has a transverse radius of curvature of infinity. To avoid problems with gravity forces the axis of rotation of this disc should be horizontal to within a few milliradians. The upper disc is contained in bearings that are mounted in the upper assembly. This upper assembly is suspended with elastic hinges such that only direct normal motion or axial motion is possible. The assembly will however always stay horizontal. The upper disc (or toroid) has curvatures so that the desired contact geometry is arrived at. The upper assembly is constructed such that the toroidal axis can be tilted relative to the horizontal plane so as to introduce spin on the contact. It can also be skewed about the normal to the contact to introduce a side slip velocity.

In order to achieve the various aspect ratios a number of special discs with varying crown curvatures were employed. These discs were made of AISI-01 steel, hardened to 7.00 GPa, ground and polished to a surface finish of less than .05 μm RMS and with an out of roundness error of less than 5 μm. Between tests the discs were inspected for surface damage and if needed, reground and polished to bring them back up to specifications. The required normal load, obtained by a dead loading technique, can be calculated from the Hertz theory for elastic bodies in contact. The maximum contact normal stress P_o is given by;

$$P_o = \frac{1}{2\pi\varphi X}\sqrt[3]{\frac{3F_zE'^2}{R_e^2}} \qquad (2\text{-}1)$$

where F_z = contact normal load [N]
P_o = Hertzian contact stress [Pa]
E' = composite elastic modulus [Pa] ;(231 GPa for steel)
R_e = equivalent disc radius [m]
$= (1/R_x + 1/R_y)^{-1}$
φ, X = Hertzian contact shape factors [-]

The various curvatures R_x and R_y as employed in this investigation are reported for each test in Appendix I-A . The Hertzian shape factors may be found in any good book on contact mechanics.

2-2 INSTRUMENTATION OF THE TRACTION TESTER.

By suitably instrumenting the disc machine the relevant experimental parameters can be measured. In the experiments reported here the sideslip, sideways traction force, toroid surface temperature, rolling velocity and the degree of asperity contact were measured. The technique of measuring each of these variables will be discussed next.

2-2-1 THE MEASUREMENT OF THE TRACTION FORCE.

A ring dynamometer type load cell was used to measure the side slip force of the upper toroid assembly. It was found necessary that this load cell was thermally isolated from the machine because temperature variations tended to introduce drift into the signal. Also the active gauges had to be protected from the splashing hot test fluid as this gave rise to noise on the signal. The electrical signal from the load cell was conditioned for noise and amplified using common mode rejection techniques. The gain on the amplifier was adjusted so that a good range on the signal was measured for each test. Calibration of the load cell was done in situ by dead loading. This calibration was checked periodically but never was there any need for recalibration.

2-2-2 THE MEASUREMENT OF SIDE SLIP.

The skew angle was measured by using a direct current displacement transducer on the upper assembly and thereby measuring the rotation angle of this assembly. This skew angle gives the amount of side slip/roll ratio through the relationship;

(2-2) $$\Delta V/U = \tan(\beta)$$

where β = side slip angle [rad]
ΔV = side slip velocity [m/sec]
U = rolling velocity [m/sec]

By measuring the amount of skew with the displacement transducer the side slip/roll ratio is obtained directly through;

(2-3) $$\Delta V/U = K\,\Delta x$$

where Δx is the displacement of the transducer and K a scale factor. The electrical output of the displacement transducer was filtered in an R-C network to provide a low-pass signal. The maximum frequency response of the R-C network was .1 sec. The displacement transducer was calibrated by rotating the upper assembly through a known angle and then calculating the amount of side slip for this angle.

2-2-3 THE MEASUREMENT OF THE TOROID SURFACE TEMPERATURE.

In the analysis and reduction of the test data it is important that the disc temperature be used as the reference inlet temperature for the film thickness. This temperature can be measured by embedding a thermocouple directly below the surface of the toroid and then to take this signal out through mercury slip rings. This method is however not very practical when a number of different toroids are involved and is also very costly from an installation point of view. With care the surface temperature can also be measured by using a trailing thermocouple that rides on the disc surface. The disadvantage of this technique is that it can be speed sensitive in its response because of frictional heating.

The latter technique was employed here and care was taken to ensure that the contact force on the thermocouple was not excessive. A reference ice bath junction ensures that the same reference level for the thermocouple is used at all times. The signal from the thermocouple is amplified using common mode rejection techniques to minimize the influence of electrical noise and other disturbances. Calibration was done by the boiling water method adjusted for sea level differences. This calibration was checked periodically. Only slight deviations were encountered. Because of the frictional heating at the junction/toroid interface a variation of about 2 °C was found in the signal between stationary discs and those rotating at a surface velocity of 120 m/s. The overall reproducibility of the temperature measurement is better than 2°C.

The temperature on the machine was regulated through the use of heaters and coolers on the test fluid. This test fluid would be allowed to circulate freely before the start of a test series in order to bring the machine up to a uniform temperature. No specific effort was made however to maintain a given set point temperature during the test and the reason for this will become clear in the analysis of the results.

2-2-4 MEASUREMENT OF THE DISC SPEED.

The rotational velocity of the bottom disc was measured indirectly through the use of a tachometer on the drive motor. Knowledge of the gear ratios and the disc diameter permitted the calculation of the surface velocity of the disc. The electrical signal from the tachometer was scaled by using a divider circuit and filtered by using a low pass R-C filter with a 2 sec time constant. This method of velocity measurement is often used to give both magnitude and direction indication. Calibration of the system was performed on a periodic basis and some major problems with the testing stemmed from this source. Initially the tachometer was directly coupled to the motor shaft. This was a simple solution but may have caused some of the problems with this system. About half way through the test series the tachometer drive was changed to an indirect system with a rubber belt to isolate it from the motor vibrations. No further problems were experienced after that point.

2-2-5 CONTACT RATIO MEASUREMENT.

In order to measure the degree of asperity contact that took place at any one time an electrical conductance circuit as shown below was employed.

The selection of the various electrical components is such that only very low voltages are applied across the two discs to minimize the risk of surface damage through arcing. The output signal of network was essentially DC in nature with only slow fluctuations in the contact conditions being recorded. The signal from this circuit will be used in Chapter 6 to analyze the amount of asperity traction that is added to the fluid traction.

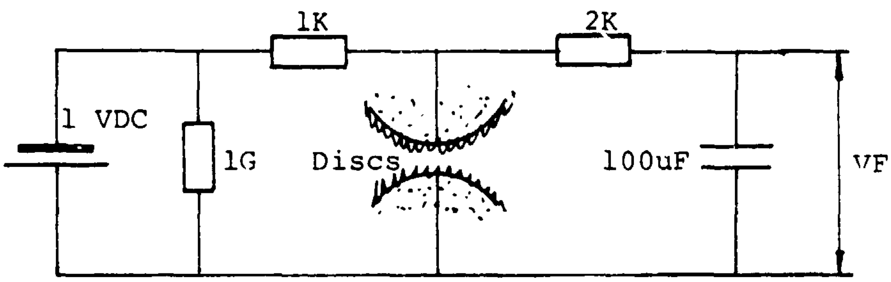

Schematic of the contact ratio measuring circuit.

2-3 TRACTION MEASUREMENTS.

Traction curves were obtained by the slow rotation of the upper assembly from a positive value of side slip/roll ratio to a negative value. The signals from the above discussed transducers were fed into a digitizer from where they were led into an Apple II+ computer for plotting and storage on magnetic media for future use. The computer would automatically trace the force versus slip curve on the screen. By reversing the direction of rotation of the machine, a duplicate set of curves can be obtained. For each experiment 500 data points were taken at fixed time periods of .2 seconds. Multiple data data points would be stored as separate entries.

After the completion of a test series the data would be recalled into memory of the computer and further manipulated. This manipulation consisted of the averaging of the multiple entries, the filling in of any gaps in the data through forward and backward interpolation, the comparison of the traces for the forward and reverse rolling direction and the centering of the traces about the center lines. After the centering operation the data would be smoothed by a 'N' point averaging technique for traction points after the peak traction points. For storage a geometric series was used so that the total traction trace was now represented by 40 data points for each measured variable. These traces were then stored on magnetic media and used for further manipulation and data extraction at a later point

2-3-1 TYPICAL TRACTION TRACES.

In total close to 400 traction curves were taken and it is not practical to reproduce every one of them here. A summary of all the traction traces is shown in Appendix I.

To show the trend that certain variables have on traction a number of typical curves were selected. Of the controlled variables it is important to show the variation of traction with speed,pressure and aspect ratio. The variation of temperature will be dealt with at a later stage. The selected traces are indicated in tabular form below.

Speed [m/sec]	TDF-88		SANTO-50	
	Flooded	Starved	Flooded	Starved
50	820804-7	820804-8	820924-7	820924-8
80	820804-9	820804-10	820924-9	820924-10
120	820804-11	820804-12	820924-11	820924-12

TABLE 2:1 Traces selected to show the influence of speed on traction.
Aspect ratio k=2 and the Hertz contact pressure P_0=1.2 GPa.

The above indicated traces are shown in Figures 2-4 to 2-7 in the grouping as indicated.

P_0 [GPa]	k [-]	TDF-88		SANTO-50	
		Flooded	Starved	Flooded	Starved
1.0	5.6	820916-3	820916-4	820923-9	820923-10
1.2	5.0	821116-9	821116-10	821102-10	821102-9
1.4	2.0	820805-3	820805-4	820924-15	820924-16
1.6	1.0	820824-3	820824-4	821019-9	821019-10
1.8	1.0	820824-9	820824-10	821019-16	821019-15

TABLE 2:2 Traces selected to show the influence of pressure on traction.

The rolling velocity is kept constant at approximately 80 m/sec. These traction traces are shown in Figures 2-8 to 2-11 in the groupings as indicated.

Aspect ratio k (-)	TDF-88		SANTO-50	
	Flooded	Starved	Flooded	Starved
1.0	820824-15	820824-16	821019-3	821019-4
2.0	820805-3	820805-4	820924-15	820924-16
5.0	821116-15	821116-16	821102-18	821102-17

TABLE 2:3 Selected traction traces to show the influence of contact aspect ratio.

Hertzian contact pressure is P_0=1.4 GPa and the rolling velocity is 80 m/sec. These traces are shown in figures 2-12 through to 2-15 for the groupings as indicated.

2-4 THE APPLICATION OF SPIN.

Spin may be introduced on the contact by tilting the upper assembly through an angle α . This angle α is referred to as the spin angle, however it is not a direct measure of the spin itself. A suitable measure of spin is given by the variable J3, see Tevaarwerk [14].

$$(2\text{-}5) \qquad J3 = \frac{3\pi}{8}\frac{m}{\bar{\mu}}\frac{\omega\sqrt{ab}}{U}\sqrt{k}$$

where; m = initial traction slope [-]
$\bar{\mu}$ = peak traction coefficient [-]
ω = spin velocity on contact [rad/sec]
k = aspect ratio b/a [-]
U = contact rolling velocity [m/sec]
a,b = contact dimensions [m]

Most of the variables in equation (2-5) are known either from the traction curves or else from the contact geometry. The group $\omega\sqrt{ab}/U$ provides for a measure of the spin intensity on the contact and it will be used here to indicate spin as such. The angular spin velocity on the contact can be related to the angle of tilt through the following:

$$(2\text{-}6) \qquad \omega/U = \frac{\sin\alpha}{(R_y\cos\alpha + e)}$$

where α = spin angle [rad]
e = center of curvature offset [m]

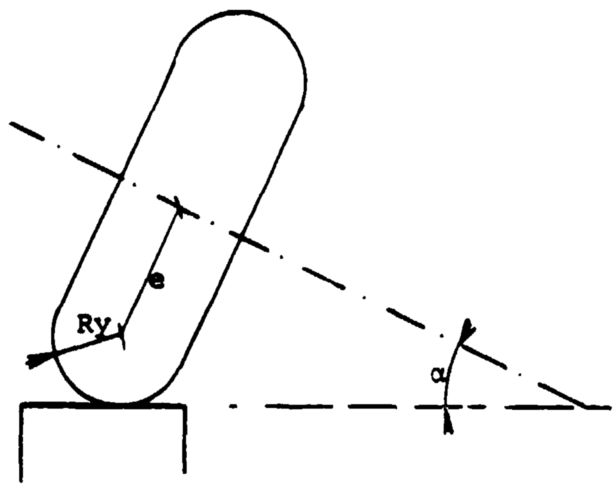

Figure 2-3: General disc arrangement for spin tests.

In some instances the distance e has a negative value i.e. the center of R_y is above the axis of rotation as shown in figure 2-3. Equation (2-6) still applies provided that the sign of the distance e is taken into account. The value of 'e' is listed in Appendix I-A together with the values for R_x and R_y. Because of the computer listing the notation differs slightly from that in the text. R_x becomes RX and R_y becomes RY. When the toroids are tilted, a slight change takes place in their rolling curvature. This was kept small however by the proper selection of the radii. A simple correction can be made for this radius change through the following expression;

(2-7) $$R_x = R_y + e/\cos\alpha$$

In most cases this correction does not amount to very much.

Traction curves with imposed spin were obtained in the same manner as described for the zero spin traction curves. Typical curves obtained are shown in figure 2-16 to 2-17 for a variety of spin conditions. A broad selection of curves was made to show the influence of spin on the traces. Below is a Table indicating the degree of spin in each test shown in Fig. 2-16 and 17.

TDF-88		SANTO-50	
Test number	$\omega\sqrt{ab}/U$ [%]	Test number	$\omega\sqrt{ab}/U$ [%]
820825-3	.294	820923-3	.605
820825-9	.336	820927-10	.400
820825-15	.370	820927-15	.474
820902-6	.400	821022-9	.336
820916-9	.631	821022-4	.294
821118-15	1.11	821101-18	1.11

TABLE 2:4 Selected traction traces to show the influence of spin on traction.

A significant feature of traction tests with spin is that at the cross over point for side slip there is a finite amount of traction left as shown in the experimental data. This is not some kind of experimental problem but results from the elastic response of the fluid to small strain. In the spin traction curves the vertical axis give the 'average traction stress' rather than the usual traction coefficient. This average traction stress is related to the traction coefficient through the mean contact pressure as;

(2-8) $$\bar{\tau} = \mu \bar{P}$$ where;

$\bar{\tau}$ = average traction stress [Pa]
μ = traction coefficient [-]
and $\bar{P}$ = mean contact pressure [Pa]

3-0 THEORETICAL ANALYSIS

In order to understand the required analysis of the experimental data it will be helpful to consider the following discussion of traction. The ability of a fluid film, trapped under high pressure in the elastically deformed region of two loaded curved elements, to transmit a tangential force from one element to the other, is commonly referred to as friction or traction. The magnitude of this force depends on several variables such as :1) the contact kinematic conditions of slip, spin and sideslip, 2)the fluid present, 3) temperature, pressure and operating speeds. We will first examine the traction behaviour under simple slip only.

Under conditions of increasing slip between the two elements an increasing traction force is transmitted up to a certain limit at which point it will decrease with further slip. See Fig. 3-1

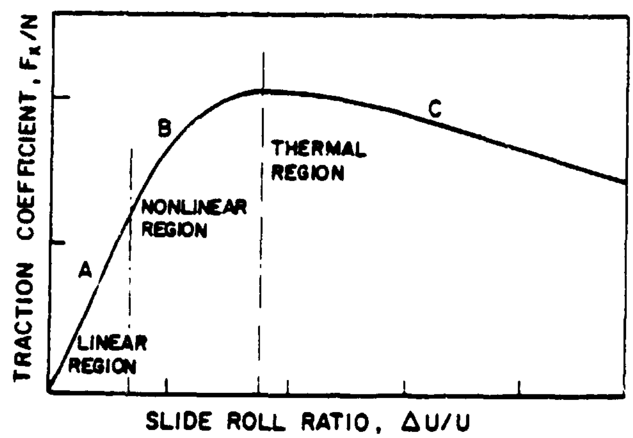

Fig. 3-1 Typical traction /slip curve.

There are three regions identified on this traction curve and the behaviour in each of these regions can best be described by the Deborah number. For a simple Maxwell viscoelastic model this number is the ratio of the relaxation time and the mean transit time, see Johnson and Tevaarwerk [9].

(A) The linear low slip region. Thought to be isothermal in nature, it is caused by the shearing of a linear viscous fluid (low De) or that of a linear elastic solid (high De).

(B) The nonlinear region. Still isothermal in nature but now the viscous element responds nonlinearly. At low De this portion of the traction curve can be described by a suitable nonlinear viscous function alone, while at high De a linear elastic element interacts with the nonlinear viscous element.

(C) At yet higher values of slip the traction decreases with increasing slip and it is no longer possible to ignore the dissipative shearing and the heat that it generates in the film. Johnson and Cameron [6] showed that the shear plane hypothesis advanced by Smith [4] does account for most of their experimental observations in this region. More recently Conry et al [22] have shown that a nonlinear viscous element together with a simple thermal correction can also describe this region.

3-1 ISOTHERMAL TRACTION ANALYSIS.

The rheological model that describes the traction under simple slip in all three regions of operation fairly well is the J & T traction model as presented by Johnson and Tevaarwerk [9];

$$(3\text{-}1) \qquad \frac{1}{G}\frac{d\tau}{dt} + F(\tau) = \dot{\gamma}$$

The dissipative function $F(\tau)$ is open to the choice of the researcher to fit the observed traction but Johnson and Tevaarwerk [9] found that the hyperbolic sine;

$$(3\text{-}2) \qquad F(\tau) = \frac{\tau_s}{\eta} \sinh(\tau/\tau_s)$$

where τ_s = non-linear shear stress parameter.

described all of their experimental results in regions (A) and (B) very well. At higher pressures and for fluids with high traction coefficients this dissipative function may be replaced by the purely plastic behaviour of the material;

$$(3\text{-}3) \qquad F(\tau) = 0 \text{ for } \tau < \tau_c \text{ ; } F(\tau) = \dot{\gamma} \text{ for } \tau = \tau_c$$

where τ_c = limiting shear strength of the fluid.

Whether the perfectly plastic behaviour of the material is intrinsic is not clear. Work by Johnson and Greenwood [23] suggests that it is possibly the result of thermal behaviour of the sinh model. For many applications the elastic/plastic traction model is adequate. It was used by Tevaarwerk and Johnson [24] and Tevaarwerk [14] to predict traction under various conditions of slip and spin. The analysis is completely isothermal in nature and for simple slip the traction is given by;

$$(3\text{-}4) \qquad J4 = \frac{2}{\pi}\left[\tan^{-1}S + \frac{S}{(1+S^2)}\right]$$

where $S = \frac{2}{3}\frac{J1}{\sqrt{k}}$

The shear strain rate in the fluid was taken to be the same everywhere in the contact and assumed to be constant throughout the film thickness. Its magnitude was taken to be;

$$\dot{\gamma} = \frac{\Delta V}{h}$$

Equation (3-4) results from the integration of stresses, caused by the shearing of an elastic element of pressure independent average shear modulus G, and the plastic stresses proportional to the local Hertzian pressure. The predicted traction from an elastic/plastic model compares very well with the experimentally observed values for combinations of slip and spin, provided that the spin or slip are not too large. Large slip or spin results in almost purely dissipative stresses over the contact area and hence non-isothermal behaviour. Traction prediction under these conditions is still possible but the thermal effects need to be brought into the picture. Tevaarwerk [25],[16] presents two techniques for calculating such spin traction curves. The latter technique requires the shape of the traction curve in the large slip regime to provide a simple correction to the isothermally predicted spin traction.

Isothermal traction analysis was used in the reduction of traction data for the first report on the results of the traction measurement, Tevaarwerk [21].

3-2 THERMAL TRACTION ANALYSIS.

The ability to separate the elastic stresses from the plastic ones can now be used to perform a thermal traction calculation. The analysis presented here follows the technique outlined by Tevaarwerk [17] and [26].

Equation (3-4) resulted from the integration of isothermal elastic and plastic stresses over the contact area of an ellipse. For the region of contact under elastic stress the shear energy is conserved and therefore does not give rise to temperature increases. The plastically deforming region however, is non-conservative and a temperature rise in the fluid is expected. This will lead to a reduction in the local plastic strength of the fluid. Equation (3-4) may therefore be better written in its elastic and plastic parts;

$$(3\text{-}5) \qquad J4 = J4_p + J4_e$$

$$(3\text{-}6) \qquad J4_e = \frac{4\,S}{\pi(1+S^2)^2}$$

$$(3\text{-}7) \qquad J4_p = \frac{2}{\pi}\left[\,\tan^{-1}S + \frac{S(S^2-1)}{(1+S^2)^2}\,\right]$$

This modification is given by τ_c/τ_o where τ_c is the average stress under thermal conditions and τ_o is the average stress under isothermal conditions. We are dealing therefore with averaged stresses in the plastic region of the contact even though the isothermal stress distribution is according to the Hertzian pressure. This seemingly contradictory assumption is supported by theoretical evidence by Tevaarwerk [25]. The modified equation would therefore be;

$$(3\text{-}8) \qquad J4_t = J4_e + \frac{\tau_c}{\tau_o}\,J4_p$$

The modification term τ_c/τ_o can be found from a thermal balance over the contact region under plastic stress. This region can be thought of as a thermal source whose heat is conducted/convected away. The length of the source is a function of the location of the onset of plastic deformation after the initial elastic region, however in this simple model we will take the source length to be "a" where this is the semi contact length in the running direction. As a simple thermal balance we will use the expression reported by Johnson and Cameron [6] for the shear plane temperature;

(3-9) $$\theta_c - \theta_o = q \frac{h}{k_f} \left[.1 + \frac{.5}{\sqrt{P_e}} \right]$$

where;

(3-10) $$P_e = \frac{a \rho_s C_s U}{k_s} \left\{ \frac{k_s}{k_f} \frac{h}{a} \right\}^2 \quad [-]$$

and
q = average thermal strength of the source [W/m²]
θ_c = shearplane temperature in the contact [°C]
θ_o = inlet temperature of the fluid [°C]
k_f = thermal conductivity of fluid in the contact [W/m°C]
h = central film th.ckness in the contact [m]
k_s = thermal conductivity of the roller material [W/m°C]
C_s = specific heat of the roller material [J/kg°C]
ρ_s = density of the roller material [kg/m³]

This expression is only valid when the heat is conducted through the film and convected away by the discs, a condition that is true for most traction drive contacts. The strength q of the source is given by;

(3-11) $$q = \tau \Delta U$$

In order to proceed any further we need a relationship between temperature and the shear strength of the fluid. A typical relationship that has its roots in the Eyring theory of fluid transport is given by;

(3-13) $$\tau(\theta) = \frac{1}{C} \left[A + BP + (\theta + D) \, Ln \left(\frac{2\dot{\gamma}CE}{\theta + D} \right) \right]$$

where ; A = viscosity temperature constant [°C]
B = pressure viscosity constant [°C/Pa]
C = non-linear shear stress constant [°C/Pa]
D = fluid solidification temperature [°C]
E = fluid viscosity constant [Pa.sec]
P = pressure of the fluid in the contact [Pa]

At first sight it seems that this equation has five disposable constants in it, however two of these constants (A and D) are derived from the atmospheric viscosity temperature relationship, and one more (B) can be obtained from the Barus viscosity pressure relationship. The constant D is known as the solidification temperature; the temperature to which the fluid should be cooled to become solid like under atmospheric pressure. Only the constants C and E need to be determined experimentally from the traction results and this will be done in the next chapter. It should be noted here that the ultimate aim is to derive the fluid traction parameters such that they apply for all the experimental conditions reported here. In the next chapter a gradual development towards this goal will take place.

By using equations (3-9), (3-10), (3-11) and (3-13) the average thermal shear stress can be obtained for a given set of conditions. In equation (3-8) we need the ratio of the average contact shear stress under thermal conditions to that under isothermal conditions. This is really the ratio of the shear stress given by equation (3-13) evaluated at the shearplane temperature θ_c (from equation 3-9) and the shear stress as evaluated at the inlet temperature conditions θ_o. The other contact conditions remain the same for this ratio calculation.

In order to verify that the fluid in the traction contact behaves as indicated by equation (3-13) a slightly rewritten form will be used so that a straight line relationship of the experimental results verifies the validity of the model (see sec 5-2).

4-0 CALCULATION OF THERMAL TRACTION CURVES.

A simple thermally influenced traction curve can now be calculated from equation (3-8),(3-9) and (3-13) provided of course that we have sufficient experimental parameters.

In almost all practical situations of contacts under traction there is a degree of sideslip and spin present. These can influence the traction behaviour rather strongly. We shall examine an exact method of incorporating the influence of sideslip and an approximate method of allowing for spin.

4-1 INFLUENCE OF SIDESLIP.

Sideslip is the slip of the two contact surfaces perpendicular to the rolling velocity. It occurs mainly because of misalignment in a system or it can be due to a sideways force. Its influence can be incorporated very simply by vectorial methods. All the calculation techniques and thermal corrections thus far discussed apply. Hence we may say that;

(4-1) $$J4 = \frac{2}{3}\,\frac{J1\,\psi}{S\sqrt{k}} \quad ; \quad J5 = \frac{2}{3}\,\frac{J2\,\psi}{S\sqrt{k}}$$

(4-2) $$\psi = \frac{2}{\pi}\left[\, \tan^{-1}S + \frac{S}{1+S^2} \,\right]$$

(4-3) where $$S = \frac{2}{3}\sqrt{\frac{J1^2 + J2^2}{k}}$$

Also equation (3-11) is modified to read;

(4-4) $$q = \sqrt{\Delta U^2 + \Delta V^2}$$

The solution techniques remain exactly the same as before.

In the experiments as performed in this investigation all the results were purposely taken under conditions of side slip so as to avoid the use of large motor generator sets. As can be seen though the analysis is identical to the longitudinal slip traction analysis and so the equations as shown in Chapter 3 are directly applicable.

4-2 INFLUENCE OF SPIN.

Spin in a contact is the result of the geometric configuration that makes up the contact and the two contacting elements. The influence of spin is not readily implemented over the entire domain of spin, however there are some simplified approximate solutions that can be applied.

4-2-1 INFLUENCE OF SPIN IN THE LOW SLIP REGION.

When the amount of slip on a contact is low it is possible that we have an elastic/ plastic stress distribution. The exact distribution depends on the combination of spin and slip. For small values of longitudinal slip then there are three separate regions of influence that we may consider as outlined by Tevaarwerk and Johnson [24] and shown in Fig. 4-1. This map is based upon the influence of spin on the 75% slip traction point.

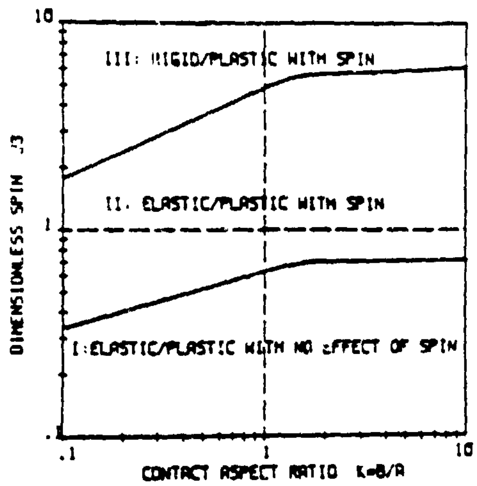

Fig. 4-1 Regions of influence of spin.

These regions are:

I) Traction can be predicted with an elastic/ plastic model without the influence of spin

II) Traction is predicted with an elastic/ plastic model with the influence of spin

III) Traction is predicted with a rigid/plastic model with influence of spin.

Because of the influence of elastic effects in region I and II it might be expected that thermal influence is small also. In region III all the shear is of a dissipative nature and hence we would expect a thermal influence. Because the rigid/plastic analysis is applicable ,a simple thermal correction is possible as outlined by Tevaarwerk [16]. This correction technique is based upon the concept that equivalent shear plane temperatures give rise to identical fluid shear strength. Hence by equating the amount of work done on the fluid due to spin to the amount of work in simple slip we can formulate a parameter called the "slide ratio". This ratio indicates the equivalent amount of simple slip that a contact has when under slip and spin.

The ratio is defined as;

$$\frac{\Delta U}{\Delta U'} = J4 + J6\frac{J3}{J1} \tag{4-5}$$

(4-6) where $\Delta U'$ = slip in the contact with spin

(4-7) and ΔU = equivalent slip in the contact without spin

and may be calculated from the rigid/ plastic analysis. Fig.4-2 shows the slide ratio as a function of the contact aspect ratio and the slip to spin ratio.

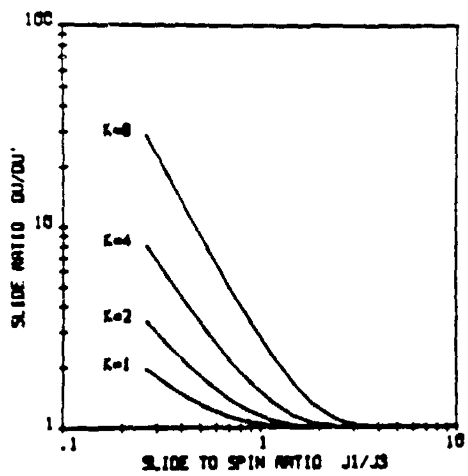

Fig.4-2 Slide ratio as a function of aspect ratio and slip/spin ratio.

There is no exact analytical expression for these curves, however they can be calculated quite readily, see Tevaarwerk [14]. In order to predict the with spin traction we also need the traction results from the rigid/plastic analysis. These curves are shown in Fig. 4-3 and can also be calculated quite readily.

The with spin traction can now be calculated quite simply by using Fig.4-3 to obtain the slide ratio for a given slip and spin. After having obtained the equivalent slip this quantity is now used in equations (3-5,3-6,3-7,3-8),(3-9),(3-11), and (3-13) to get the average thermally influenced shear strength of the fluid. From this we calculate the traction coefficient. B using Fig.4-3 find the dimensionless traction at the indicated slip/spin condition, multiply by the traction coefficient just obtained to get the actual value of the current traction coefficient.

4-2-2 INFLUENCE OF SPIN IN THE REGION OF LARGE SLIP.

The essence of the argument for using the rigid/ plastic (and hence the simplified thermal correction) analysis in Region III is that the entire stress distribution consists of plastic stresses. In the above case it is caused by the large spin component, however there is no difference if it is brought on by a rather large value of slip and small values of spin. In fact any time that we are dealing with traction in the thermal region one can apply the methods as for region III.

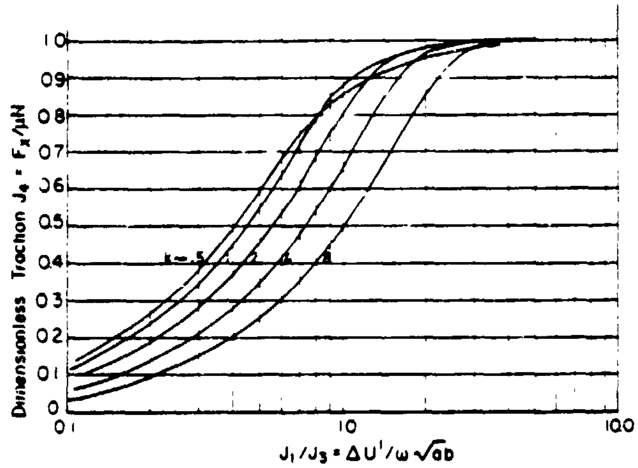

Fig.4-3 Spin traction curves as a function of aspect ratio and slip/spin ratio.

4-2-3 THERMAL INFLUENCE OF SMALL SPIN.

The thermal influence of small spin values in the region of combined elastic and plastic effects can also be included quite readily if the traction calculation techniques as outlined by Tevaarwerk [14] are followed. It is merely required that the plastic traction stresses are integrated due to slip and due to spin. From these integrals an equivalent amount of slip can be calculated by the same methods as outlined by Tevaarwerk [16]. This method is used in this report to calculate the thermal small spin traction curves because the methods outlined in 4-2-1 would ignore any elastic effects in the fluid. More information on this method will appear in a future publication.

5-0 EXTRACTION OF THE TRACTION PARAMETERS.

In order to use the technique as outlined above for the prediction of traction one does have to have the values of the thermal constants and those that govern the initial linear range. We shall deal with the extraction of the parameters for the two ranges separately.

5-1 EXTRACTION OF THE SHEAR MODULUS PARAMETERS.

As discussed in chapter 3 the initial linear slope on a traction curve can be the result of either a viscous or an elastic response of the material in the contact to the strain implied. The parameter that determines the actual response is the dimensionless grouping of the relaxation time of the material in the contact and the transit time of this material through the contact. For a simple Maxwell type material this number is known as the Deborah number and is given by;

$$De = \frac{\eta\, U}{a\, G} \qquad (5\text{-}1)$$

where η = viscosity of the fluid in the contact [Pa.sec]
U = transit velocity of fluid in the contact [m/sec]
a = semi contact length in rolling direction [m]
G = shear modulus of the fluid in the contact [Pa]

Now under the assumptions of a simple pressure distribution according to Hertz, a constant film thickness in the contact and a constant shear modulus over the contact area the initial small strain behaviour for the material will be elastic if the Deborah number is larger than 10 and will be viscous in response if the Deborah number is less than .1 . In between these two values the response is due to a mixed viscoelastic behaviour.

Many assumptions have been made before arriving at this point, however even with more complicated analyses where the pressure is allowed to influence the viscous and elastic properties it is found that the transition points occur at about the same Deborah numbers. Also for the range of parameters normally encountered in traction drives and testers the Deborah number is such that the initial slope of the traction curve is almost always governed by the elastic properties of the material in the contact. In the analysis of the data as performed here this assumption is implicit.

5-1-1 SHEAR MODULUS FOR CONSTANT PROPERTIES.

When the initial linear response is completely elastic it is quite easy to calculate the value for the actual modulus that caused this slope. Under the assumptions of constant properties throughout the contact this modulus can be extracted from the initial slope using the following equation;

$$G = \pi m \frac{P_o\, h}{4\, a} \quad [Pa] \qquad (5\text{-}2)$$

where m = initial linear elastic slope [-]

P_o = maximum Hertz pressure in the contact [Pa]

h = film thickness in the contact [m]

a = semi contact size in the rolling direction [m]

This equation is applicable regardless of whether the slope is measured under longitudinal slip or under side slip.

In Appendix II the results of the slopes from the experiments analyzed for modulus are indicated in the column labeled GB. Only the slopes from the spin free experiments were analyzed for shear modulus. These results were calculated with the isothermal value for the film thickness as indicated by H0 in this Appendix. The film thickness H0 was calculated from the expression for the central film thickness as reported by Hamrock and Dowson [32]. In order to modify the value of the shear modulus to allow for inlet shear heating the printed value under GB should be multiplied by the value of YI. Values for YI were calculated based upon the inlet shear heating theory of Wilson and Murch [33].

Examination of these results shows that there appears to be very little influence of pressure on the modulus. This is caused by the fact that some of the slope response is due to the creep compliance of the discs used to test the traction fluid.

5-1-2 SHEAR MODULUS WITH A SIMPLE COMPLIANCE CORRECTION.

One of the criticisms that is often raised at the above analysis is that it neglects the influence of the disk compliance on the measured slope. Disk compliance is the result of the elastic creepage of the disk material due to the tractive stresses on the surface. The traction response in the initial linear range is affected by this disk creepage in that it makes the slopes lower than if the discs were infinitely stiff. An exact correction of the modulus for the disc compliance is not possible at the moment. The analysis that is presented here is that due to Johnson and Roberts [8].

If we let m' be the slope of the traction curve for dry rolling bodies, then from the addition of the compliances of the discs and the film a simple corrective term for the shear modulus may be derived as shown in equation (5-3). From this expression it is obvious that when the measured slope approaches the dry slope the corrected value for the shear modulus tends to infinity.

$$G_c = G \frac{m'}{(m' - m)} \qquad (5\text{-}3)$$

where G_c = simple compliance corrected modulus

The dry slope m' can be calculated from the expression given by Kalker [27] as;

$$m' = \frac{G_s}{Q\,P_o} \qquad [-] \tag{5-4}$$

where G_s = shear modulus of the disc material [Pa]
Q = Kalker coefficient [-]

The value of the Kalker coefficient depends on the aspect ratio of the contact and the direction of slip. Below is a table which gives these values for the aspect ratios and tests as reported here.

Table of Kalker Coefficients Q

aspect ratio k	coefficient Q
1	.56
2	.70
5	.81

The fluid shear modulus as calculated by this method are indicated in Appendix II under the column GC. Again to modify this result for inlet shear heating it should be multiplied by the factor YI. From the results it may be observed that there is now a definite increase in the modulus as the contact pressure increases.

5-1-3 SHEAR MODULUS WITH A COMPLEX MODULUS CORRECTION.

Some of the drawbacks on the foregoing analysis are that we are still using the compliance of the total film and of the total disc system and then combining them for a correction term. A much more detailed compliance correction was developed by Johnson, Nayak and Moore [28] . These compliance corrections were based on the fact that elastic effects can only occur at high enough pressures, so that for a normal lubricated contact only a portion would be elastic in response, the remainder being viscous. Suitable charts for the correction term to be used with the simple modulus were presented for longitudinal slip and for an aspect ratio of 1 and a line contact. In using this data here we should be aware that the tests presented here are obtained under conditions of side slip only. The error introduced by this is expected to be about 40% for the contact aspect ratios as used here and this is based upon the simple dry slope ratios from Kalker's theory.

Since the correction factors are reported in graphical form a more suitable method based upon a correlation of the results will be used here. It may be expected that the new correction factors are an improved form of the 'simple correction term' as used in the previous section so that the basic form of the expression can be retained. From the shape of the curves this appears to be the case. By employing simple shift correction factors the following equation can be derived;

(5-5) $$G_j = G\left\{\frac{2.25-1.25C' + (.25C'-.2)/k}{C'-m/m' + (.25C'-.3)/k}\right\} \quad [Pa]$$

where C'= fraction of semi contact length under elastic response [-]
m = measured slope [-]
m'= dry calculated slope [-]
G_j= fully corrected modulus [Pa]
k = contact aspect ratio [-]

The fraction C' can be calculated from the assumption that no elastic effects occur if the viscosity is less than .1 MPa.s . With the knowledge of the pressure viscosity coefficient and assuming a Hertzian pressure distribution, C' can be calculated from;

(5-6) $$1 - C'^2 = \frac{Ln\ [100000/\ \eta(\theta)]}{\alpha(\theta)\ P_o}$$

where $\eta(\theta)$ = atmospheric viscosity [Pa.sec]
$\alpha(\theta)$ = pressure viscosity coefficient $[Pa^{-1}]$

The fluid shear moduli calculated by this technique are listed in Appendix II under the lable GJ. The value of C' is also indicated. Because of the nature of the expressions in equation (5-5) it is possible to get a negative value for the shear modulus from this analysis. When this was the case a zero value would be entered in the data column. From the results it can be seen that the magnitude of the modulus does increase but so does the amount of scatter. For the time being it is not recommended to use this method of shear modulus correction.

5-1-4 COMPLEX CORRECTION WITH REDUCED PRESSURE EFFECTS.

As discussed in Chapter 3 the assumptions of Hertzian pressure distributions in the contact area do not hold when a fluid film is present. Due to the hydrodynamic action the pressure distribution is more peaky. This will have an influence in the calculation of the elastic region C as used in the foregoing analysis. To estimate the influence of the reduced pressure the shear modulus was calculated along the previous method but with the reduced pressure in equation (5-6). The reduced pressure may be calculated from the pressure ratio as given below;

(5-7) $$P_r = 1 - 4\ G_e^{-.25}\ YI^{-3}\ e^{(-2.3/k)}$$

where G_e = Johnsons elasticity constant [-]
YI = Inlet shear heating factor [-]
k = aspect ratio (b/a) [-]
P_r = fraction of the theoretical Hertz pressure [-]

The reduced contact pressure is then the product of the Hertzian peak pressure times the pressure ratio. The results including this effect are presented in Appendix II in the column labled GP for the modulus and as CP for the semi elastic contact length. Also the reduced film thickness due to inlet shear heating was used. As can be seen from the results in Appendix II there is not a significant change in the value of C and CP and hence the influence of reduced pressure is not very strong on the modulus.

5-2 EXTRACTION OF THE LARGE STRAIN PARAMETERS.

The large slip region , that is the region beyond the traction peak, is exclusively governed by the dissipative element in the rheological equation. All the elastic effects have completely disappeared so that it is now quite easy to extract the governing parameters for this region. In essence what is required is a reverse analysis of the traction calculation normally used for the calculation of the traction curves. As we shall see only two parameters are truly required to fit this large strain region.

Of the five parameters shown in equation (3-13) , two derive from the simple fit of the atmospheric temperature viscosity data to the Vogels viscosity equation;

$$\eta(\theta) = V0\, e^{\frac{A}{(\theta+D)}} \qquad (5\text{-}8)$$

The constant B comes from the description of the Barus pressure viscosity relationship in the form;

$$\eta = \eta(\theta)\, e^{\frac{B\,P}{(\theta+D)}} \qquad (5\text{-}9)$$

This form can be directly derived from the Roelands equation for viscosity pressure. Table 5-1 shows the viscosity constants as used for the two fluids tested, together with the thermal parameters as used in (3-9) and (3-10). These constants remained the same throughout the analysis and prediction of the data.

	Santo50	TDF-88	Units
V0	1.69E-04	6.75E-05	[Pa.sec]
A	585	777	[°C]
D	75	84	[°C]
B	2.98E-06	2.98E-06	[°C/Pa]
k_s	15	15	[W/m°C]
k_f	.15	.15	[W/m°C]
ρ_s	7800	7800	[kg/m^3]
C_s	500	500	[J/kg°C]

Table 5-1 Fluid and roller material constants used in the analysis.

It remains therefore to find the constants E and C. These can be derived from the thermal region of the traction curve itself by curve fitting equation (3-13) to it. For this purpose it is better to write this equation in a slightly different form;

$$(5\text{-}10) \qquad \frac{\tau}{\theta+D} = \frac{1}{C}\left[\frac{A + BP}{\theta+D} + \text{Ln}\left(\frac{2\dot{\gamma} C E}{\theta+D}\right)\right]$$

For the temperature θ we will use the shear plane temperature θ_C as calculated by equation (3-9). From the above equation it is apparent that if this relationship holds then the results from the traction measurements should form a straight line when plotted in the above fashion. The slope of this line reflects the value for C while the intercept is indicative of the value for E.

In these calculations the shear strain rate is considered to be constant over the contact area and throughout the thickness of the film. Its magnitude is given by;

$$\dot{\gamma} = \Delta U/h \qquad [\text{sec}^{-1}]$$

where h = central filmthickness [m]

The central filmthickness is calculated from the expressions by Hamrock and Dowson [32]. Further modifications to this film thickness to allow for inlet shear heating were made by using the Wilson and Murch [33] approach.

5-3 ANALYSIS OF THE EXPERIMENTAL RESULTS.

From the experimental traction data the curves as selected in Chapter 2 were analyzed in the above fashion and the results plotted in Fig. 5-1 through 5-6. For the remainder of the traction curves the resulting values of E and C are shown in Appendix III under the columns E1,C1,R1 and E2,C2,R2. The difference between these constants is that the suffix '1' denotes isothermal inlet conditions while suffix '2' denotes the results with inlet shear heating effects. In each case a best fit value of C and E were selected and the corresponding R values indicate the regression coefficient obtained.

In order to reproduce the original traction curves we will need three separate and distinct constants (G,E,C). However if the values of C2 and E2 are examined in Figures 5-1 to 5-6, or in Appendix III it can be observed that for a given fluid these parameters do not change much. This suggest that more than one traction curve can be analyzed in the above fashion to get just one pair of values for a whole family of traction curves.

5-3-1 MULTIPLE TRACTION CURVE REGRESSION.

Multiple curve regressions were carried out for the groups of traction curves as shown in the report and the results are shown in Fig. 5-7 to 5-12. In each case it may be observed that the fit is reasonable. An even better fit can be obtained if those curves that have some asperity contact are left out. This was done for the results as reported in Fig.5-13 and 5-14. These two figures include all the traction tests for the two fluids as shown in Chapter 3 with the exception of those tests where some asperity contact took place. As can be seen from these two figures the degree of fit is remarkably good if we remember the fact that the traction tests were taken under such varying conditions of speed, aspect ratio, contact pressure and inlet temperature. This suggest that perhaps as few as two constants are required to describe the large strain traction region on a traction curve taken under any condition, provided that it is fully flooded. For partially flooded traction curves a different approach will be used.

6-0 TRACTION PREDICTION

We will now turn to the prediction of the traction traces that we have analyzed so far. There are several ways in which this can be done depending upon the source of our data. First we will compare the theoretical and experimental data based upon the constants as derived from the curves themselves. This serves to illustrate that the general shape of the experimental traction curves is adequately predicted by theory. This will be done for curves without and with spin.

Next we will restrict the prediction technique so that we will use only constants as fitted to a whole family of experimental traction traces. From the comparison of predicted with the experimental results we should be able to ascertain the validity of the fact that the non-linear traction constants E and C are common to all the traction curves and can therefore be thought of as being intrinsic to the fluid, at least for a good range of the experimental conditions. Again non spin and spin traction results will be examined.

Thirdly we will take the effect of asperity traction into account. In order to do that we require that the theoretical prediction technique be used to to correctly predict the fluid traction portion of the experimental data only. The difference between the fluid portion and the experimentally observed traction will be taken as the traction due to asperities in contact.

6-1 PREDICTION WITH INDIVIDUAL CONSTANTS.

To see the accuracy of the prediction technique with the elastic/plastic thermal method the first way to predict the traction traces is by using the very constants that were derived from them. For each trace this means the three fluid parameters of shear modulus, and the two parameters from the nonlinear thermal analysis. At this point it is possible to ignore the influence of asperity traction since this has gone into the constants that were obtained from the curves. To ignore this asperity traction is not correct however for the sake of comparison the starved traces are included here. Fig 6-1 and 6-2 show the experimental traction traces without starvation and in Fig 6-3 and 6-4 compare the predicted traces (continues lines) with the experimental results (symbols). These predictions are for the traces without spin. Fig 6-5 and 6-6 compare the theoretical traction traces with the experimental data for contacts under spin. All these predictions are based upon individual constants. The original experimental spin traction curves are shown in Fig 2-16 and 2-17. Similarly Fig 6-11 and 6-12 show the experimental traction traces that include some asperity contact. The comparisons between predicted and experimental traces for these are shown in Fig 6-13 and 6-14. The constants used in the prediction are listed under the trace numbers in Appendix II and III.

From the comparison the prediction technique appears quite successful with good fit in the initial traction region and in the nonlinear region. At larger slip the prediction of traction is above the experimental. The reason for this is thought to be that the disc temperature in the experimental traces increases with increasing slip. In the theoretical predictions however it is kept constant. The experimental traces will therefore show a lower traction than the theoretical. For further clarification on the various predictions and curve numbers see Table 6-2.

6-2 PREDICTION WITH MULTIPLE FITTED CONSTANTS.

That the predictions as described above give good predictions is more or less expected because otherwise there would be a serious fault in the analysis somewhere. However based upon the multiple curve fit that we did for the non-linear parameters it is tempting to use these for the theoretical predictions. This means that we would only have two non-linear constants for the entire traces as predicted in Fig. 6-3 ,6-4, 6-5 and 6-6. Also with this technique we can separate the asperity traction from the fluid traction by predicting what the traction for the particular conditions would have been based upon the fluid traction only. Comparison with the experimental traces allows us to separate the asperity traction as a function of the number of asperities in contact. The number of asperities in contact can be obtained directly from the voltage fraction from the experiments.

In order to use the theoretical prediction technique as outlined we will need a relationship for the dependency of the shear modulus on temperature and pressure. For the range of variables as shown in Fig 6-1 and 6-2 the modulus was fitted to the following expression;

(6-1) For Santo50: $G_c = .131 + .122\ P_o\ -.002\ \theta_o$ [GPa]
and TDF88 : $G_c = .077 + .061\ P_o\ -.0007\theta_o$ [GPa]

Also the non-linear constants were obtained from the curve fit shown in Fig. 5-13 and 5-14. These constants are;

(6-2) Santo50 : E2 =1.3557E-06 C2=2.803E-05
TDF88 : E2 =1.1402E-06 C2=3.108E-05

The comparison between experimental and predicted traction traces shown in Fig. 6-7, 6-8, 6-9 and 6-10 were based on these constants only. The accuracy in the prediction is very good especially if we consider that only two non-linear thermal and one isothermal constant are used for the entire prediction of the traces. This proves that the elastic/plastic thermal model is in fact adequate as a traction model. Further improvements could be made if for example a Roelands type viscosity pressure relationship were used and if some thermal allowance were made for the increase in the disc temperature with increasing slip. All in all though the prediction is very good keeping the simplicity of the model in mind.

6-3 THEORETICAL TRACTION PREDICTION WITH ASPERITY CONTACT.

So far we have only dealt with the fluid traction in the contact. We have carefully selected traces that were free of asperity contact for our data prediction However we know from the experimental results that asperity contact does occur under conditions of starvation where inadequate fluid is supplied to the inlet of the disc, or under conditions of high temperature and low speed where the film formation capability of the fluid is insufficient. With the help of the prediction technique for the fluid traction in the contact we can obtain the influence of the asperity traction for a given asperity contact condition.

The experimental traction curves that have varying degrees of asperity contact are shown in Fig. 6-11 and 6-12. The theoretically predicted traces by the method used in section 6-2 are shown in Fig 6-15 and 6-16. These traces are for the pure fluid traction only. Any difference between them and the experimental traces must be due to the asperity traction. This difference can be obtained by superimposing one curve on the other and measuring the average difference between the two traces. It would be expected that only some average difference can be obtained in this way. The table below gives these averaged differences for the sets of traction traces.

Asperity Traction for TDF88			Asperity Traction for Santo50		
Volt. Fract. (-)	Fz (N)	Asp. Tract. (N)	Volt. Fract. (-)	Fz (N)	Asp. Tract. (N)
.75	600	13.5	.78	600	18.5 *
.8	600	13.5	.68	600	11.9
.8	600	10.4	.85	600	8.5
.91	600	6.1	.86	1200	18.6 *
.85	800	6.0	.69	1000	13.2
.94	400	6.5	.96	600	3.9
.69	1000	9.3 *	.94	400	3.4
			.85	400	4.5

Table 6-1: Asperity traction forces for the traction curves shown in Fig. 6-11 and 6-12. The items with a '*' were not included in the final correlation.

Figures 6-21 a,b below show the results from this table in a more direct form.

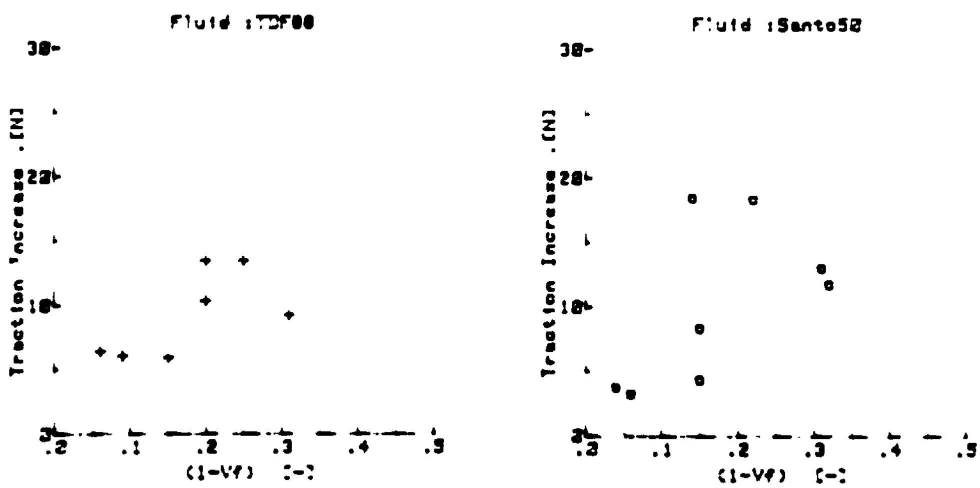

Fig 6-21a,b: Relationship between traction increase due to asperity contact and the contact fraction for TDF88 and Santo50.

6-3-1 ANALYSIS OF THE ASPERITY TRACTION.

From the results in the table it can be seen that the amount of extra traction resulting from the asperity contact is roughly proportional to the contact fraction.

This contact fraction is given by;

(6-3) $C_f = 1 - VF$

where VF = Voltage fraction of the film

This voltage fraction is measured for each experiment and is an indication of the the separation of the discs. The contact fraction C_f is a direct indicator of the number of asperities that are in contact. Leather et al [29] shows that the average number of contact points is related to the contact fraction as follows;

(6-4) $f = C_f / (1 - C_f)$

when we are dealing with a rolling/ sliding circular contact. At small values of C_f we see that the number of asperity contacts is directly proportional to the contact fraction. Even at values of $C_f = .2$ the error in assuming linearity is only 25%

The other point that we need to address is the relationship between asperities in contact and the traction increase that results from this. For the theory of asperity contact by Greenwood and Williamson [30] the surface roughness is assumed to be Gaussian in its height distribution and in its peak distribution. For this form of distribution they showed the following for the contact of asperities between dry surfaces;

i) the number of contacts is proportional to the load.
ii) the average contact area per asperity is load independent.
iii) the average pressure per asperity is load independent.

We will assume that conditions ii) and iii) hold even for lubricated contacts. Condition i) is not applicable here because the load is not only carried by the asperities but by the fluid film as well. We will however assume that all the load is carried by the film so that the number of asperities in contact will have no influence on the local pressure in the contact. Even though the averages of the asperity contact pressure and the areas are constant for surfaces with Gaussian roughness distribution it is possible that the larger contact areas predominate in the traction response. Also the traction from the asperities will depend on the shear behaviour of the material at the asperities. This material could be some traction fluid trapped under the asperity contact itself, forming a micro traction contact, or it could be some solid material such as some boundary lubrication additive or perhaps even the disc material itself.

The implications of these two possibilities are quite different for a traction contact and it is important for us to establish which mechanism predominates. The two possible forms of asperity traction can be stated in the following two hypotheses;

I) : the increase in <u>traction force</u> is proportional to the number of contacts or,

II) : the increase in traction coefficient is proportional to the number of contacts.

We shall use the experimental data to test the two hypotheses and establish which is the more correct form to use. We can do this by fitting straight line relationships to the actual asperity traction data and observing the degree of fit obtained. The equations that will be used are as follows;

(6-5) for hypothesis I) : $F_y(\text{asperity}) = f * C3$

„ „ „ II) : $F_y(\text{asperity})/F_z = f * C3$

Testing the two hypotheses on the asperity traction data we obtain the following results;

	Santo50			TDF88		
	R^2	F	C3	R^2	F	C3
For hypothesis I) :	.39	4.5	25	.56	7.5	23
For hypothesis II) :	.41	4.8	.033	.2	1.5	.023

Where R^2 is the square of the regression coefficient and F is numerical value for the 'F' test used in statistics, see for example Draper and Smith [31]. It is not very clear from these values which of the hypotheses are correct. In both cases however the degree of fit indicated is very low. This can be corrected somewhat by eliminating some outstanding data points. After eliminating the points indicated by a star (*) in Table 6:1 we obtain the following results;

	Santo50			TDF88		
	R^2	F	C3	R^2	F	C3
For hypothesis I) :	.89	43	24	.85	28	37
For hypothesis II) :	.71	12	.028	.64	9	.055

The above values now clearly favour hypothesis I) over II). Furthermore the dependence of the asperity traction seems pretty nearly independent of the type of fluid in the contact. This suggests that we are dealing with the traction due to some common material in both cases such as an additive or perhaps even the disc materials themselves. Lumping all the asperity traction data together results in the following values;

Hypothesis I) :	$R^2 = .75$	F=32	C3=25
Hypothesis II) :	$R^2 = .46$	F=9	C3=.03

Again hypothesis I) is clearly more plausible than II). From this analysis the dependence of asperity traction on the contact fraction is given by;

(6-6) $F_y(\text{asperity}) = (1-VF)/VF * 25$ (N)

The overall degree of correlation between this expression and the experimental results may be observed from Fig. 6-22 .

Expression (6-6) can now be used in the prediction of the traction curves which have a significant amount of asperity contact in them. The asperity traction should be added in as a proportion of the plastic traction, ie. when all the traction is due to complete plastic like slip in the contact then the full amount of asperity traction is added in. On the other hand when the contact traction is solely due to elastic effects the fact that asperities are in direct contact does not result in a higher traction,. The reason for this is that the initial traction slope is mostly due to the elastic creep of the disc material and so the elastic deformation of the asperities in contact would be the same as the remainder of the roller material in the contact. Not until actual sliding of one asperity past another occurs will the effect of asperity contact reveal itself in an increased traction. In fact it is entirely conceivable that for very rough surfaces in dry contact the effect of asperity contact is one whereby the initial elastic slope is lower than when the surfaces are smooth.

Fig. 6-17 to 6-20 compares the predicted with the experimental traction curves with the asperity traction included. The agreement between theory and experiment is very good in most cases, considering the rather simple modeling that is used here.

FIGURES SHOWING BASIC EXPERIMENTAL DATA				FIGURES SHOWING THE COMPARISON WITH PREDICTED.		
Fig. #	Fluid name	Spin	Starved /flooded	Fitted Constants.	Fixed Constants.	Including asp. traction
6-1	TDF88	none	flooded	6-3	6-7	N/A
6-2	Santo50	none	flooded	6-4	6-8	N/A
2-16	TDF88	yes	flooded *	6-5	6-9	6-19
2-17	Santo50	yes	flooded *	6-6	6-10	6-20
6-11	TDF88	none	starved	6-13	6-15	6-17
6-12	Santo50	none	starved	6-14	6-16	6-18

*** Partially starved results**

Table 6-2: Comprehensive overview of the figure numbers showing the experimental and predicted data.

7-0 CONCLUSION

Ultra high speed traction tests were perf .med on two traction fluids commonly employed. The range of the tests variables were; contact pressure from 1 to 1.8 GPa, disc surface velocity from 50 to 120 m/sec, fluid inlet temperature from 50 to 120 'C , contact spin from 0 to 1.5% and inlet fluid supply from fully flooded to fully starved. A total summary of all the traction tests performed may be found in Appendix I. The resulting traction curves were reduced to three constants by using the Johnson and Tevaarwerk isothermal traction model coupled to a thermal correction technique for large slip and spin results. The three constants are the elastic shear modulus and two non linear thermal parameters and are reported in Appendix II and III.

Theoretical traction predictions were performed for a representative number of curves that showed the influence of rolling velocity, of contact pressure and of aspect ratio. To establish the accuracy of the thermal model the predictions were performed with increasing levels of independence of experimentally determined parameters. In the final resulting prediction only two non linear thermal parameters were used for the prediction of 15 different traction curves covering the entire range of variables as used in the investigation, with the exception of the influence of asperity traction. Comparison of these theoretical curves and corresponding experimental traces show very good agreement, in support of the Johnson and Tevaarwerk modified thermal model.

The influence of asperity traction was extracted from the experimental curves with starvation by predicting the traction under fully flooded conditions and using the difference to predict the asperity traction as a function of the number of asperities in contact. It was found that the amount of traction force per asperity in contact was pretty well independent of the traction contact conditions and also of the traction fluid. Comparison between theoretically predicted traction curves including the effect of asperity traction and experimental curves shows reasonable agreement.

It is felt that the degree of success that is shown by the theoretical predictions can be further improved upon by using the Roelands pressure viscosity equation and also by making allowance for the rising temperatures of the traction discs as slip increases. This will introduce one more disposable constant for the fundamental fluid traction data however it will result in an improved prediction of traction.

8-0 REFERENCES

[1] Loewenthal, S. H., " A Historical Perspective of Traction Drives and Related Technology ". Advanced Power Transmission Technology. G.K. Fisher, ed., NASA CP-2210, 1983.

[2] Clark, O.H., Woods, W.W. and White, J.R. "Lubrication at Extreme Pressure with Mineral Oil Films". J. Appl. Phys., 22 , (1951), #4, pp. 474-483.

[3] Hewko, L.O., "Contact Traction and Creep of Lubricated Cylindrical Rolling Elements at Very High Surface Speeds". ASLE Trans., 12 , (1969), pp. 151-161.

[4] Smith, F.W. "Rolling Contact Lubrication-The Application of Elasto hydrodynamic Theory". Trans . Am. Soc. Mech. Engrs. 87 , (1965), Series D, p. 170 .

[5] Smith, R.L., Walowit, J.A. and McGrew, J.M. "Elastohydrodynamic Traction Characteristics of 5P4E Polyphenyl Ether". J. Lubr. Technol. Trans. ASME., 95 , (1973), pp. 353-362.

[6] Johnson, K.L. and Cameron, R. "Shear Behaviour of Elastohydrodynamic Oil Films at High Rolling Contact Pressures" Proc. Inst. Mech. Eng. (London), 182 , pt. I, #14, 1967, pp. 307-319.

[7] Niemann, G. and Stoessel, K. "Reibungszahlen bei elasto-hydrodynamisher Schmierung in Reibrad- und Zahnradgetrieben". Konstruktion, 23 , #7, (1971), pp. 245-260.

[8] Johnson, K.L. and Roberts, A.D. "Observations of Viscoelastic Behaviour of an Elastohydrodynamic Lubricant Film". Proc. Roy. Soc. (London), Series A, 337 , #1609, (1974), pp. 217-242.

[9] Johnson, K.L. and Tevaarwerk, J.L. "Shear behaviour of Elastohydrodynamic Oil Films". Proc. Roy. Soc. (London), Series A, 356 , #1685, (1977), pp. 215-236.

[10] Daniels, B.K. "Non-Newtonian thermo-viscoelastic EHD Traction from combined slip and spin" ASME Preprint 78-LC-2A-2. ASLE/ASME Lubrication Conference, Minneapolis, Minnesota, October 24-26,1978.

[11] Hirst, W. and Moore, A.J. "The effect of temperature on traction in elastohydrodynamic lubrication". Phil. Trans. Roy. Soc. of London, Sept. 1980, Series A, 298 , #1438, pp. 183-208.

[12] Alsaad, M., Bair, S., Sandorn, D.M. and Winer, W.O. "Glass Transition in Lubricants: Its Relation to Elastohydrodynamic Lubrication"., J. Lubr. Technol. Trans. ASME, 100 , (1978) pp. 404-417.

[13] Johnson, K.L., "Introductory Review of Lubricant Rheology and Traction". Proc. of the Leeds-Lyon Conference, Leeds 1978, pp. 155-161.

[14] Tevaarwerk, J.L. "Traction Drive Performance Prediction for the Johnson and Tevaarwerk Traction Model". NASA TP-1530 ,(1979).

[15] Magi, Mart, "On Efficiencies of Mechanical Coplanar Shaft Power Transmissions". Chalmers University of Technology, Gothenburg, (1974).

[16] Tevaarwerk, J.L. "A Simple Thermal Correction for Large Spin Traction Curves" J. Mech. Design. Trans. ASME., 103 , #2, (1981), p440.

[17] Tevaarwerk, J.L. "Thermal Influence on the Traction behaviour of an Elastic/Plastic model" Proc. of the Leeds-Lyon Conference, Leeds 1980, pp. 302-309.

[18] Loewenthal, S,H., Anderson, N.H. and Nasvytis, A.A. "Performance of a Nasvytis Multiroller Traction Drive." NASA TP-1378, (1978).

[19] Kemper, Y. "A High Power Density Traction Drive", SAE Paper 790849, (1979).

[20] McCoin, D.K. and Walker, R.D. "Design study of continuously variable roller cone traction CVT for Electric Vehicles", NASA CR-159841, Sept., 1980.

[21] Tevaarwerk, J.L. "Traction Contact Performance Evaluation at High Speeds". NASA CR-165226, Sept., 1981.

[22] Conry,T.F., Johnson,K.L. and Owen,S. "Viscosity in the Thermal Regime of Traction". Proc. of the Leeds-Lyon Conference, Lyon 1979, pp. 219-227.

[23] Johnson,K.L., and Greenwood, J.A. "Thermal Analysis of an Eyring fluid in EHL Traction", Wear, 61 (1980), p 353.

[24] Tevaarwerk, J.L. and Johnson, K.L. "The Influence of Fluid Rheology on the Performance of Traction Drives", J. Lubr. Technol. Trans. ASME., 101 , (1979), p 266.

[25] Tevaarwerk, J.L. "Traction Calculations using the Shear plane Hypothesis" Proc. of the Leeds-Lyon Conference, Lyon 1979, pp. 201-213.

[26] Tevaarwerk, J.L. "Traction in Lubricated Contacts ". Proc. of the Int. Symposium on Contact Mecnanics and Wear of Rail/Wheel systems. Vancouver 1982

[27] Kalker, J.J. "On the Rolling Contact of Two Elastic Bodies in the Presence of Dry Friction". Ph.D. Dissertation, Technische Hogeschool, Delft, 1967

[28] Johnson, K.L., Nayak, L. and Moore, A.J. "Determination of Elastic Shear Modulus of Lubricants from Disc Machine Tests". Proc. of the Leeds-Lyon Conference, Leeds 1978, pp. 204-208.

[29] Leather, J.A. and McPherson, P.B, "The Practical use of Electrical Measurements in Lubricated Contacts", Proc. of the Leeds-Lyon Conference, Lyon 1977, pp. 155-162.

[30] Greenwood, J.J. and Williamson, J.P.B., "The Contact of nominally flat Rough Surfaces", Proc. Roy. Soc. A, 295 , p300, 1966.

[31] Draper, N.R. and Smith, H. Applied Regression Analysis. John Wiley and Sons, Inc. 1981.

[32] Hamrock, B.J. and Dowson, D., "Isothermal Elastohydrodynamic Lubrication of Point Contacts, Part III - Fully Flooded Results." , J. Lubr. Technol. Trans. ASME., 99 , (1977), #2, pp. 264-276.

[33] Murch, L.E. and Wilson, W.R.D. , " A Thermal Elastohydrodynamic inlet zone analysis." , J. Lubr. Technol. Trans. ASME. , 97 , (1975), #2, p212.

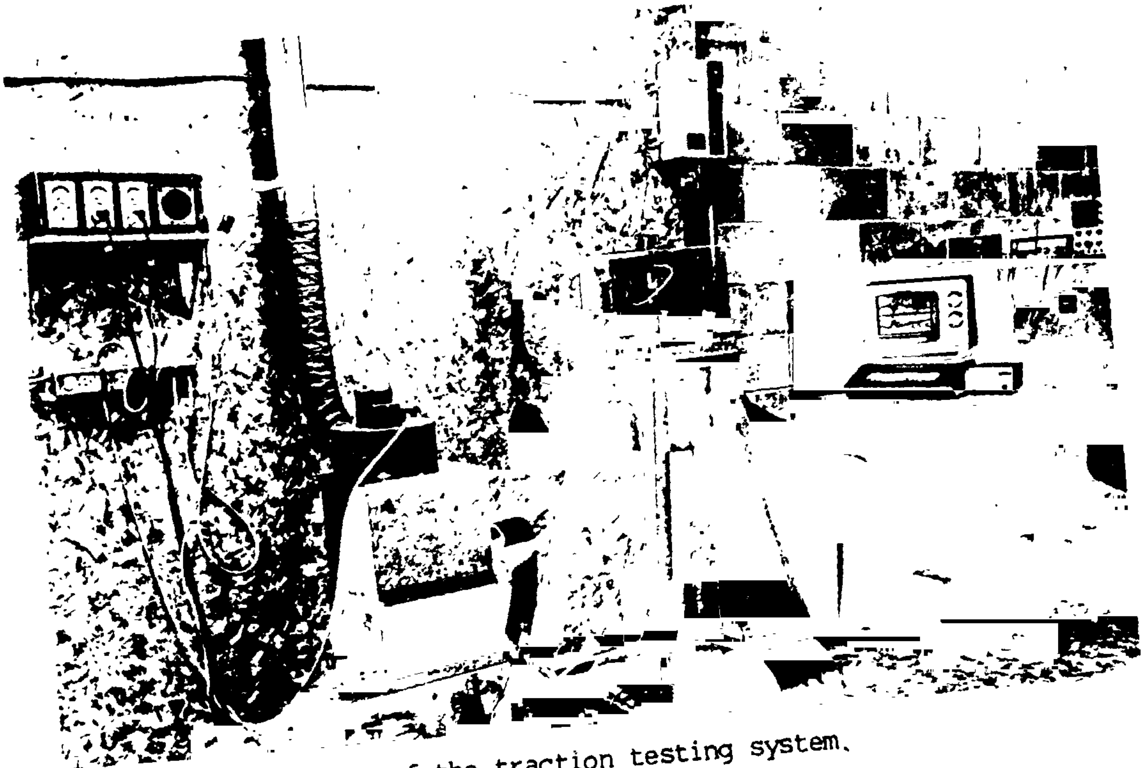

Fig. 2-1: Overview of the traction testing system.

Fig. 2-2: Overview of the Microcomputor Datalogger system used for the traction tests.

Fig. 2-3a: Overview of the actual traction tester (LHS).

Fig. 2-3b: Close-up view of the traction tester (LHS).

ORIGINAL PAGE IS
OF POOR QUALITY

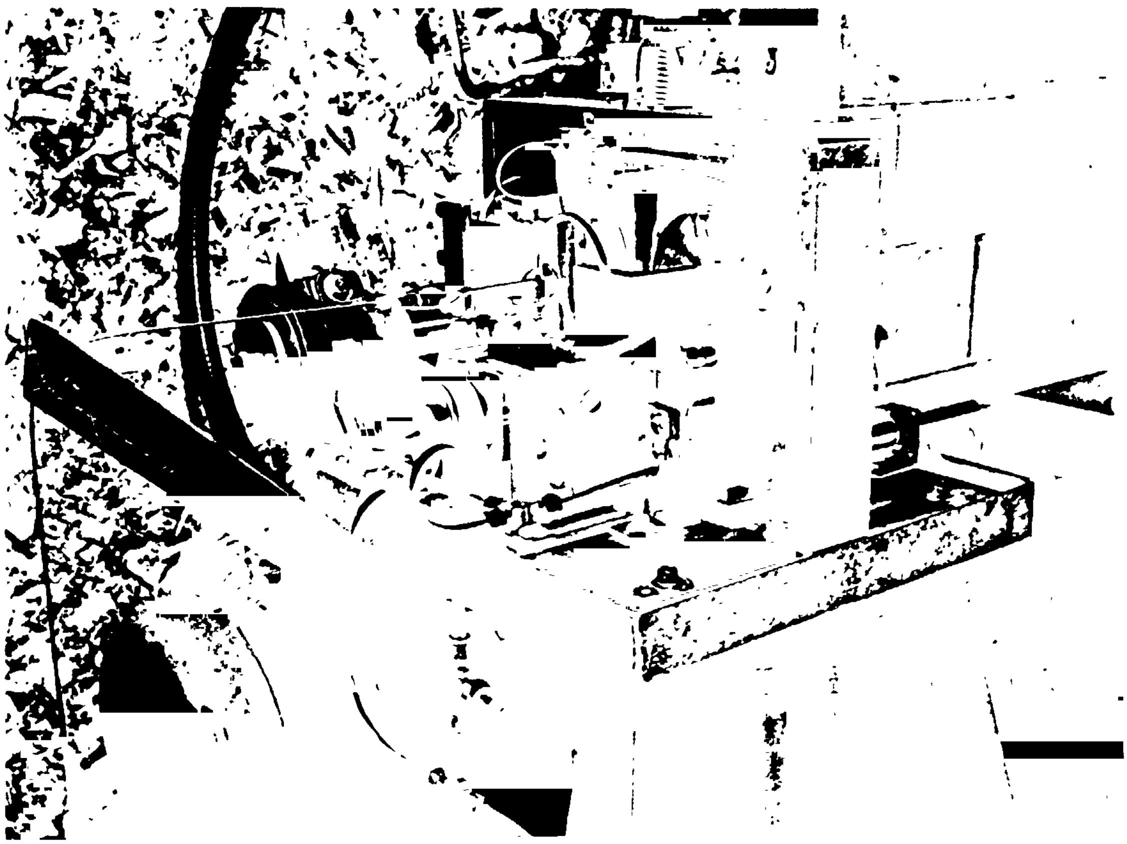

Fig. 2-3c: Overview of the actual traction tester (RHS).

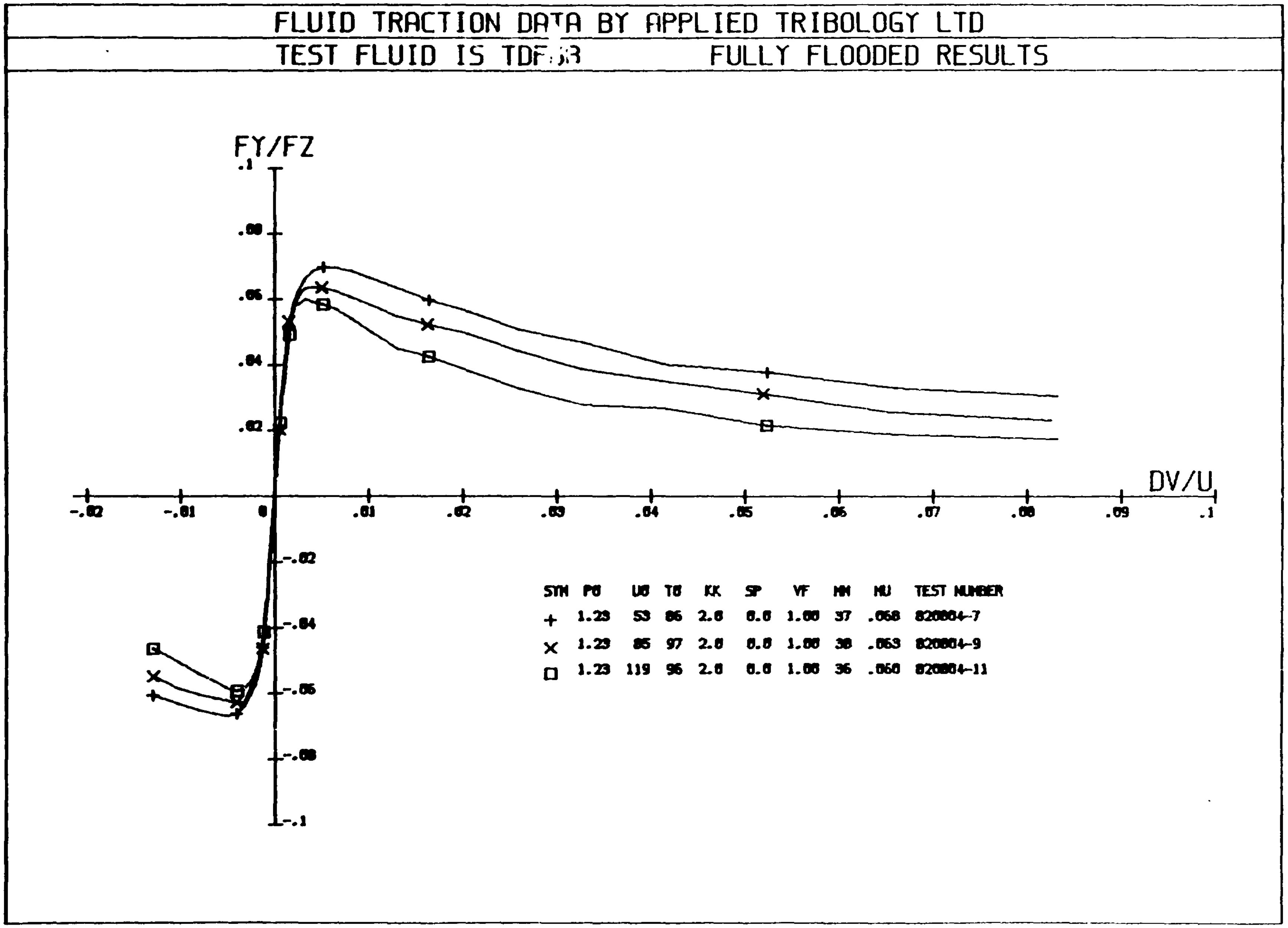

Fig. 2-4 Experimental traction results for TDF88. Flooded results for increasing speed.

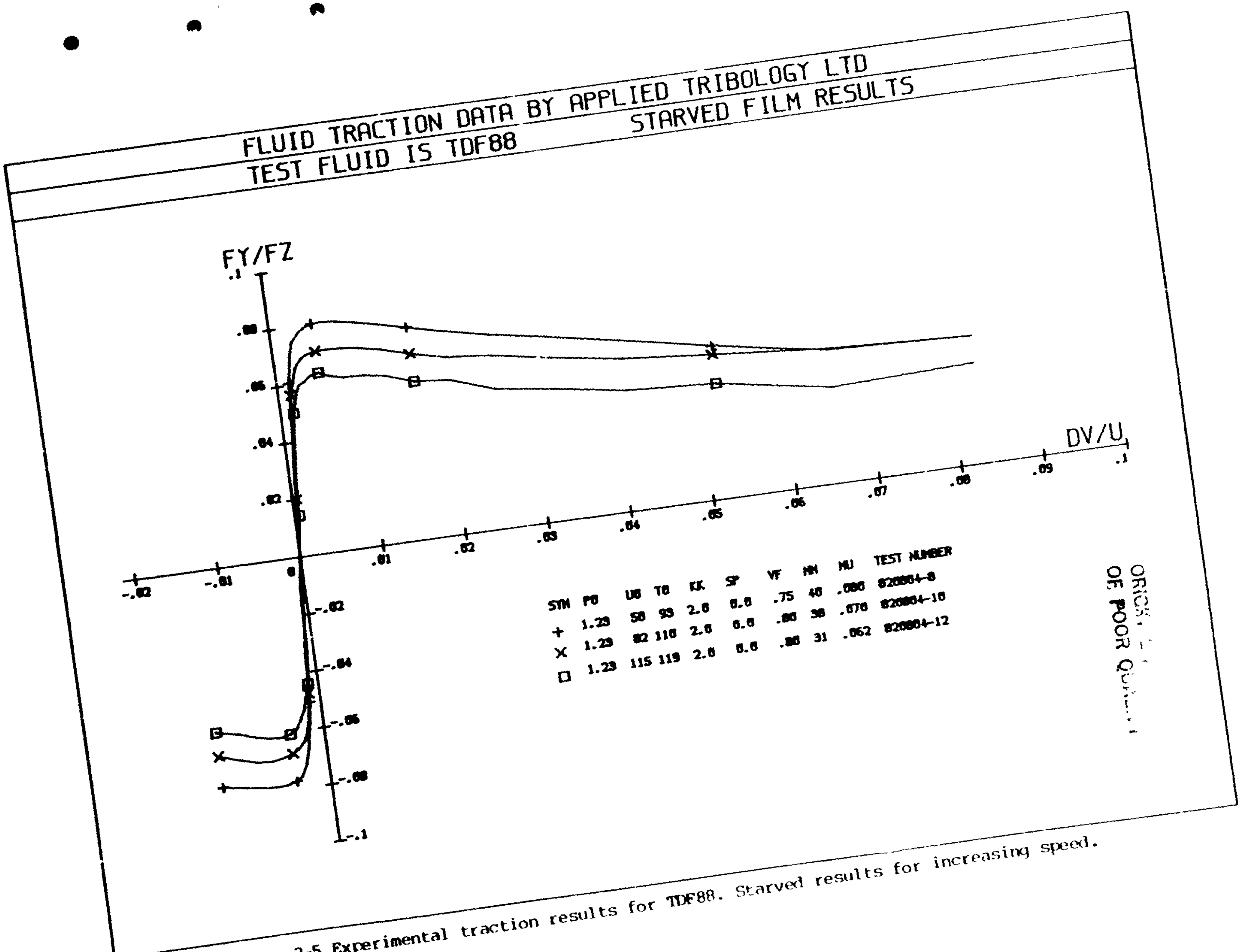

Fig. 2-5 Experimental traction results for TDF88. Starved results for increasing speed.

ORIGINAL PAGE IS
OF POOR QUALITY

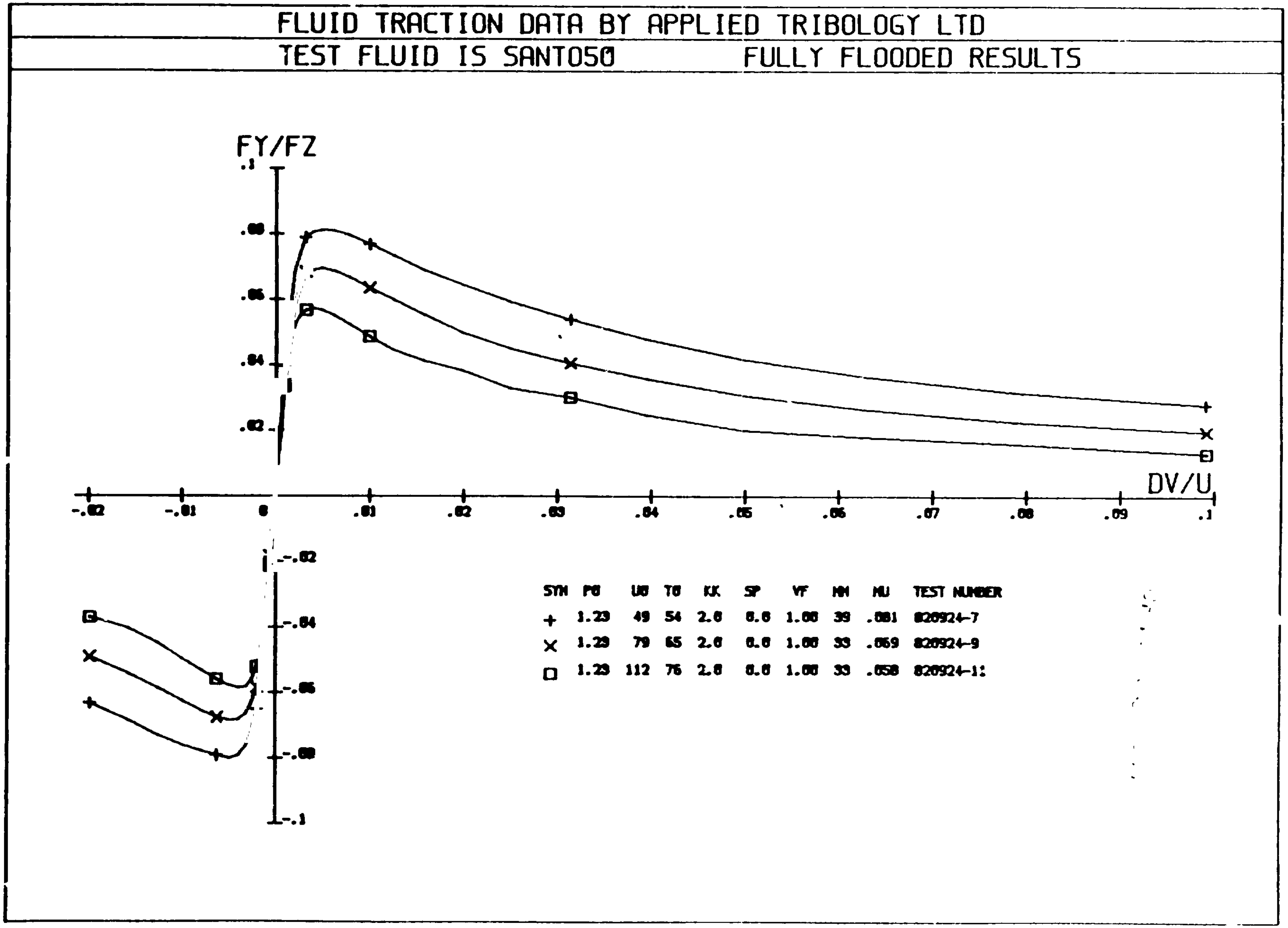

Fig. 2-6 Experimental traction results for SANTO50. Flooded results for increasing speed.

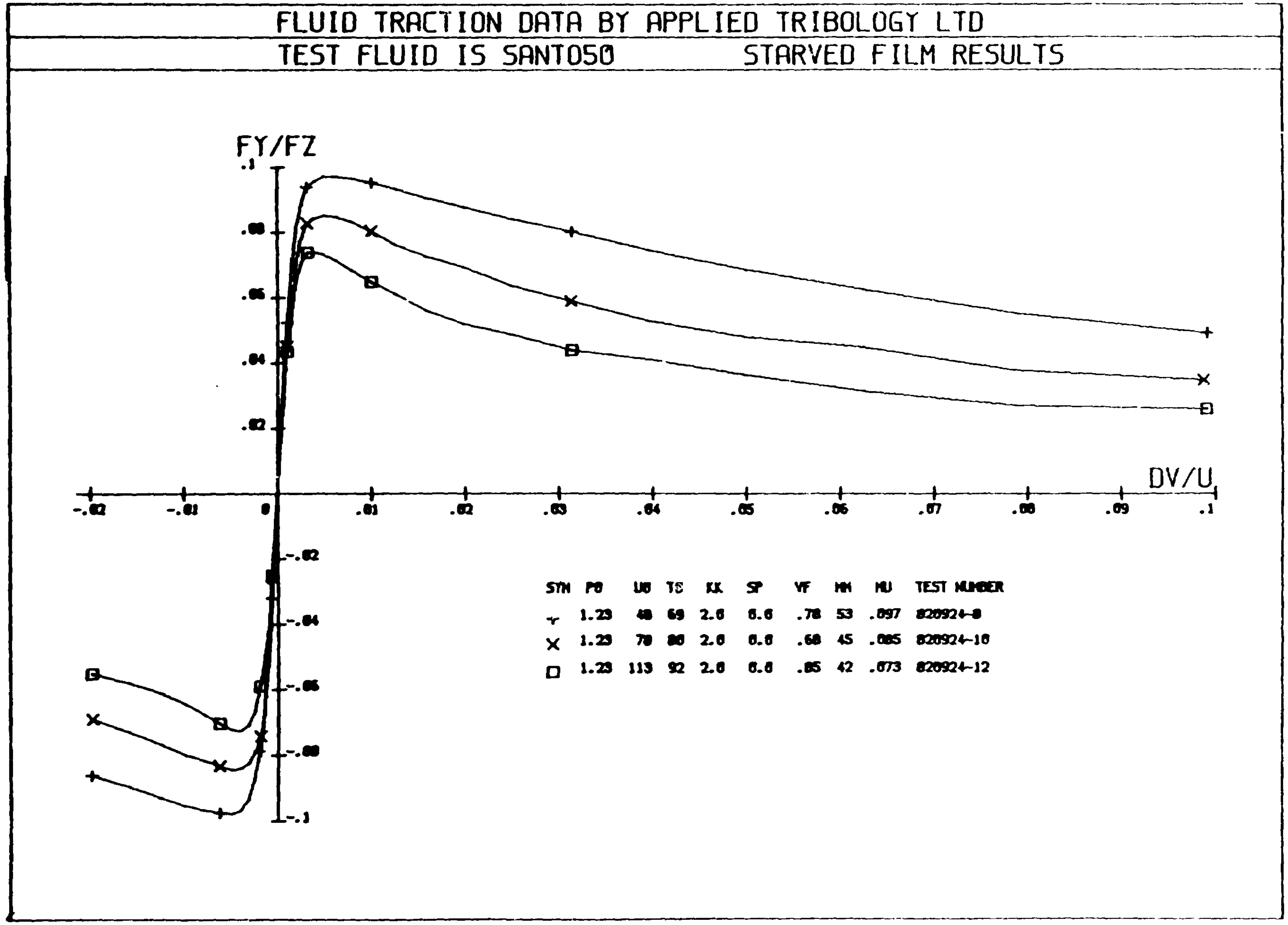

Fig. 2-7 Experimental traction results for SANTO50. Starved results for increasing speed.

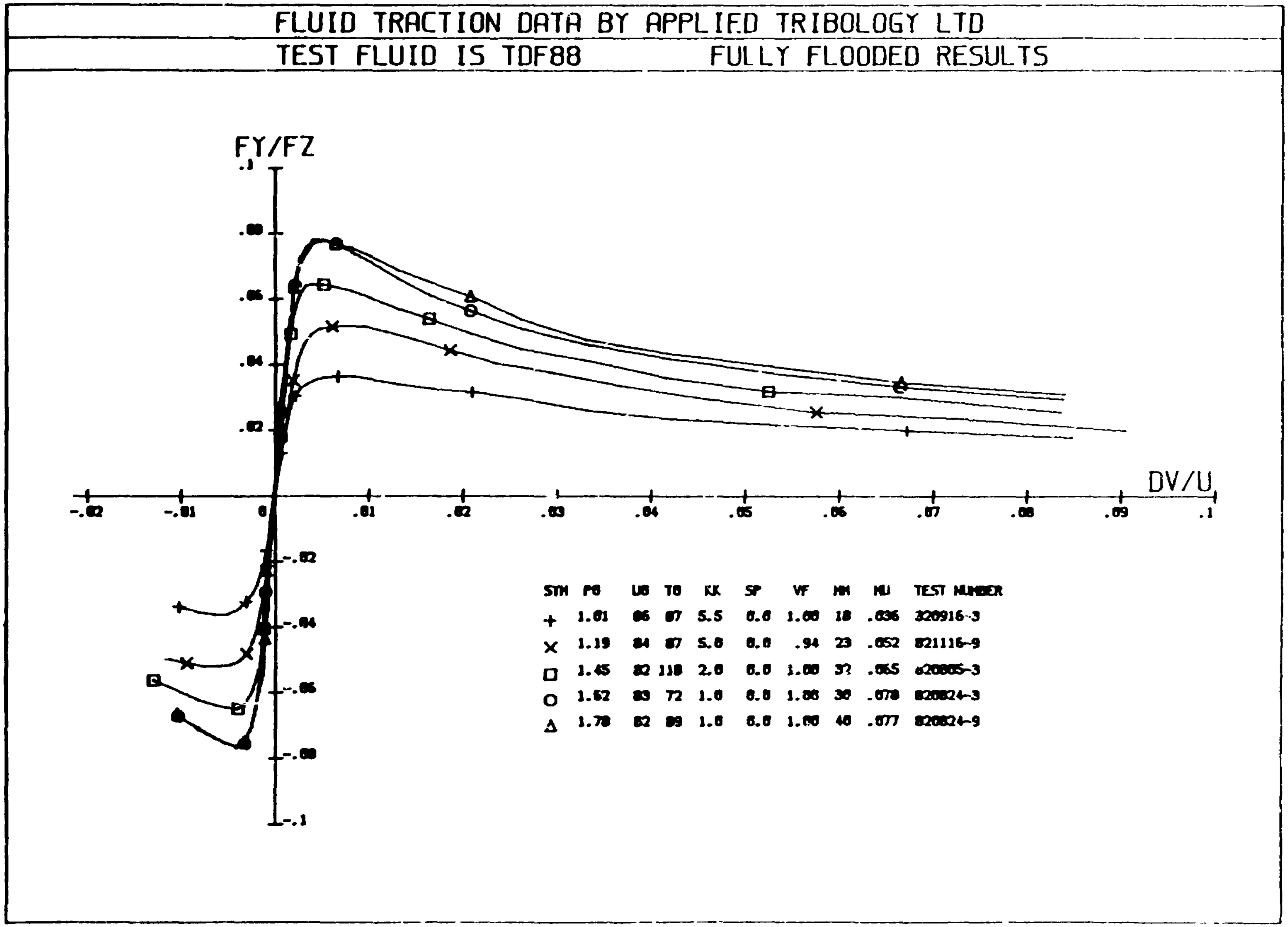

Fig. 2-8 Experimental traction results for TDF88. Flooded results for increasing pressure.

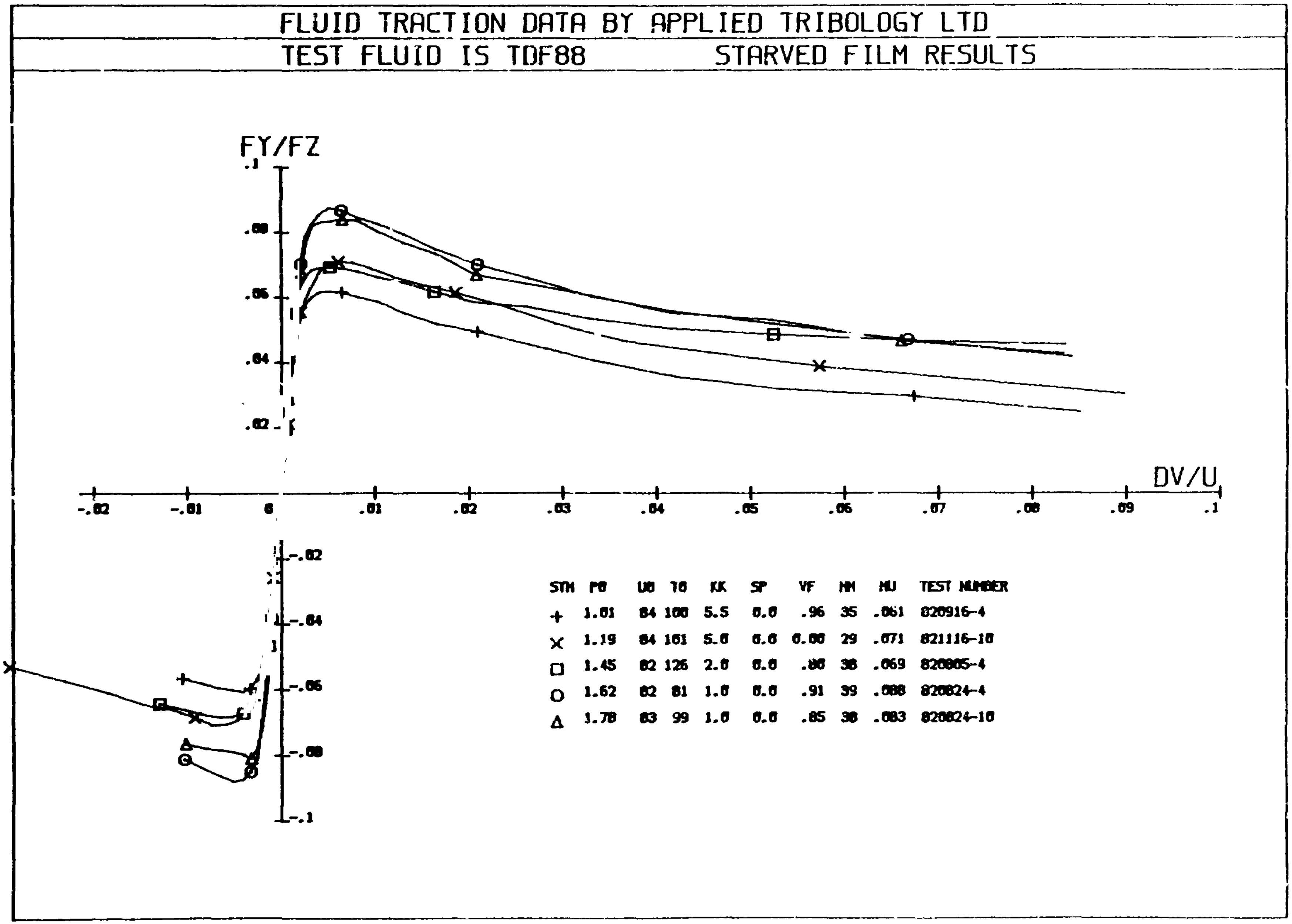

Fig. 2-9 Experimental traction results for TDF88. Starved results for increasing pressure.

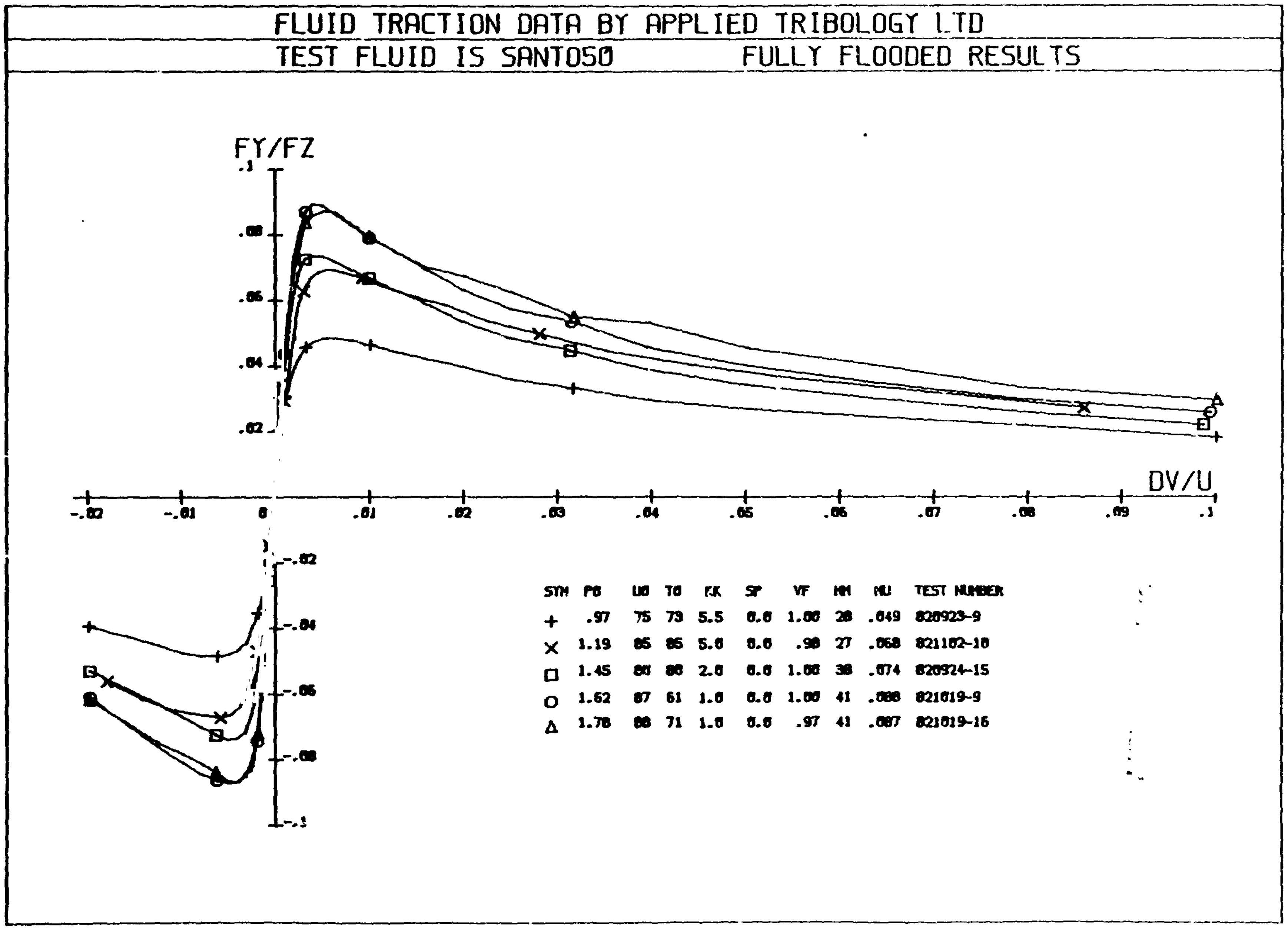

Fig. 2-10 Experimental traction results for SANTO50. Flooded results for increasing pressure.

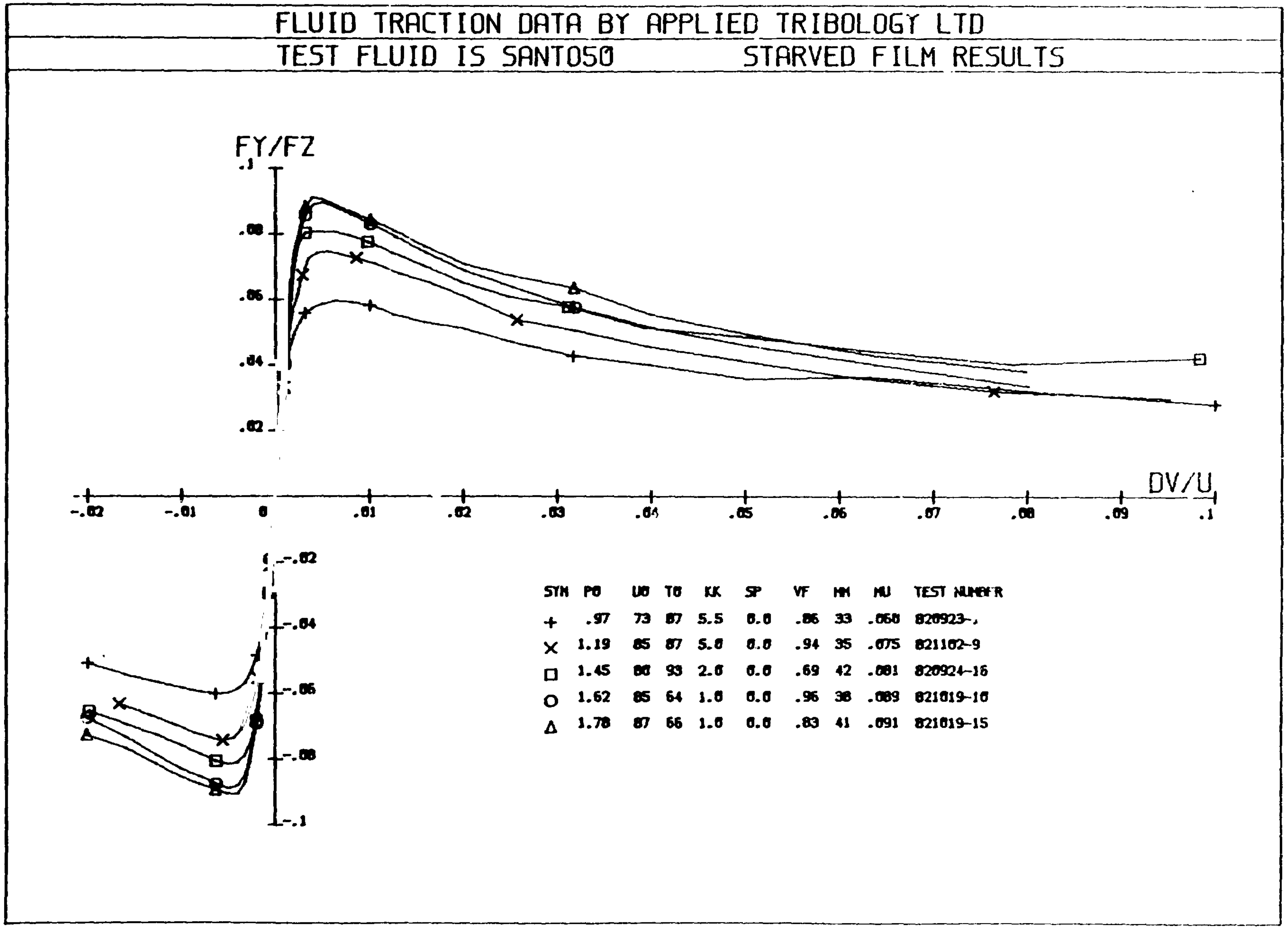

Fig. 2-11 Experimental traction results for SANTO50. Starved results for increasing pressure.

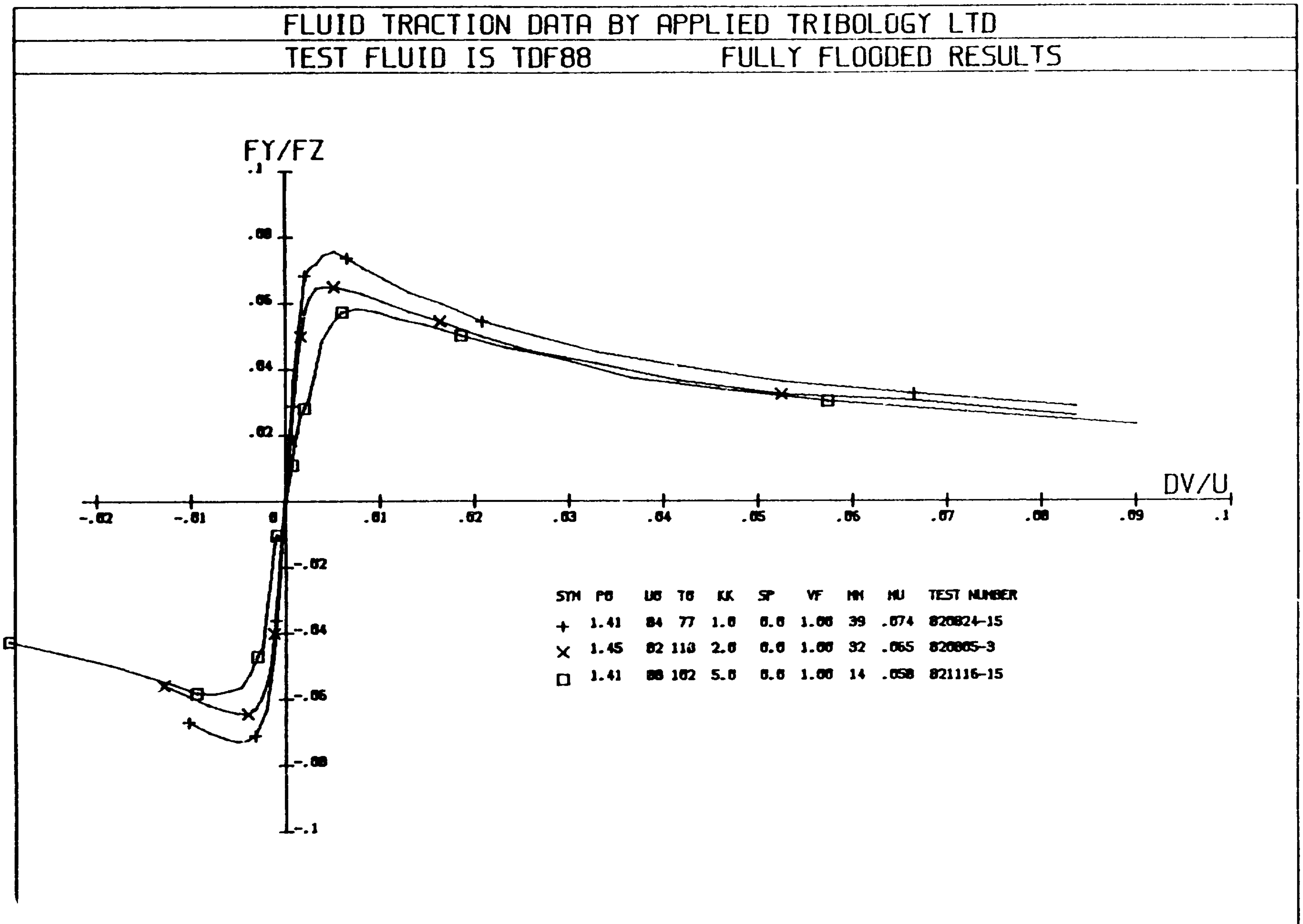

Fig. 2-12 Experimental traction re..'ts for TDF88. Flooded results for increasing aspect ratio.

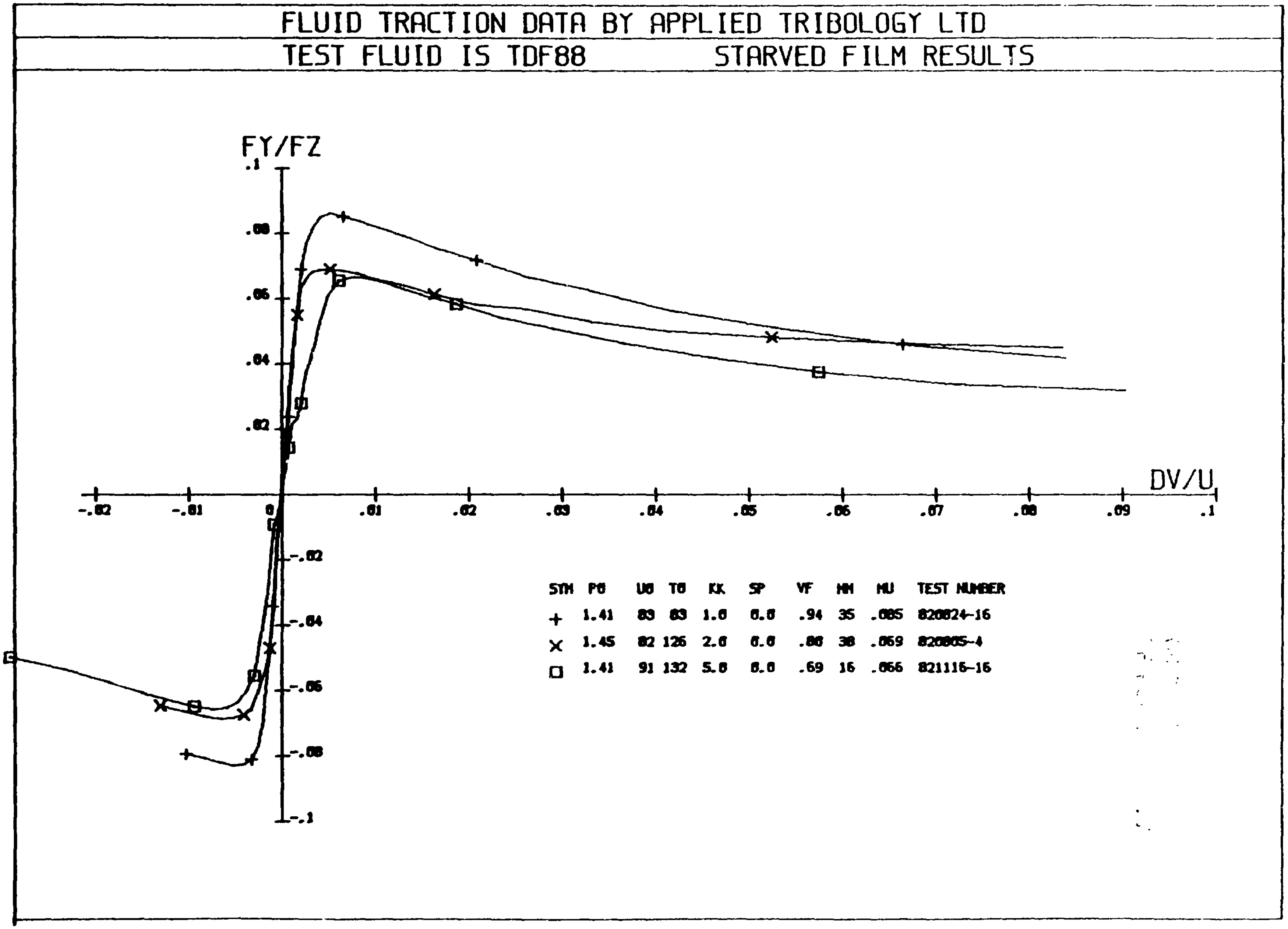

Fig. 2-13 Experimental traction results for TDF88. Starved results for increasing aspect ratio.

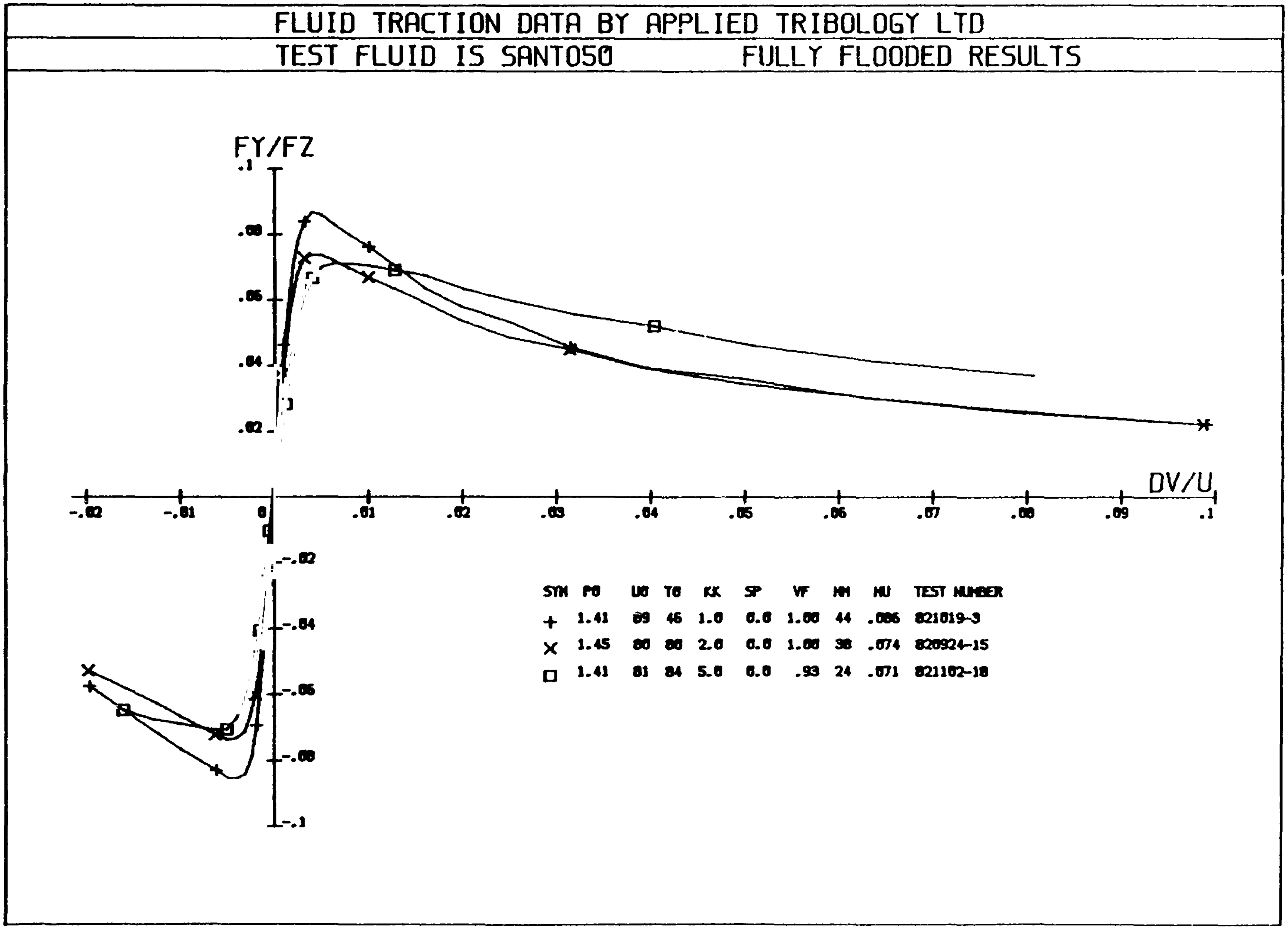

Fig. 2-14 Experimental traction results for SANTO50. Flooded results for increasing aspect ratio.

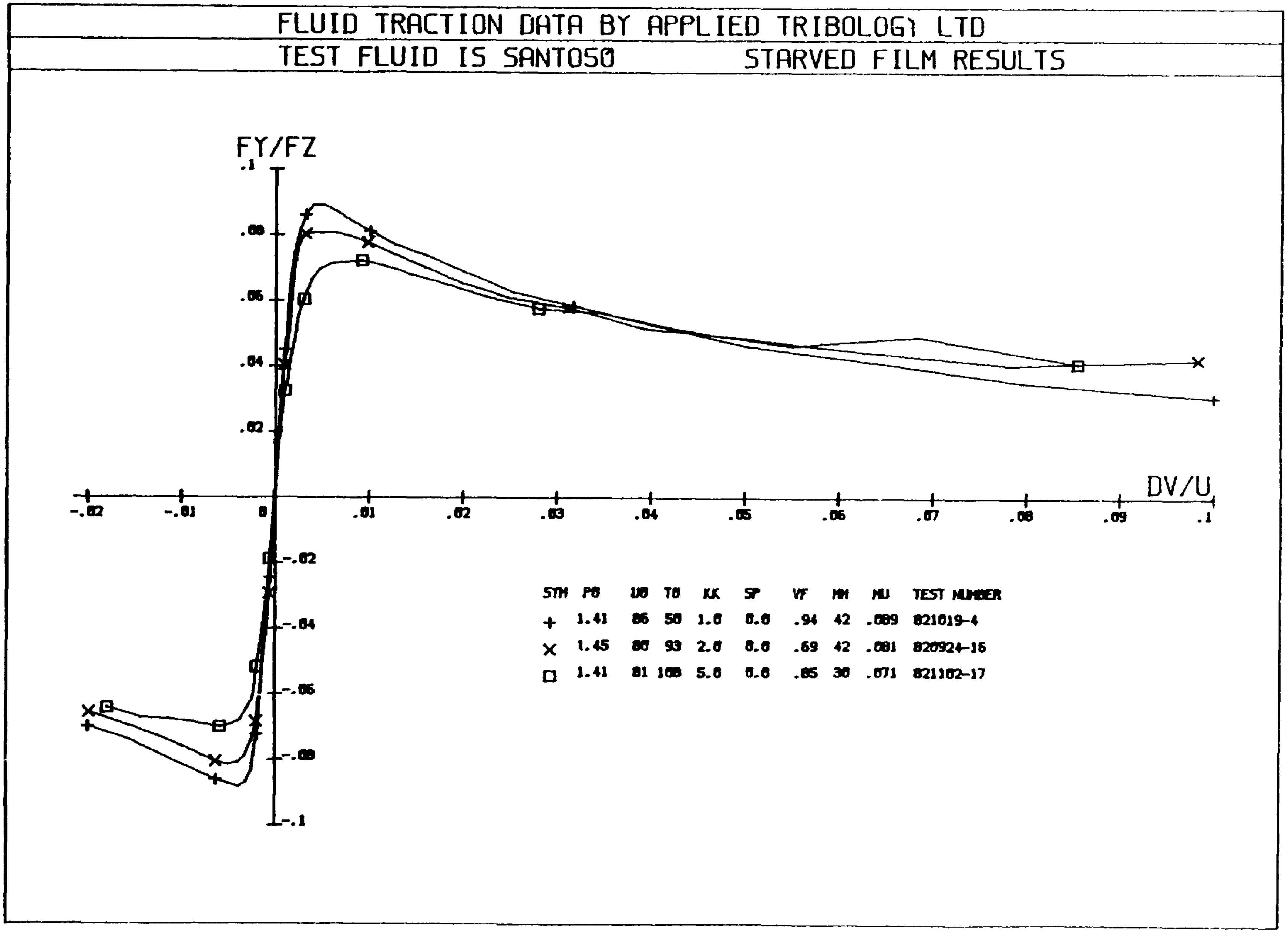

Fig. 2-15 Experimental traction results for SANTO50. Starved results for increasing aspect ratio.

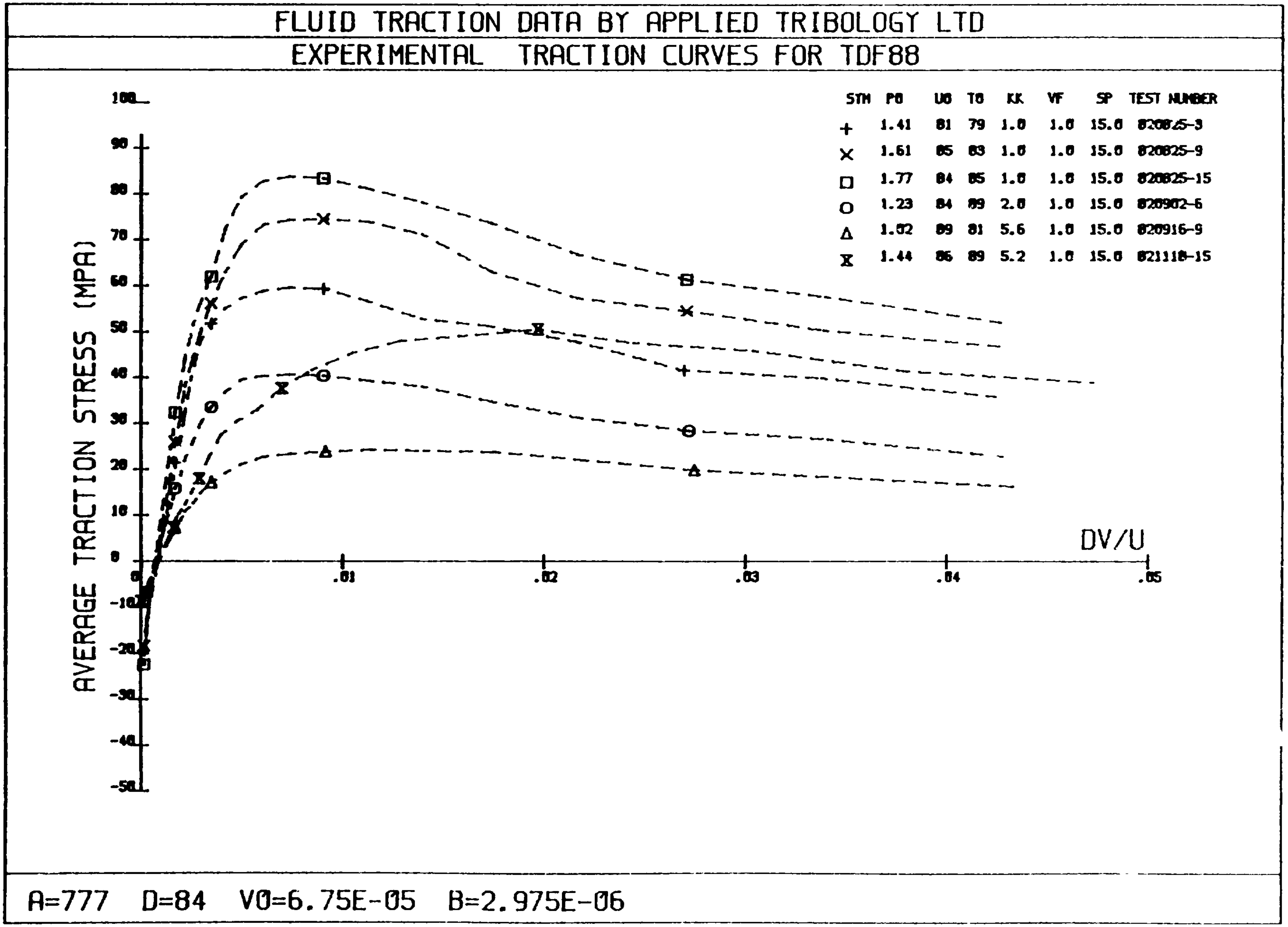

Fig. 2-16 Experimental traction results for TDF88. Spin traction curves

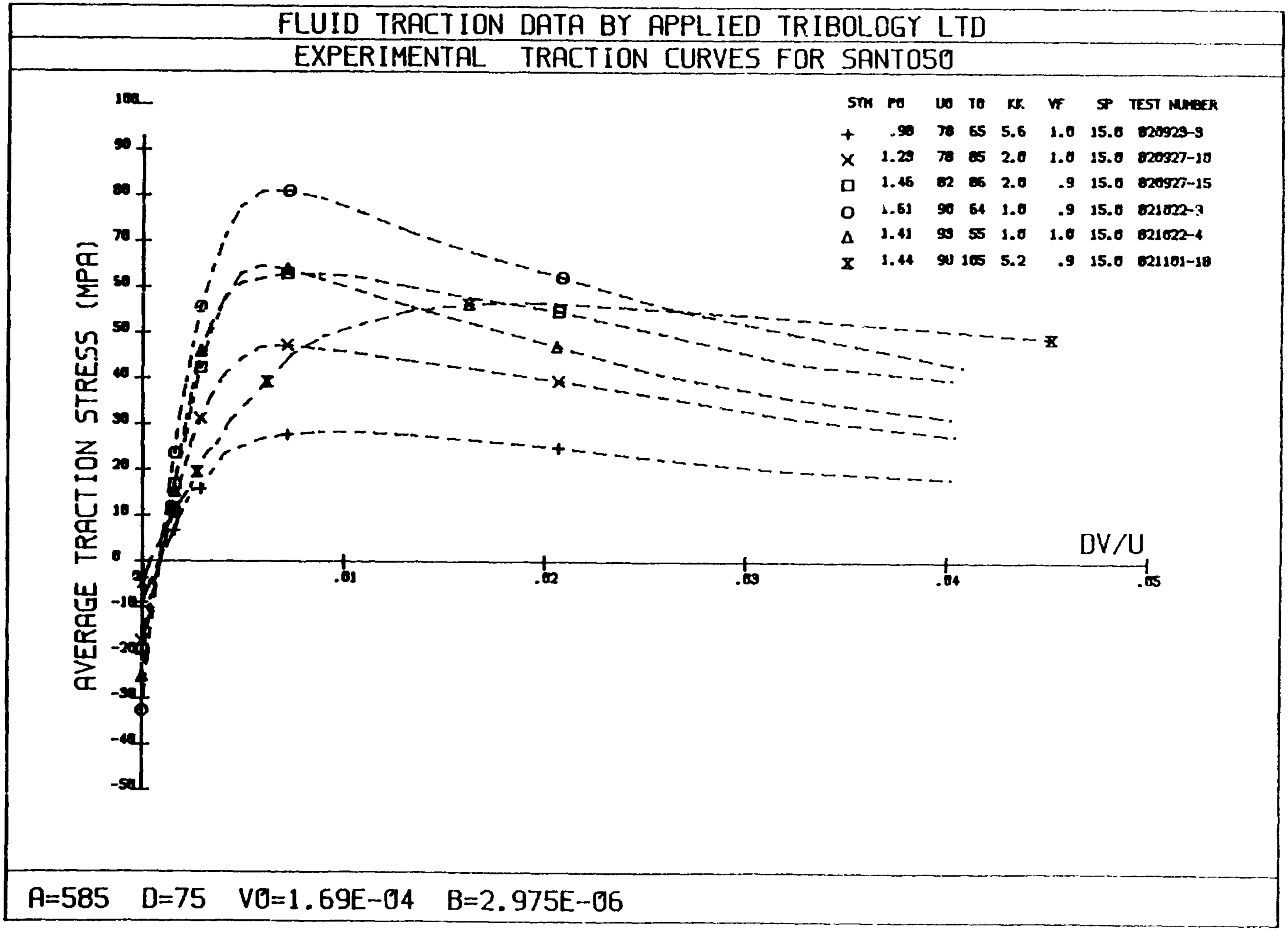

Fig. 2-17 Experimental traction results for SANTO50. Spin traction curves

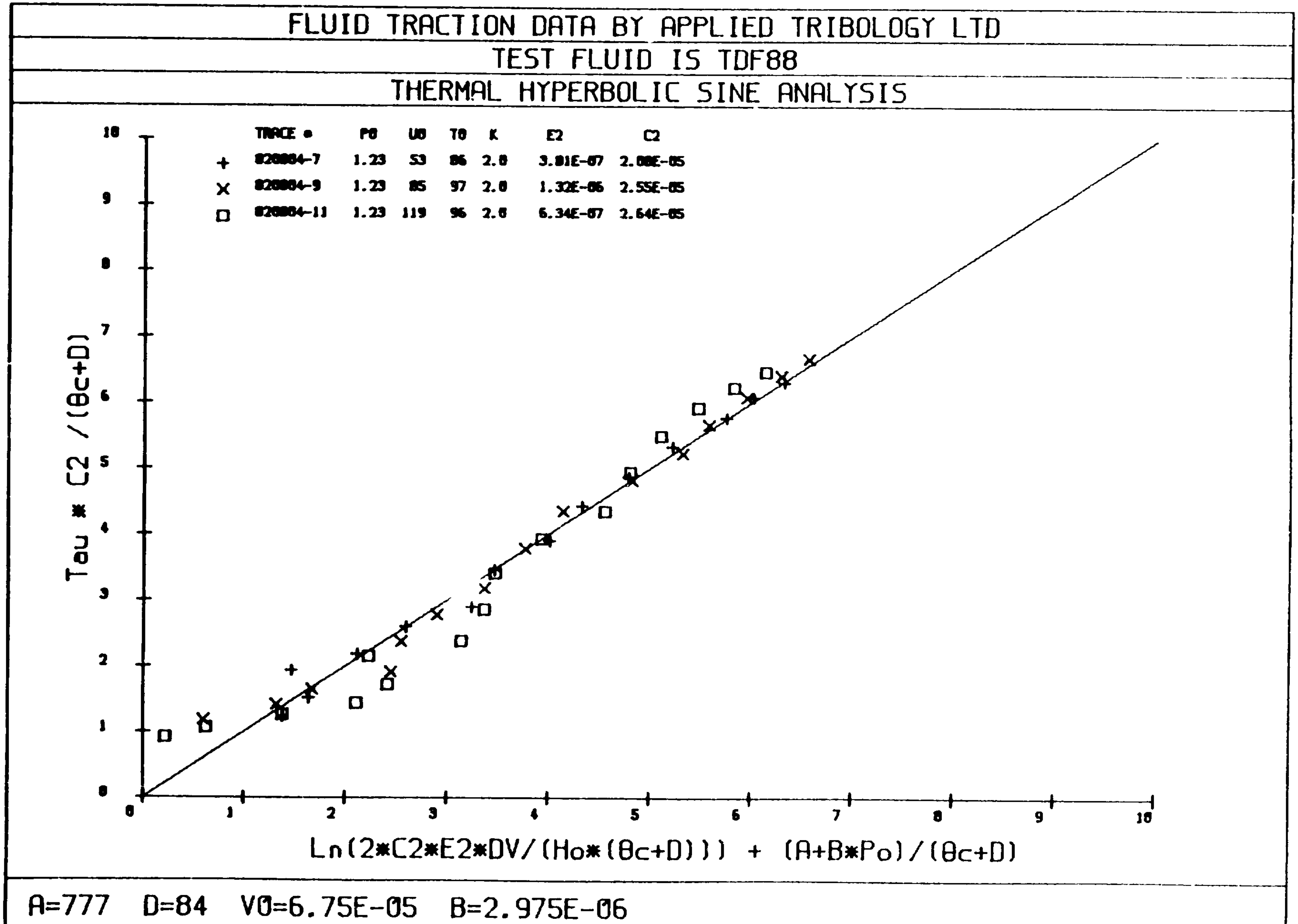

Fig. 5-1 Regression line for individual thermal constants on TDF88 for increasing speed.

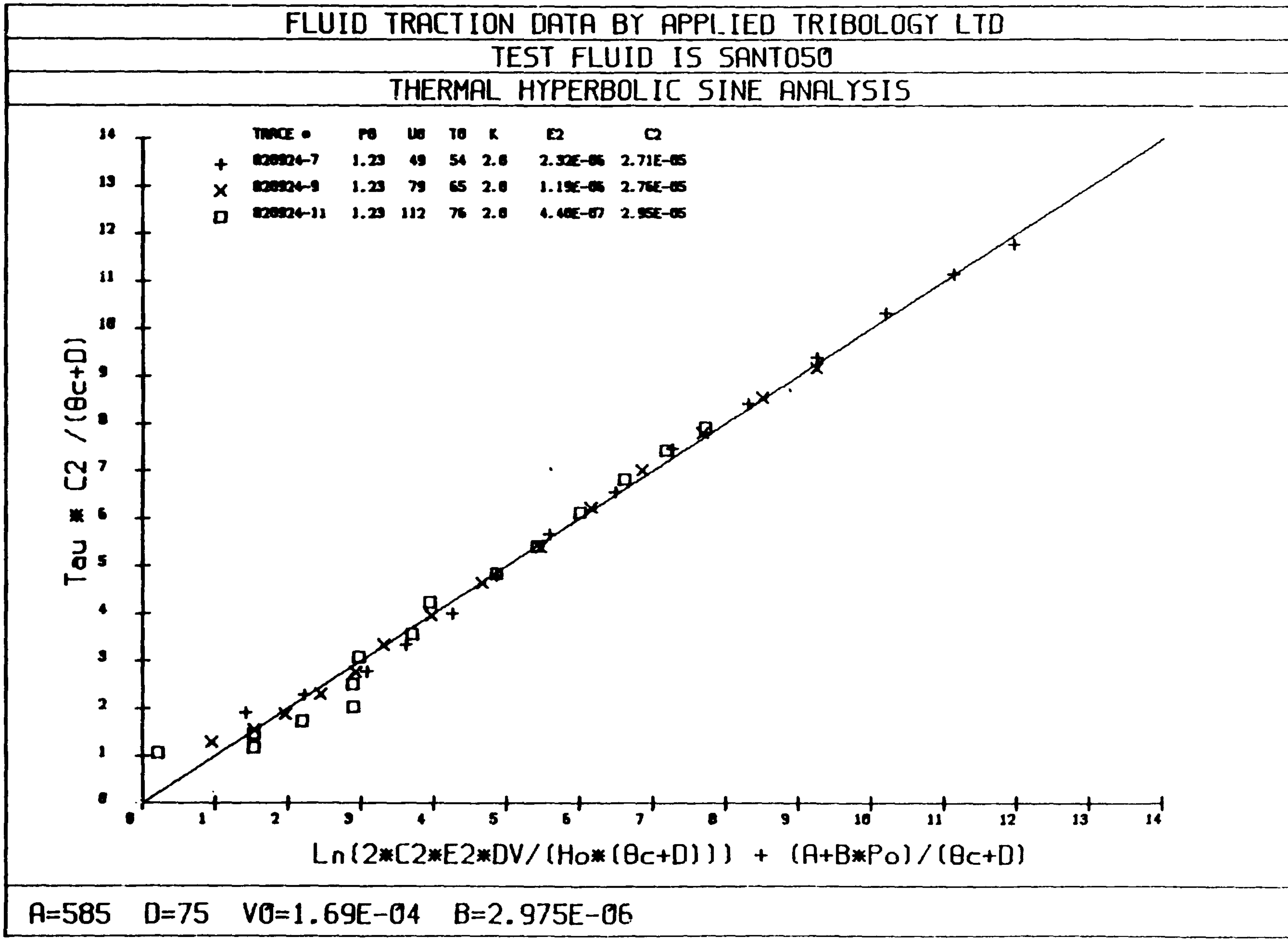

Fig. 5-2 Regression line for individual thermal constants on SANTO50 for increasing speed.

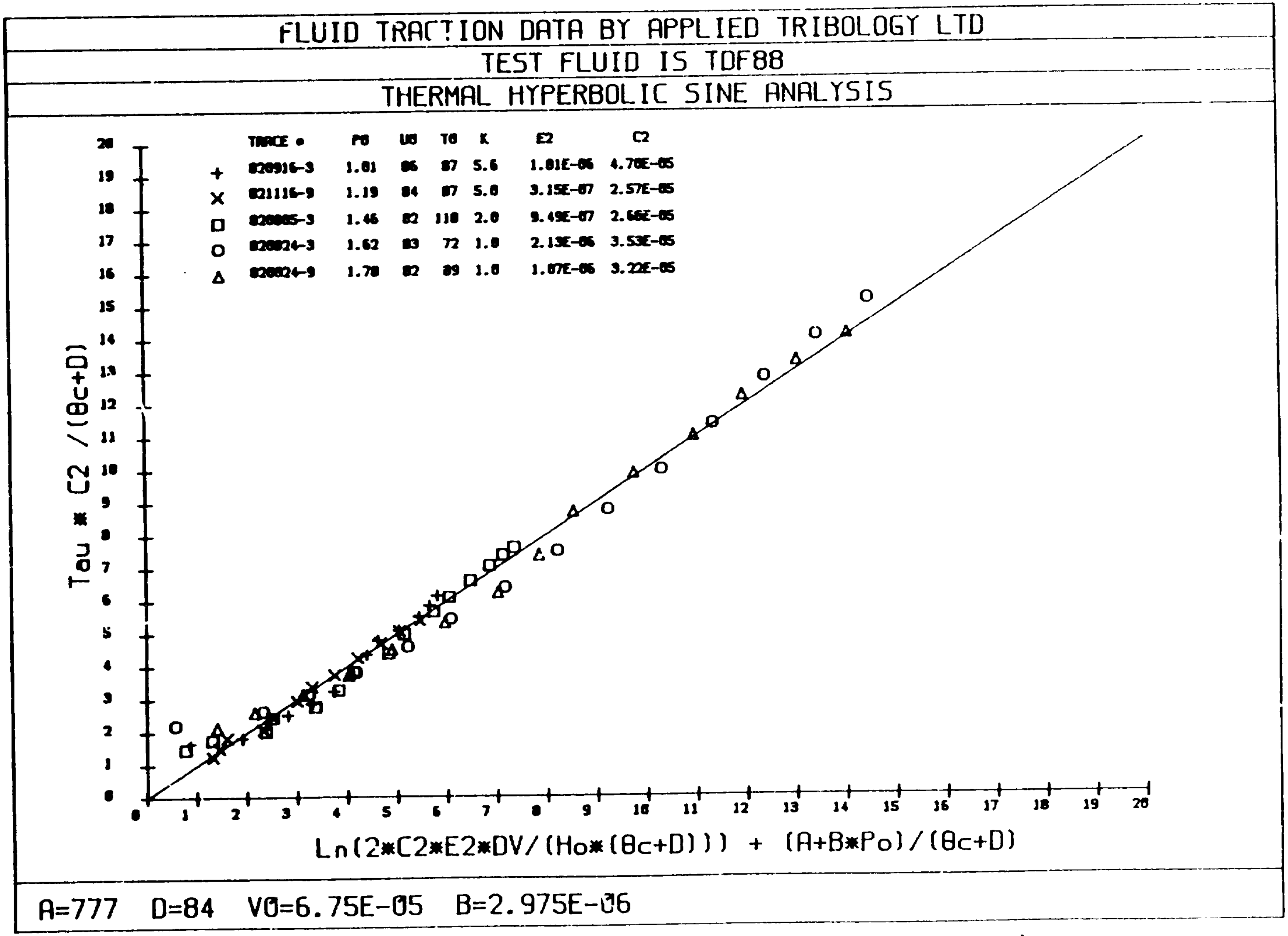

Fig. 5-3 Regression line for individual thermal constants on TDF88 for increasing pressure.

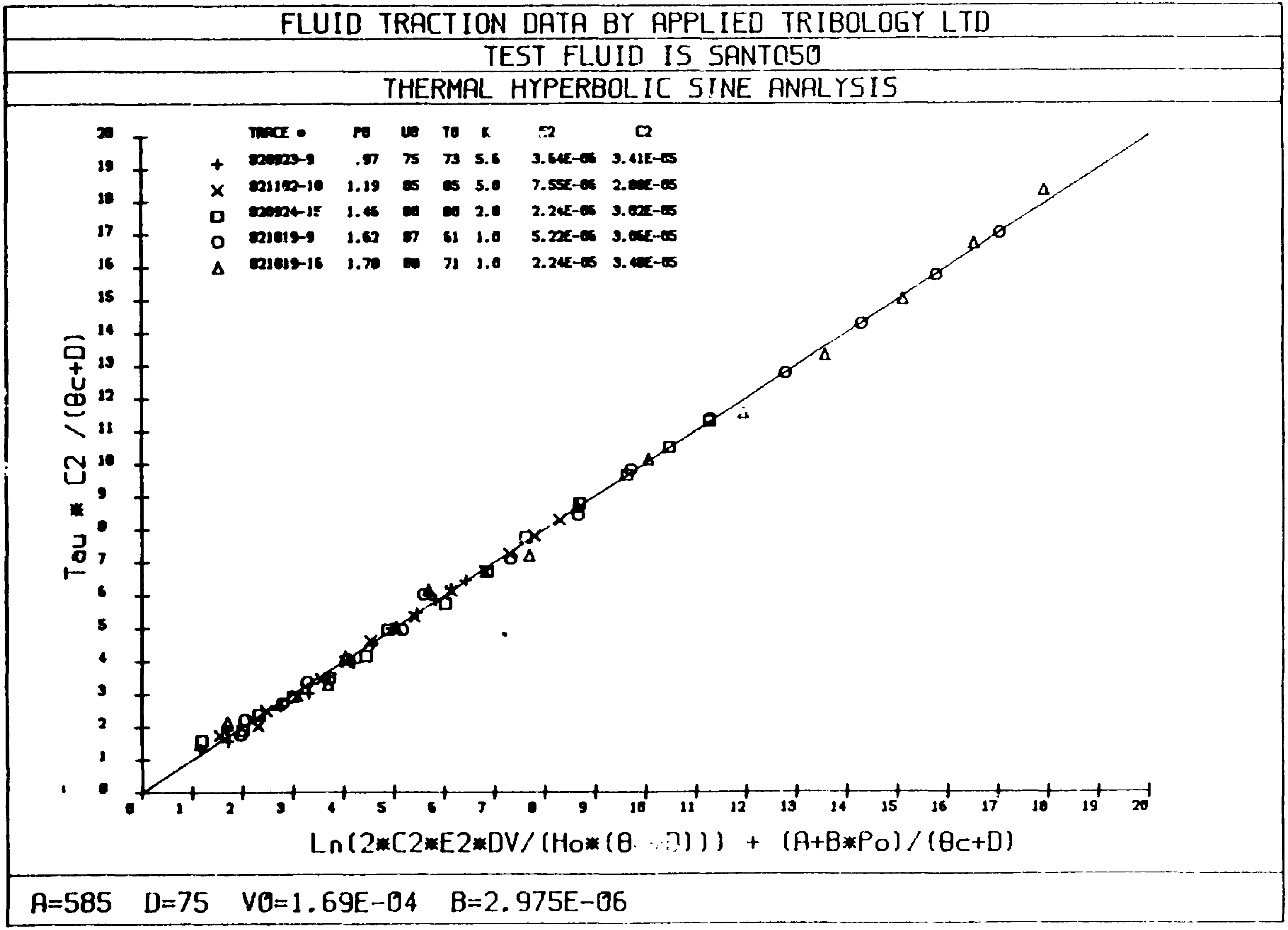

Fig. 5-4 Regression line for individual thermal constants on SANTO50 for increasing pressure.

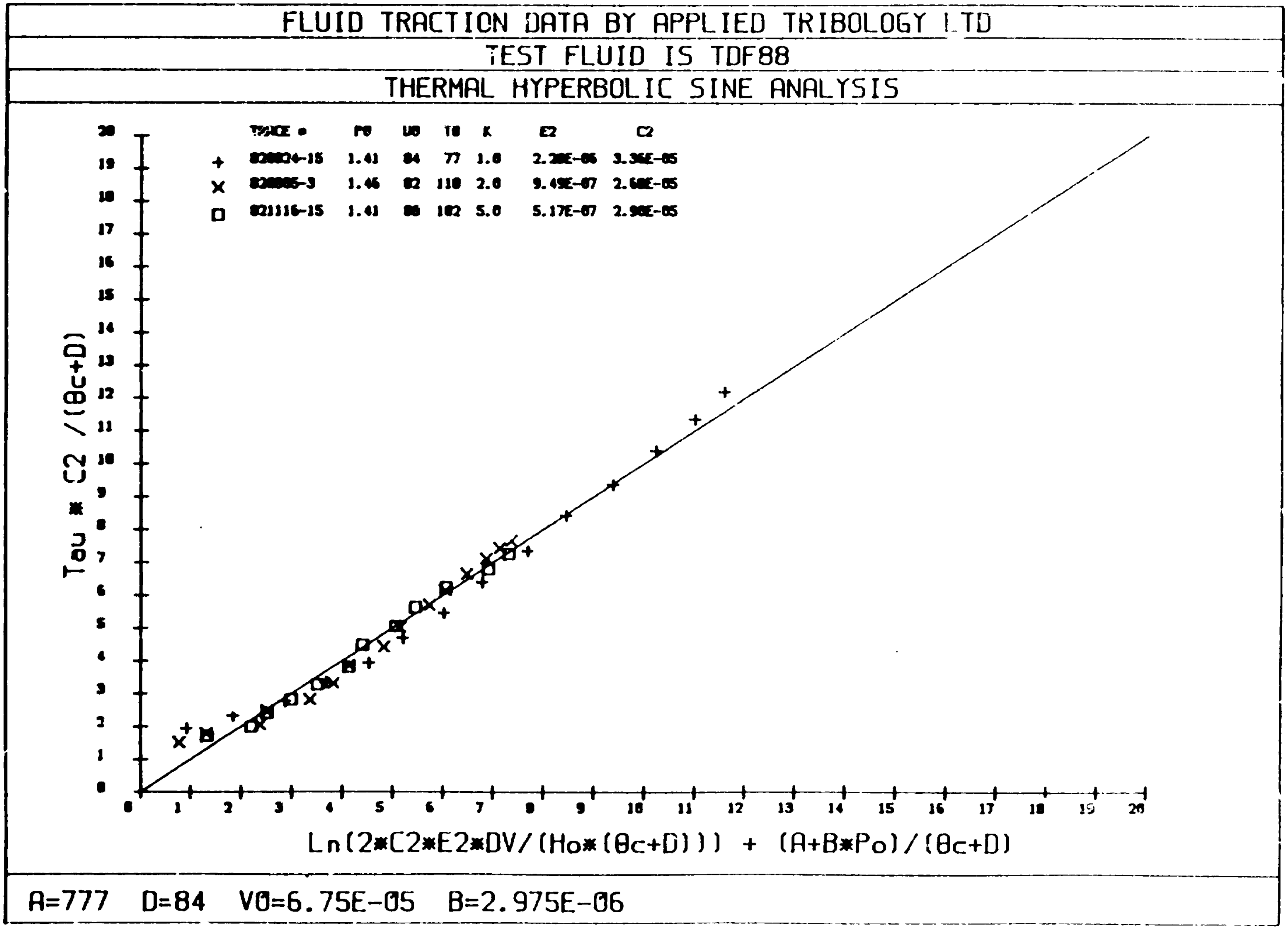

Fig. 5-5 Regression line for individual thermal constants on TDF88 for increasing aspect rati

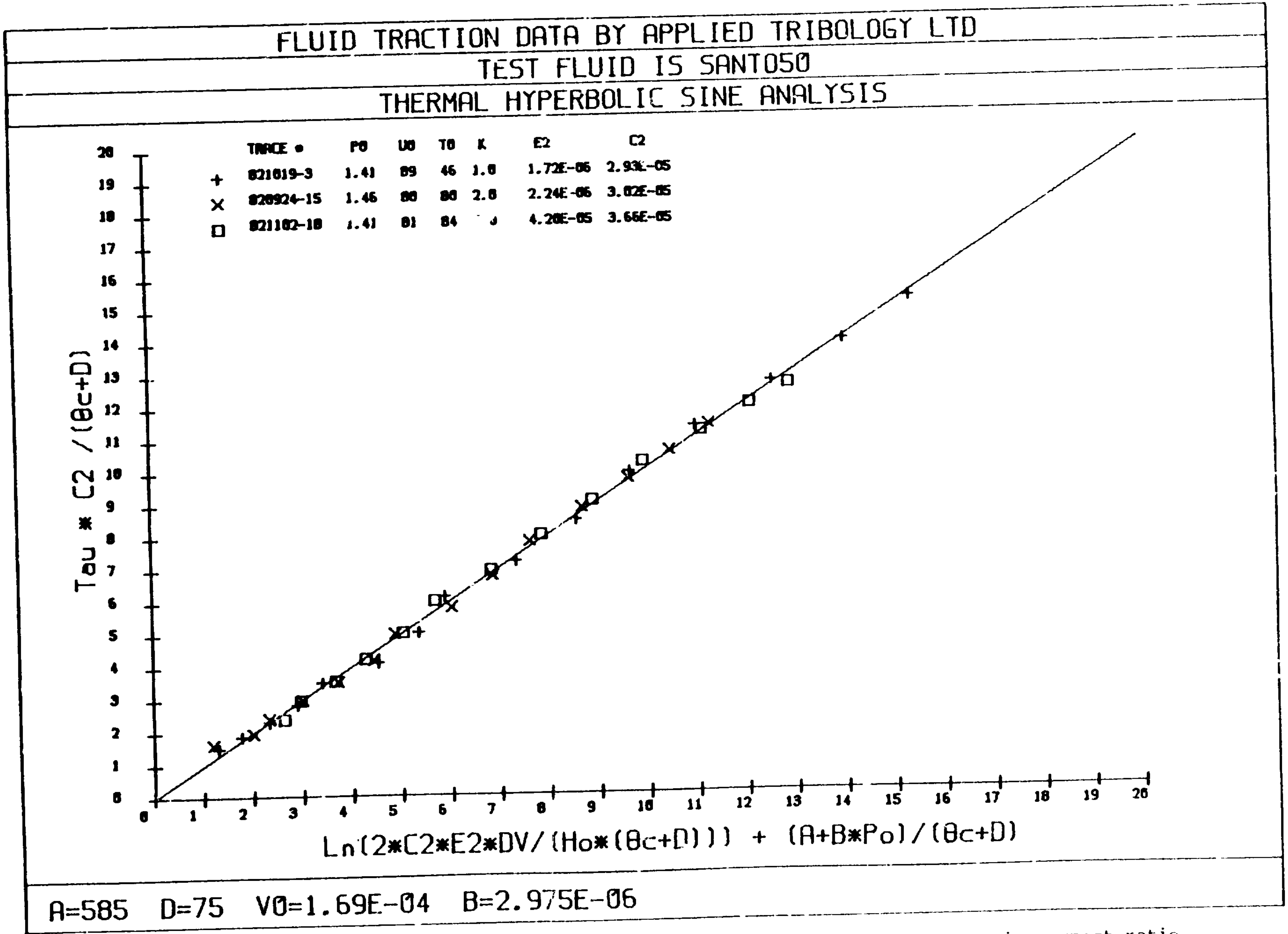

Fig. 5-6 Regression line for individual thermal constants on SANTO50 for increasing aspect ratio.

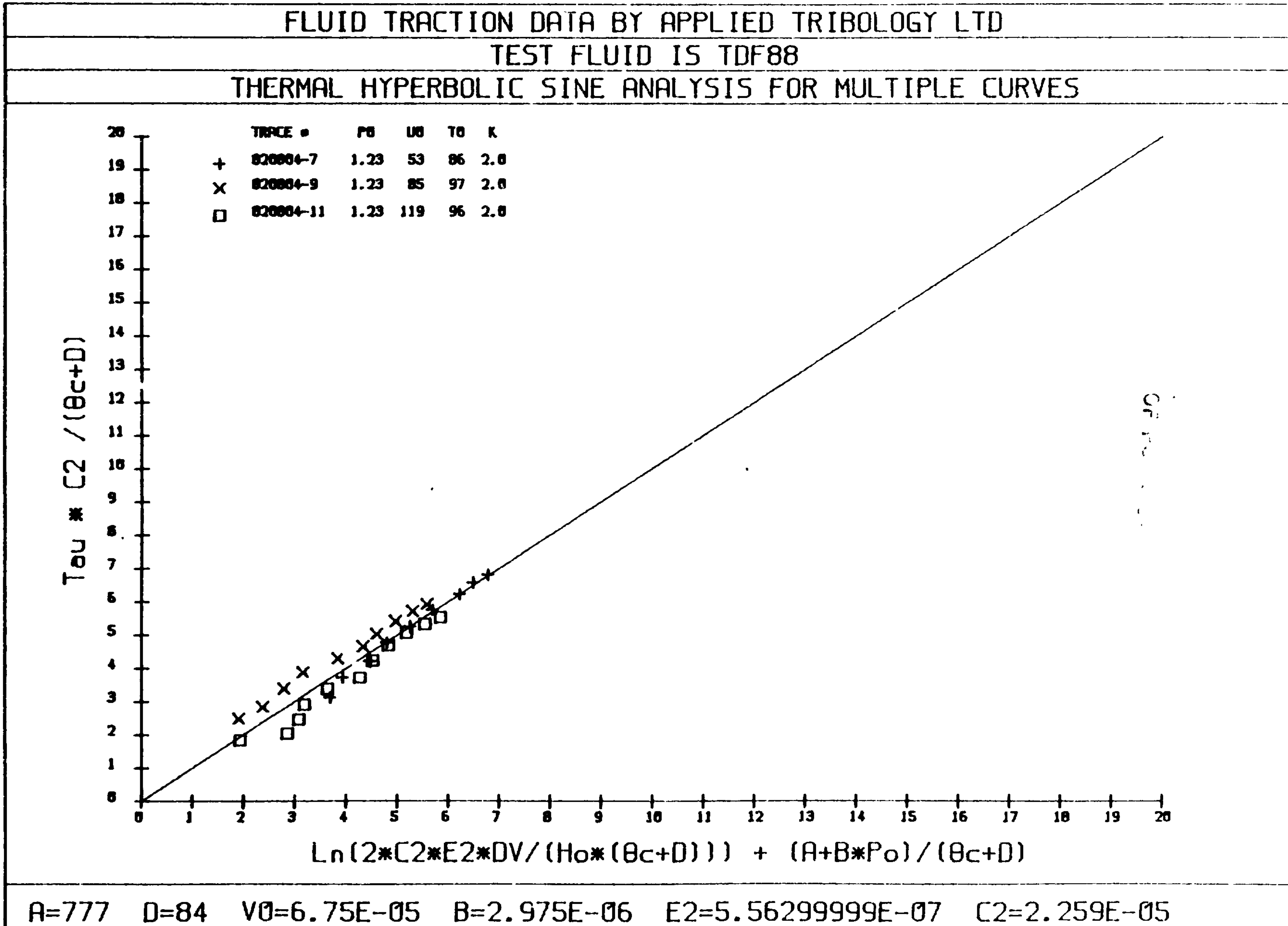

Fig. 5-7 Regression line for combined thermal constants on TDF88 for increasing speed.

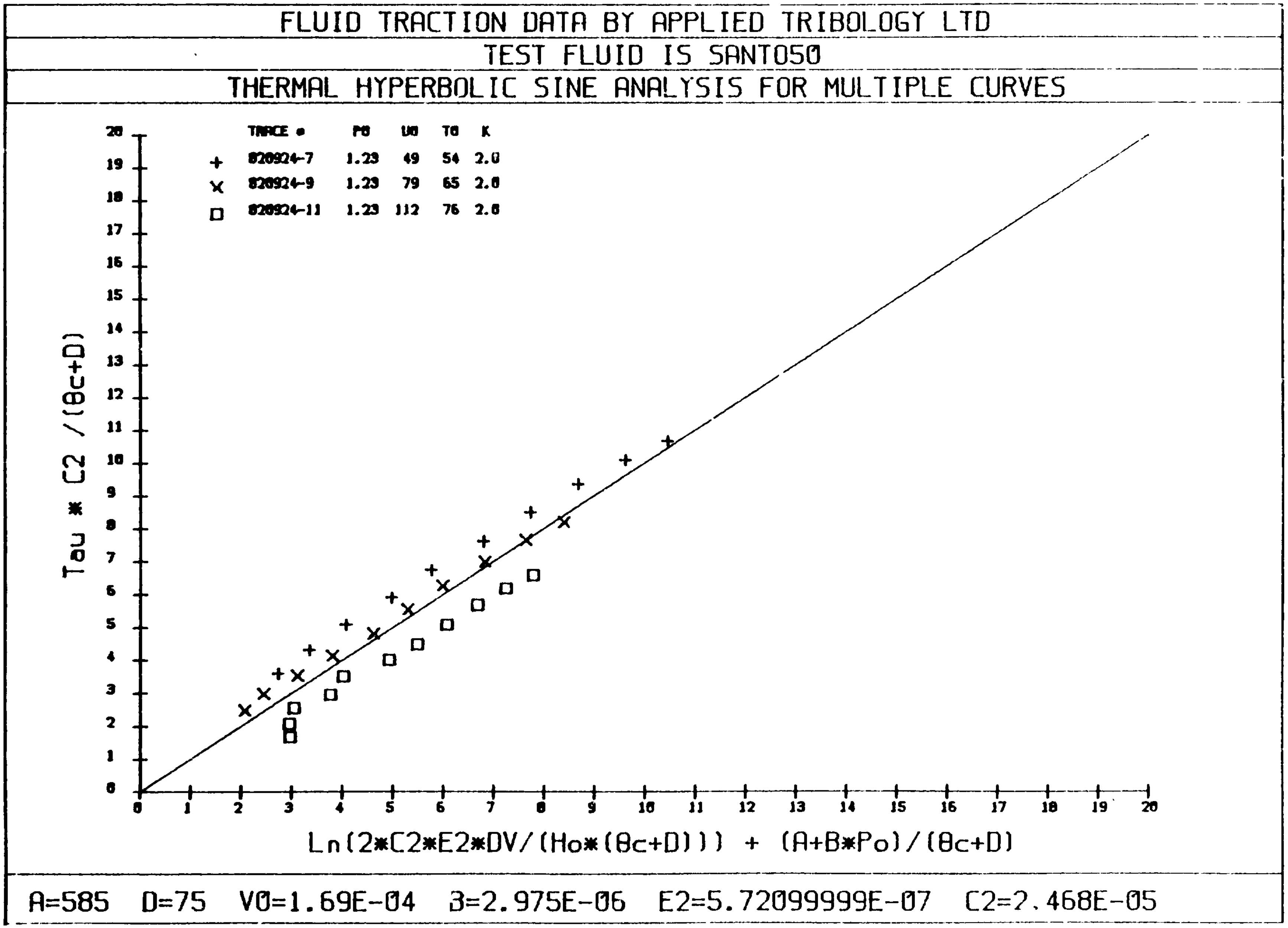

Fig. 5-8 Regression line for combined thermal constants on SANTO50 for increasing speed.

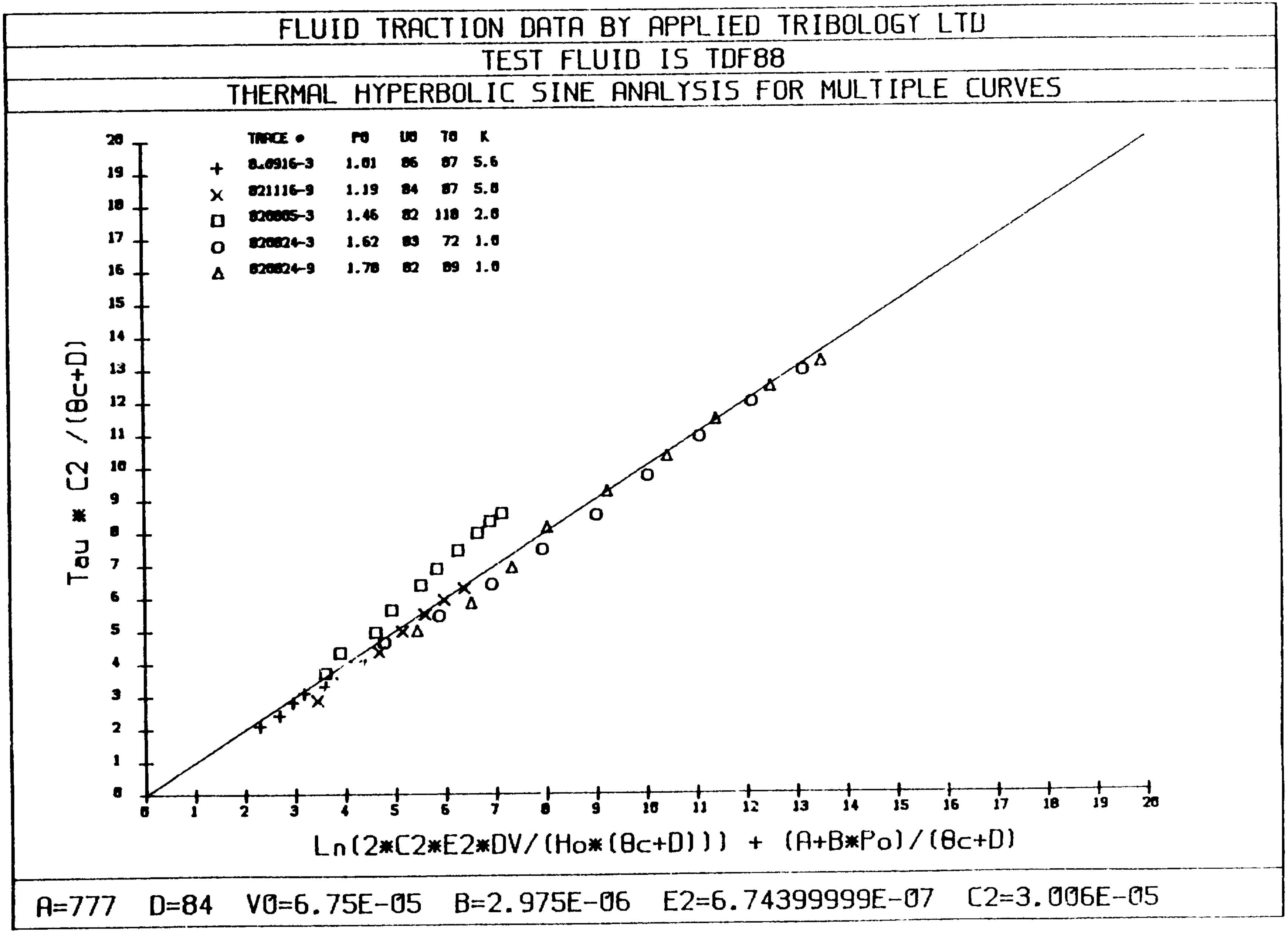

Fig. 5-9 Regression line for combined thermal constants for TDF88 for increasing pressure.

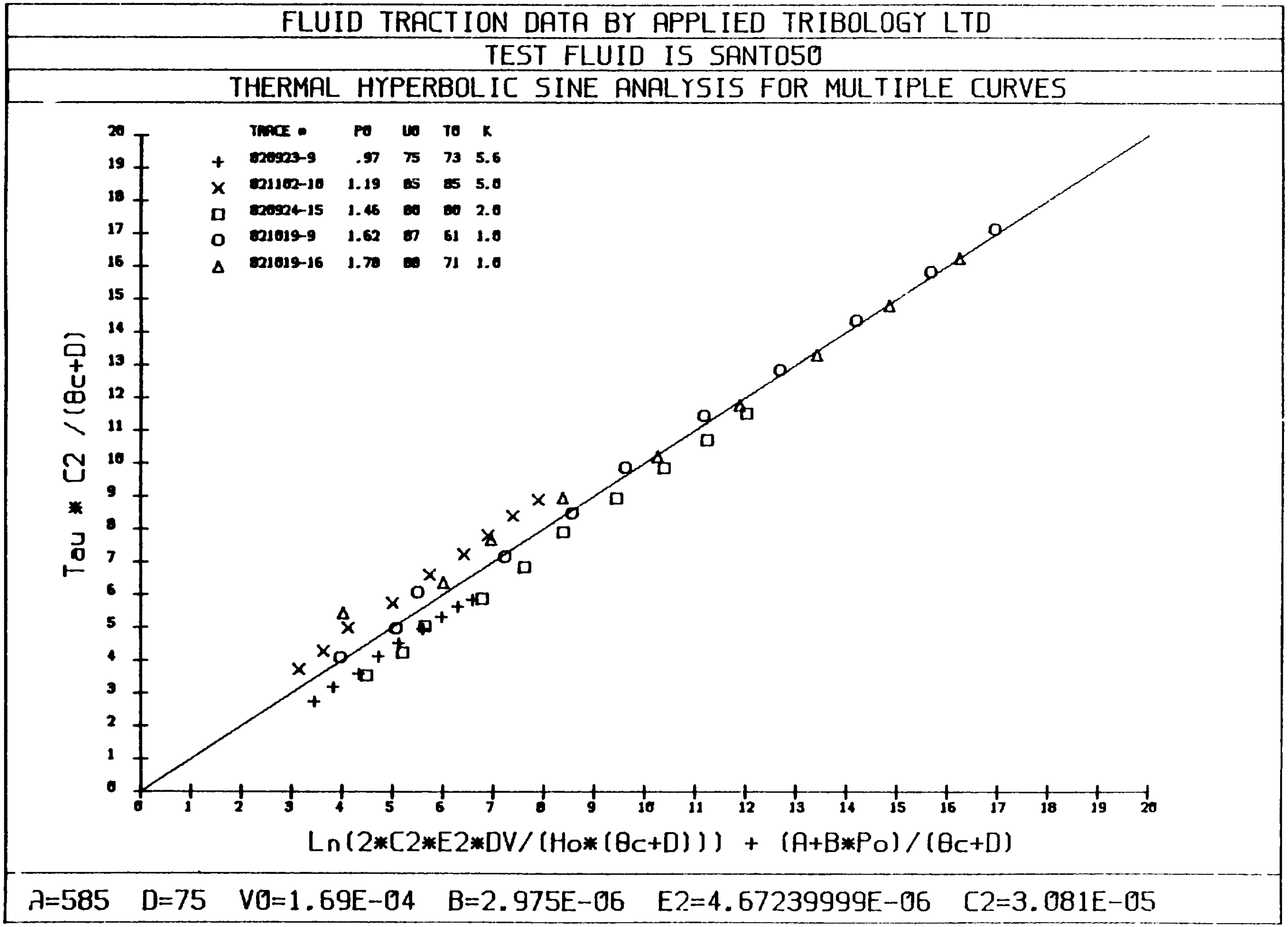

Fig. 5-10 Regression line for combined thermal constants for SANTO50 for increasing pressure.

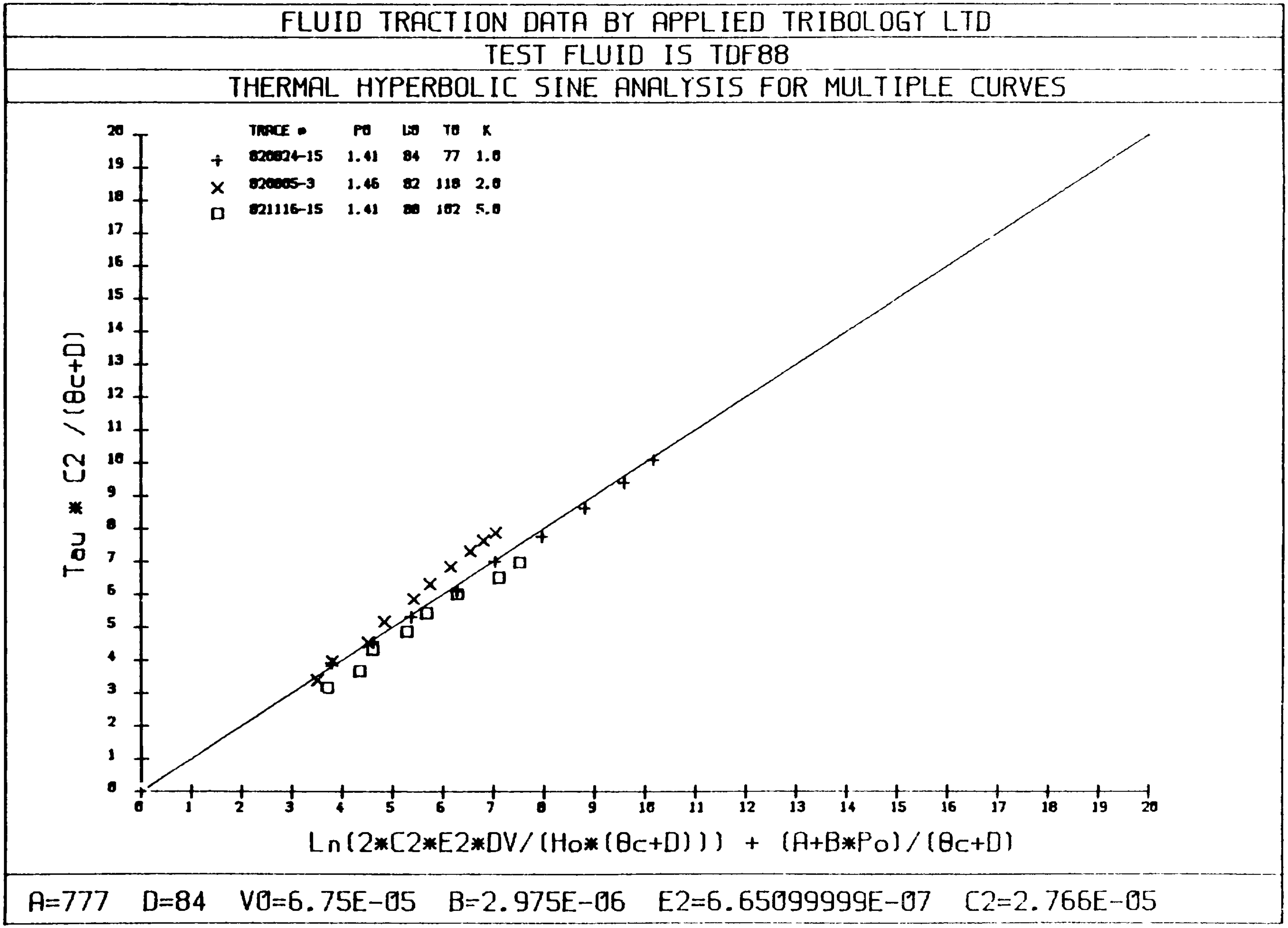

Fig. 5-11 Regression line for combined thermal constants for TDF88 for increasing aspect ratio.

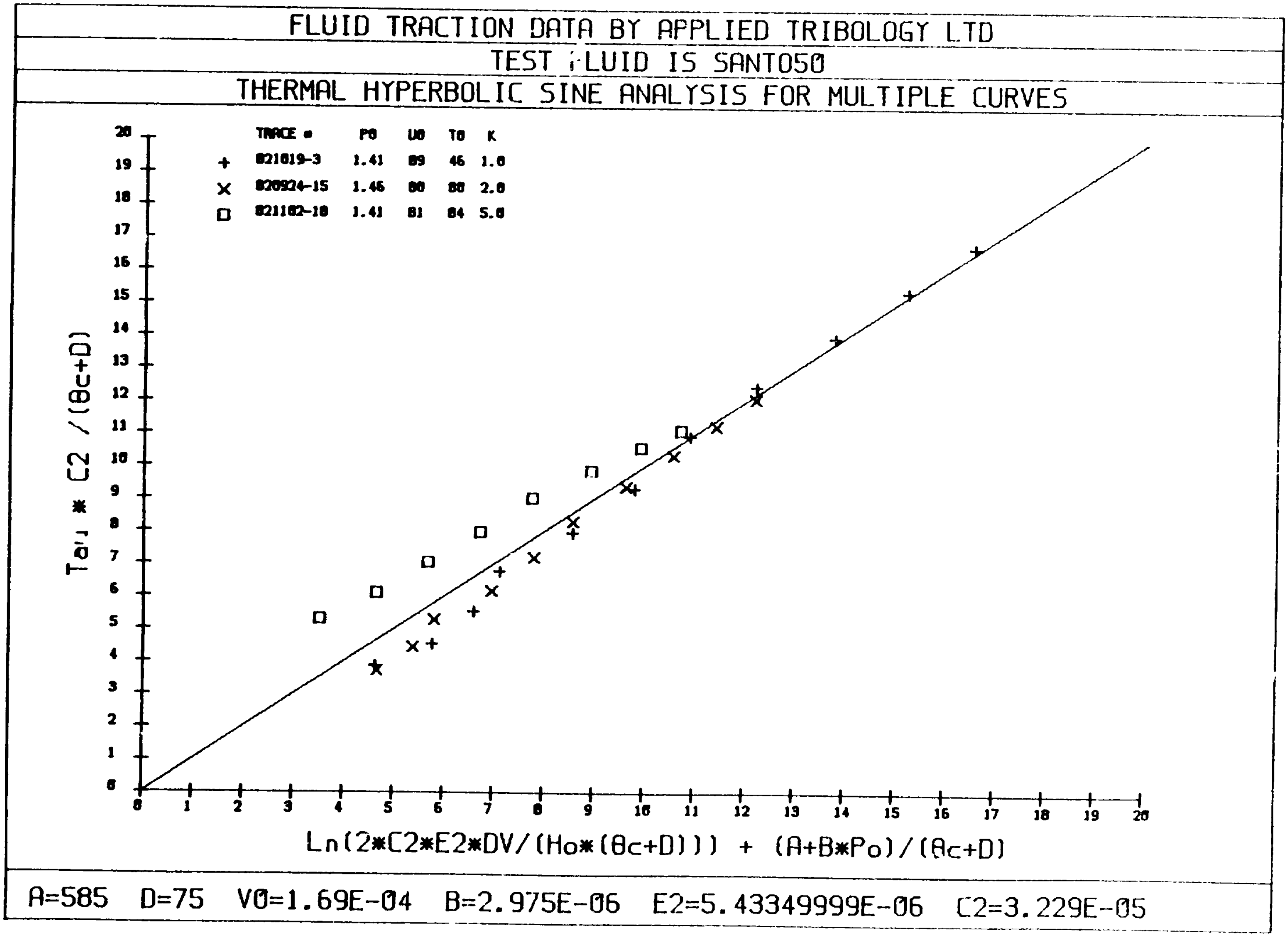

Fig. 5-12 Regression line for combined thermal constants for SANTO50 for increasing aspect ratio.

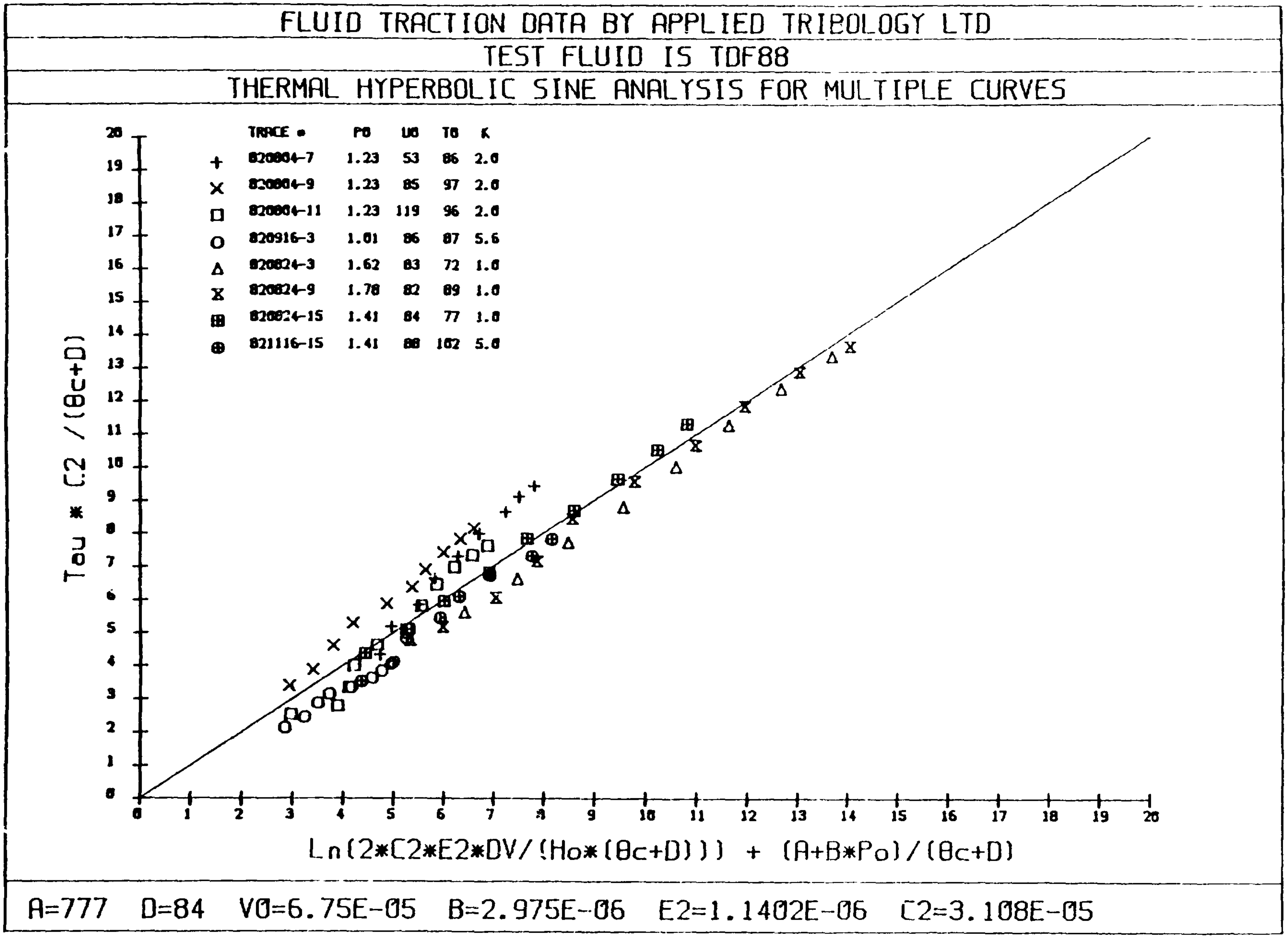

Fig. 5-13 Regression line for combined thermal constants for TDF88 for various conditions of speed, pressure, aspect ratio and inlet temperature

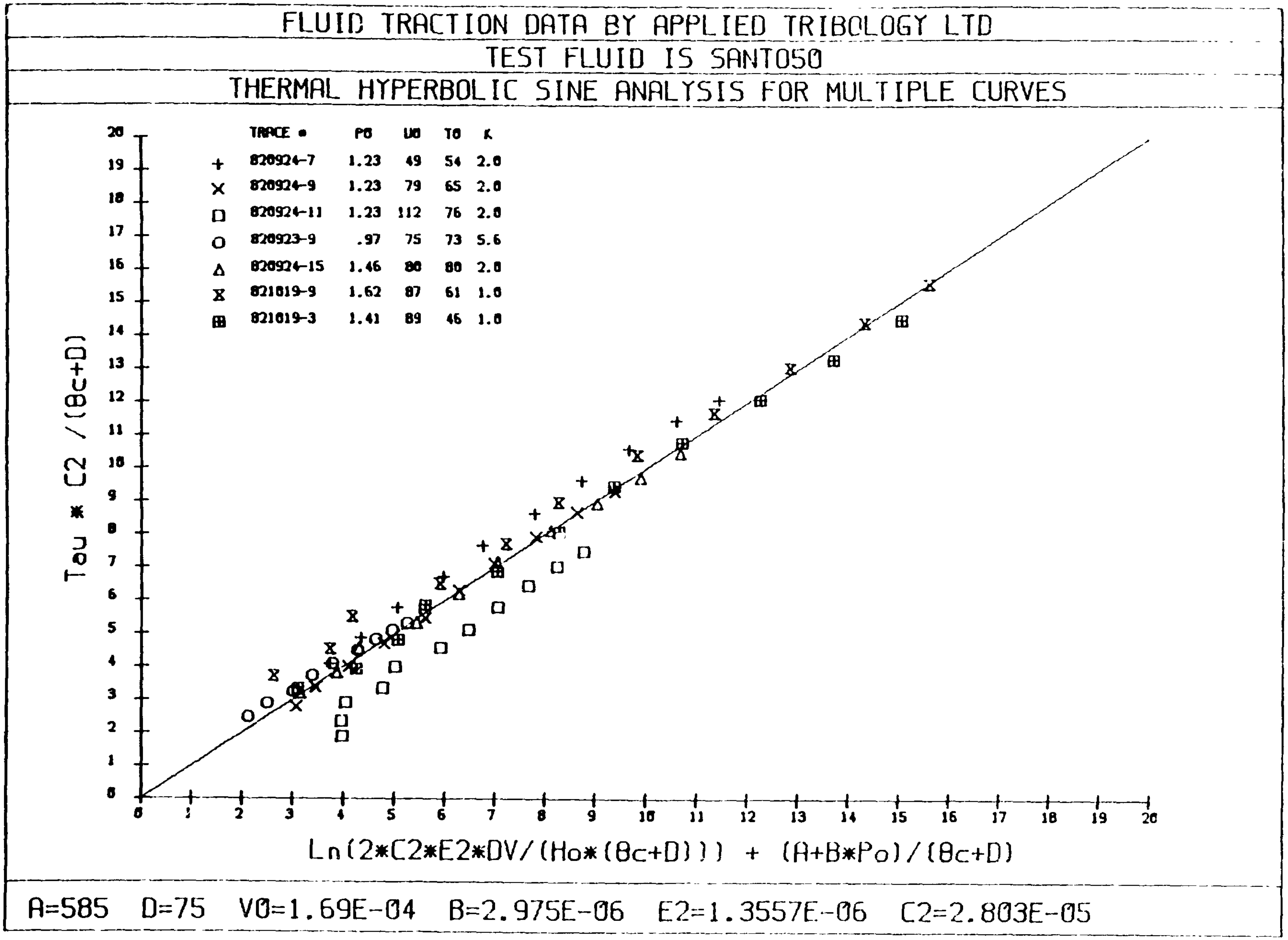

Fig. 5-14 Regression line for combined thermal constants for SANTO50 for various conditions of speed, pressure, aspect ratio and inlet temperature.

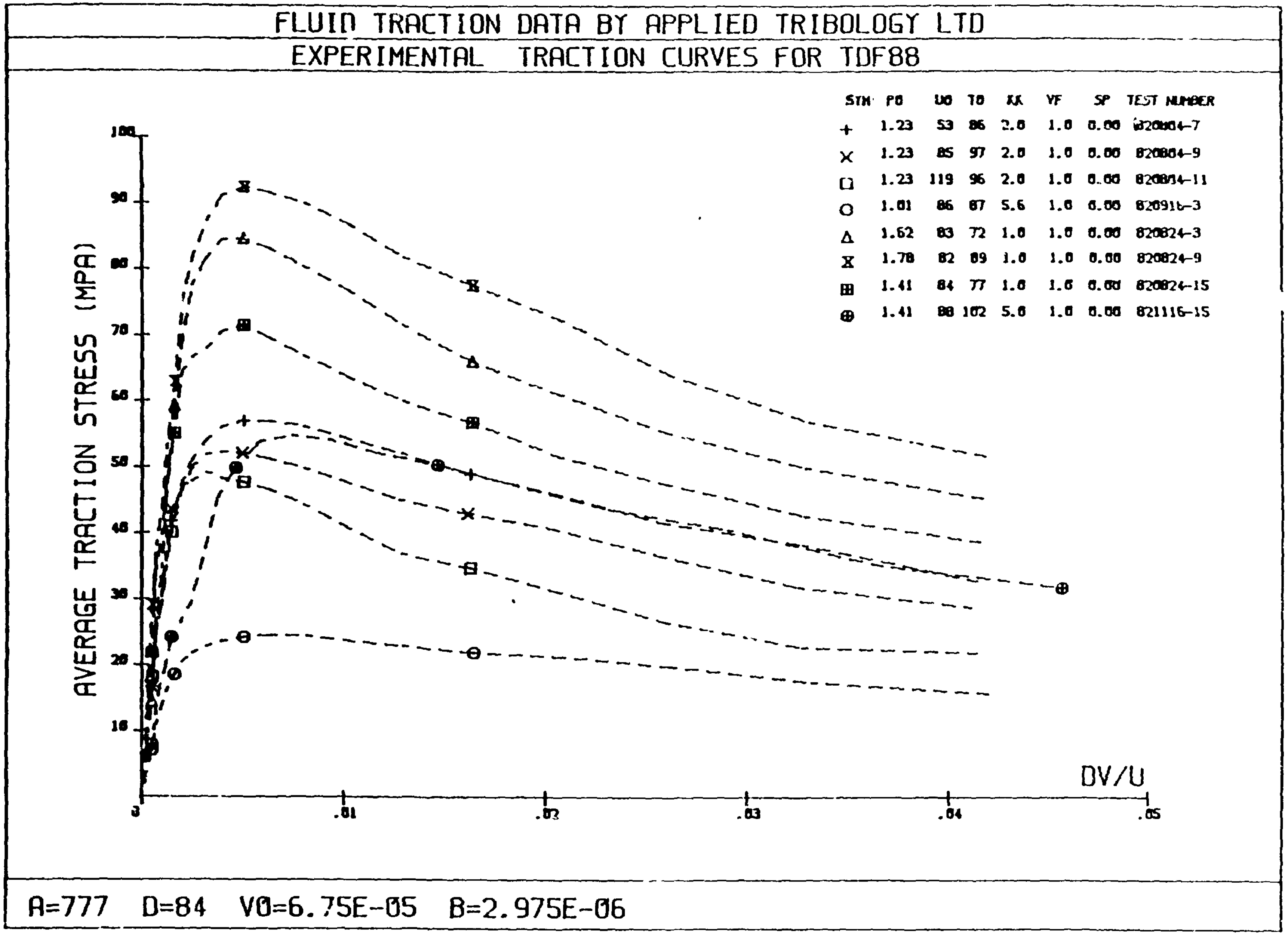

Fig. 6-1 Experimental side slip traction curves for TDF88 at various pressures, temperatures, aspect ratios and rolling velocities.

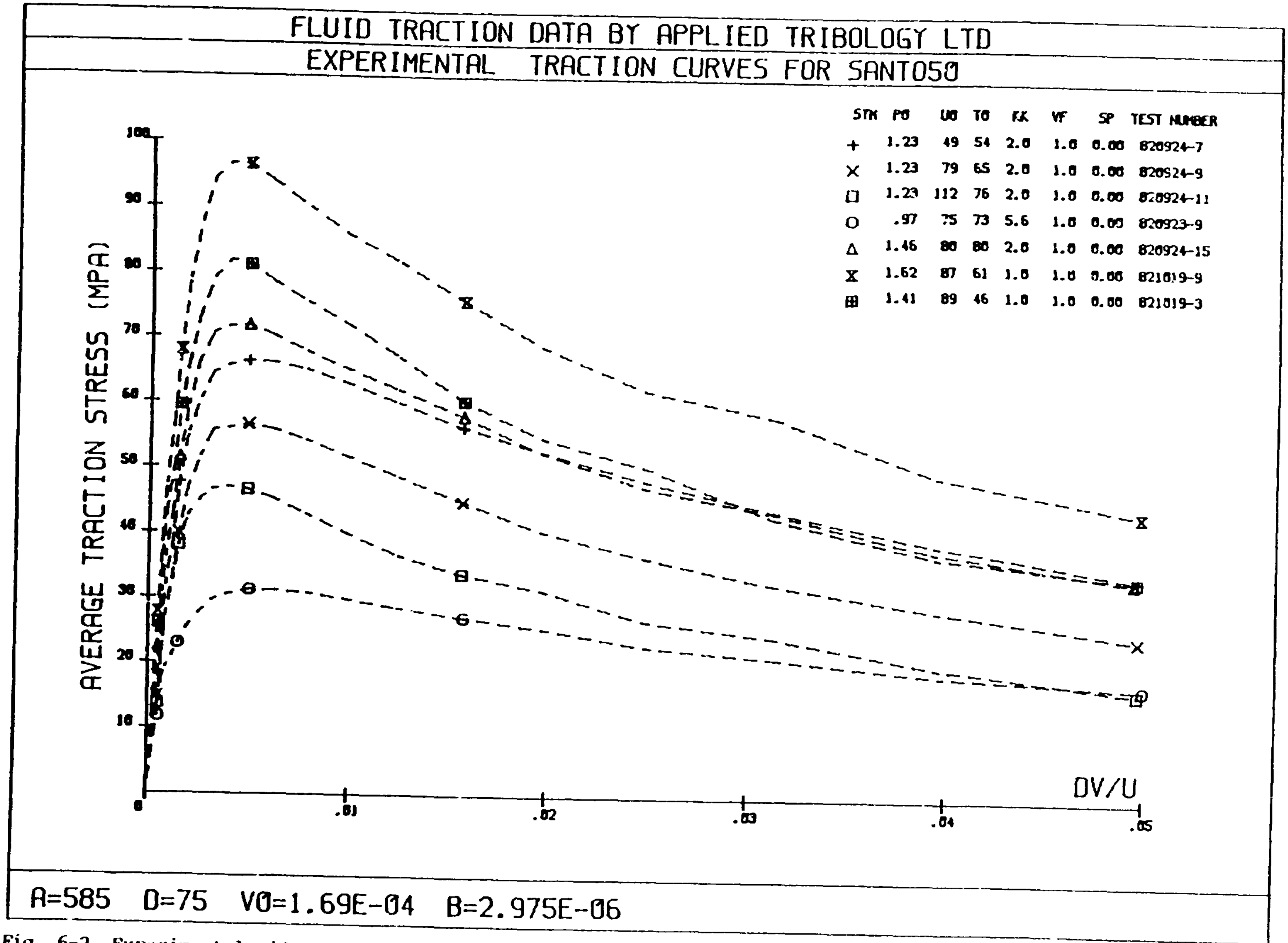

Fig. 6-2 Experimental side slip traction curves for SANTO50 at various pressures, temperatures, aspect ratios and rolling velocities.

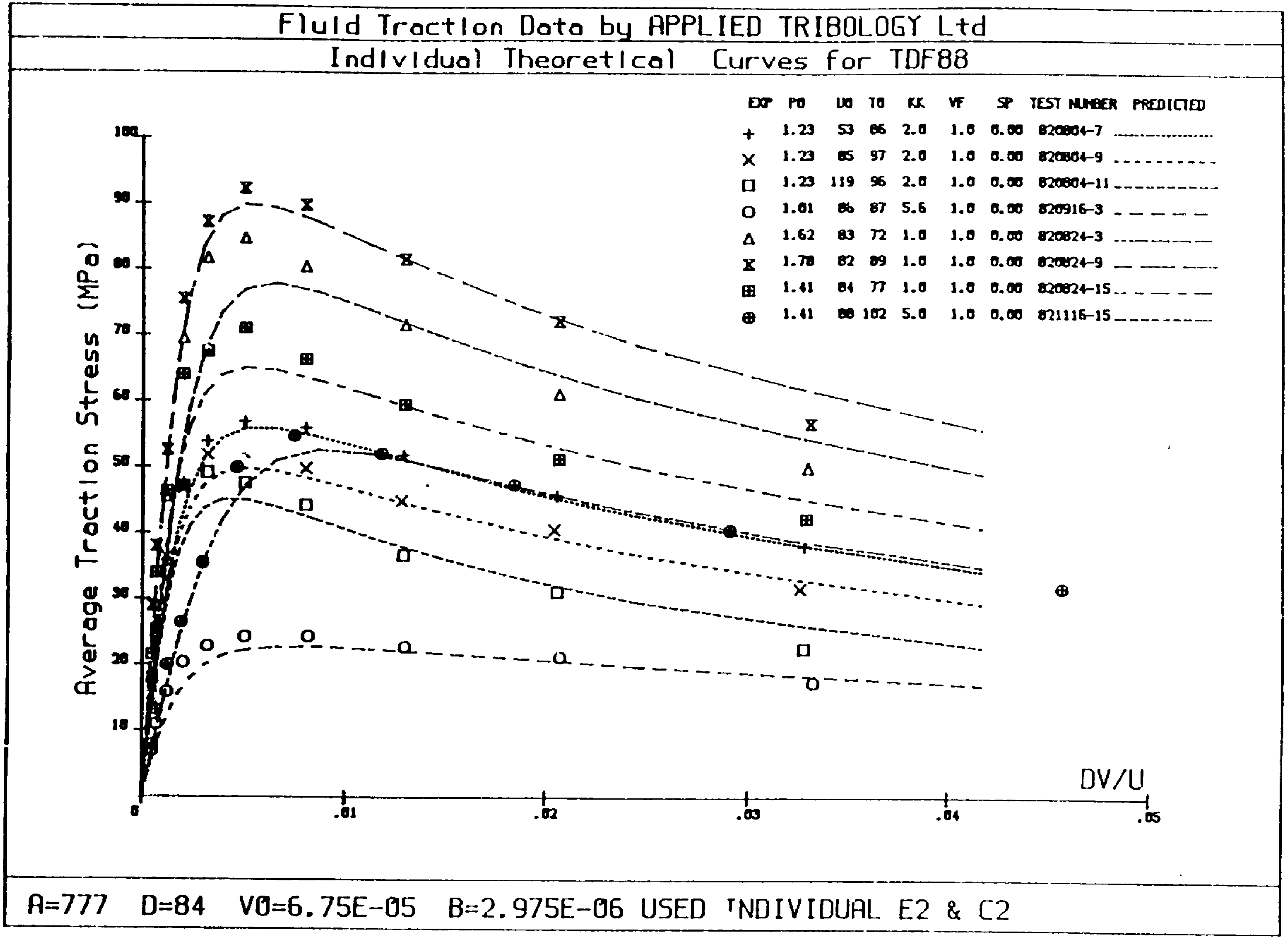

Fig. 6-3 Comparison of experimental with theoretically predicted traction curves for TDF88 based upon individually fitted thermal constants and shear modulus at various pressures, temperatures, rolling velocities and aspect ratios.

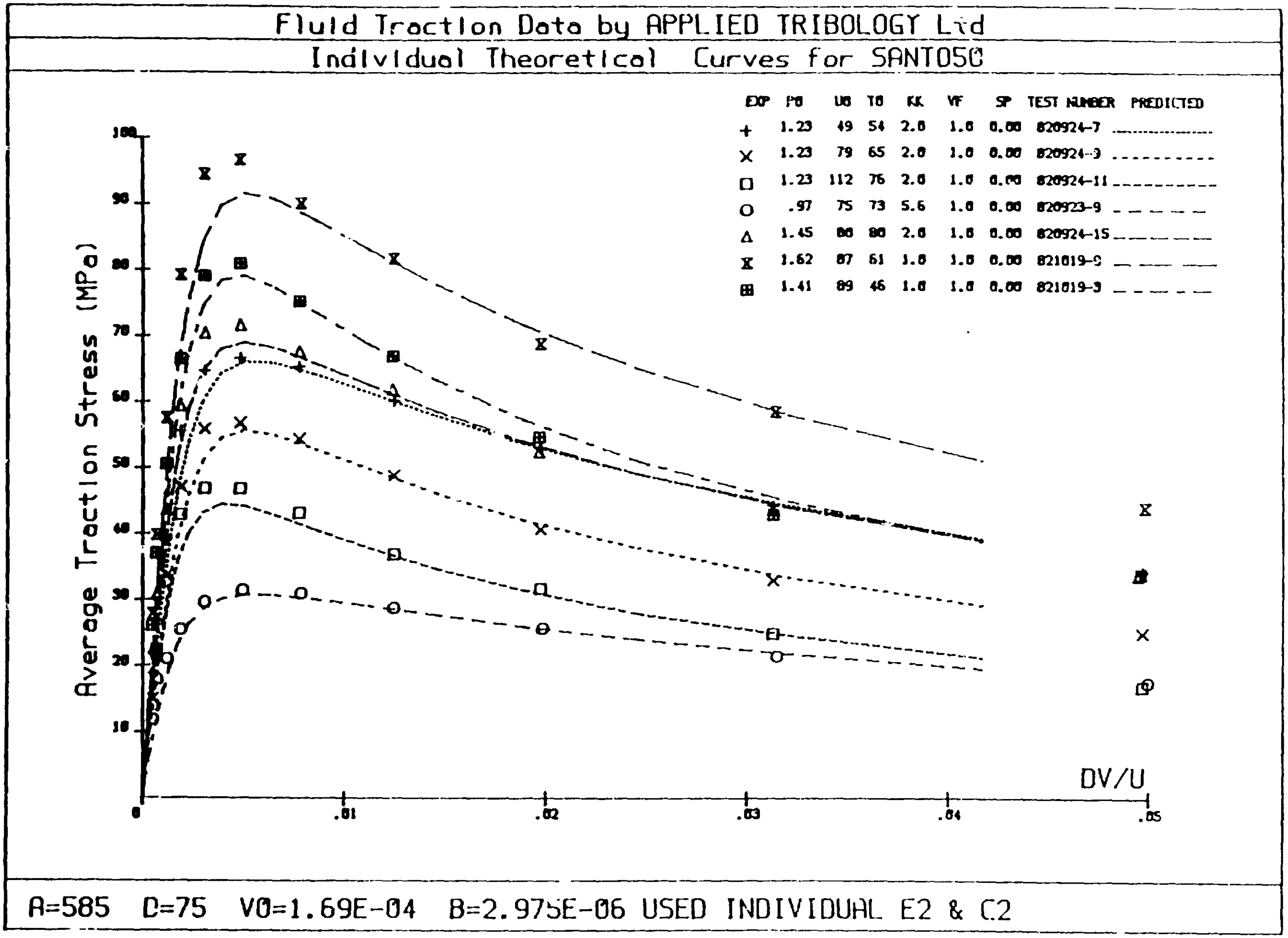

Fig. 6-4 Comparison of experimental with theoretically predicted traction curves for SANTO50 based upon individually fitted thermal constants and shear modulus at various pressure, temperatures, rolling velocities and aspect ratios.

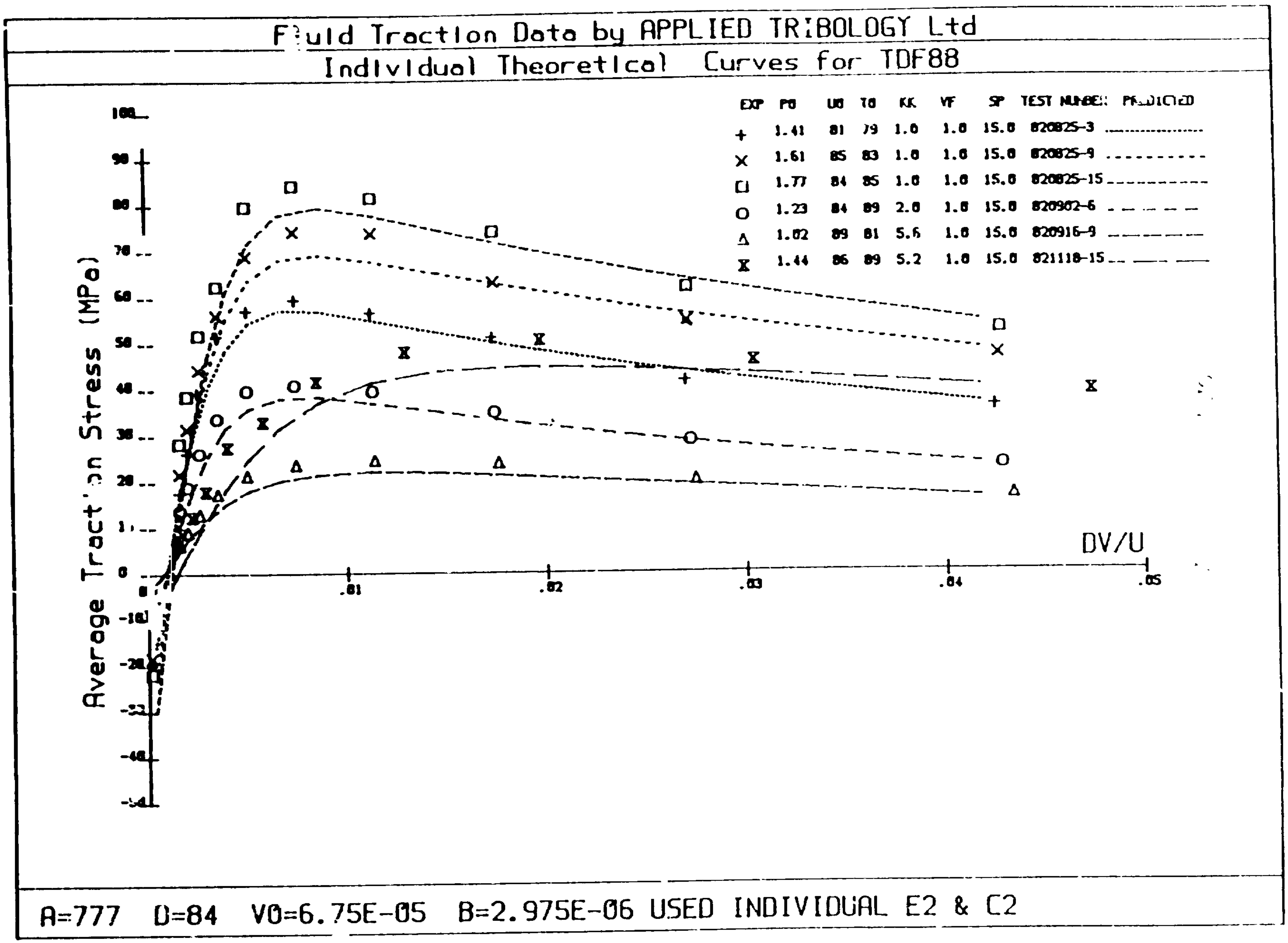

Fig. 6-5 Comparison of experimental with theoretically predicted traction curves for TDF88 based upon individually fitted thermal constants at various pressures, temperatures, rolling velocities, aspect ratios and spin.

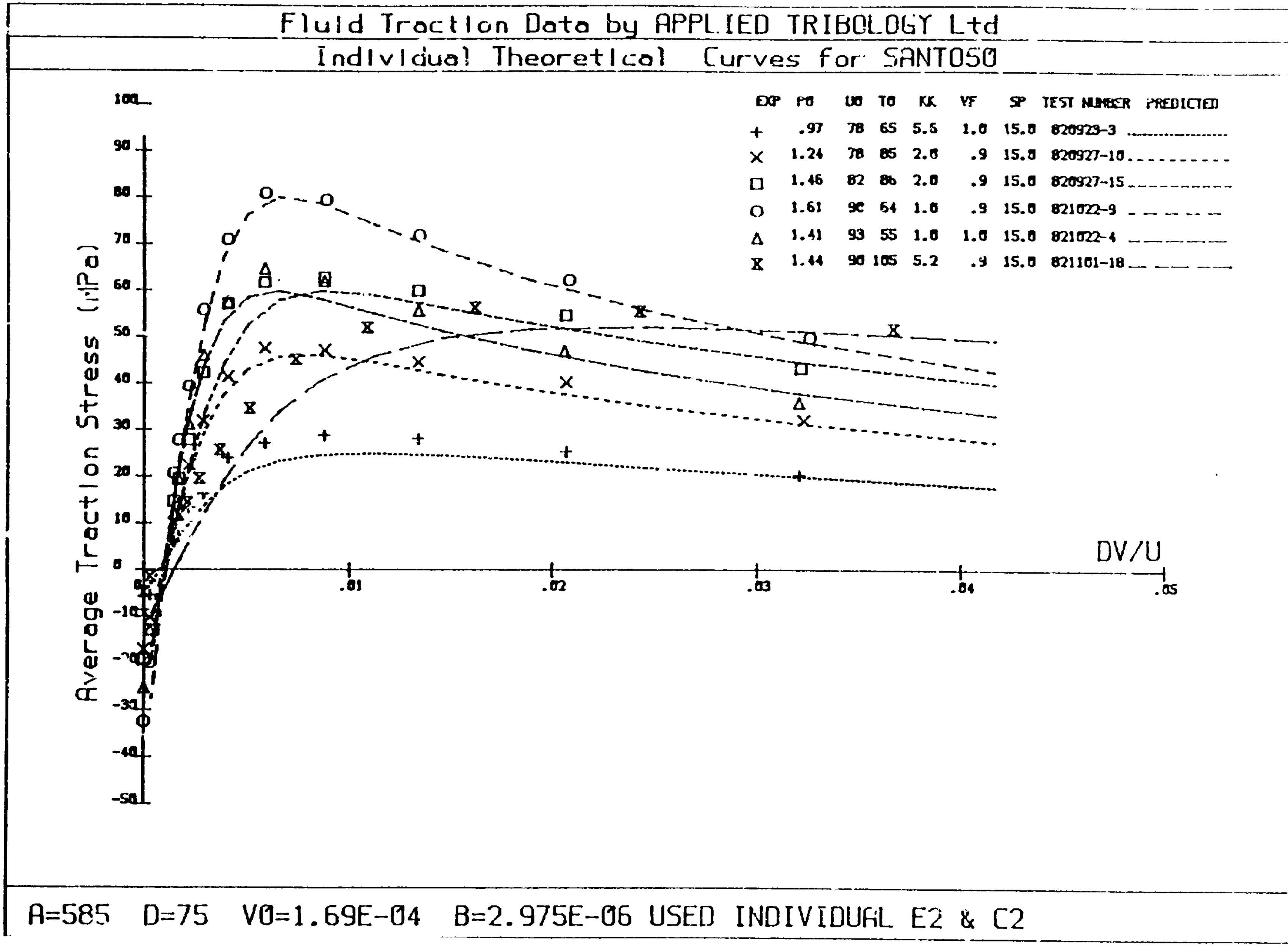

Fig. 6-6 Comparison of experimental with theoretically predicted traction curves for SANTO50 based upon individually fitted thermal constants at various pressures, temperatures, rolling velocities, aspect ratios and spin.

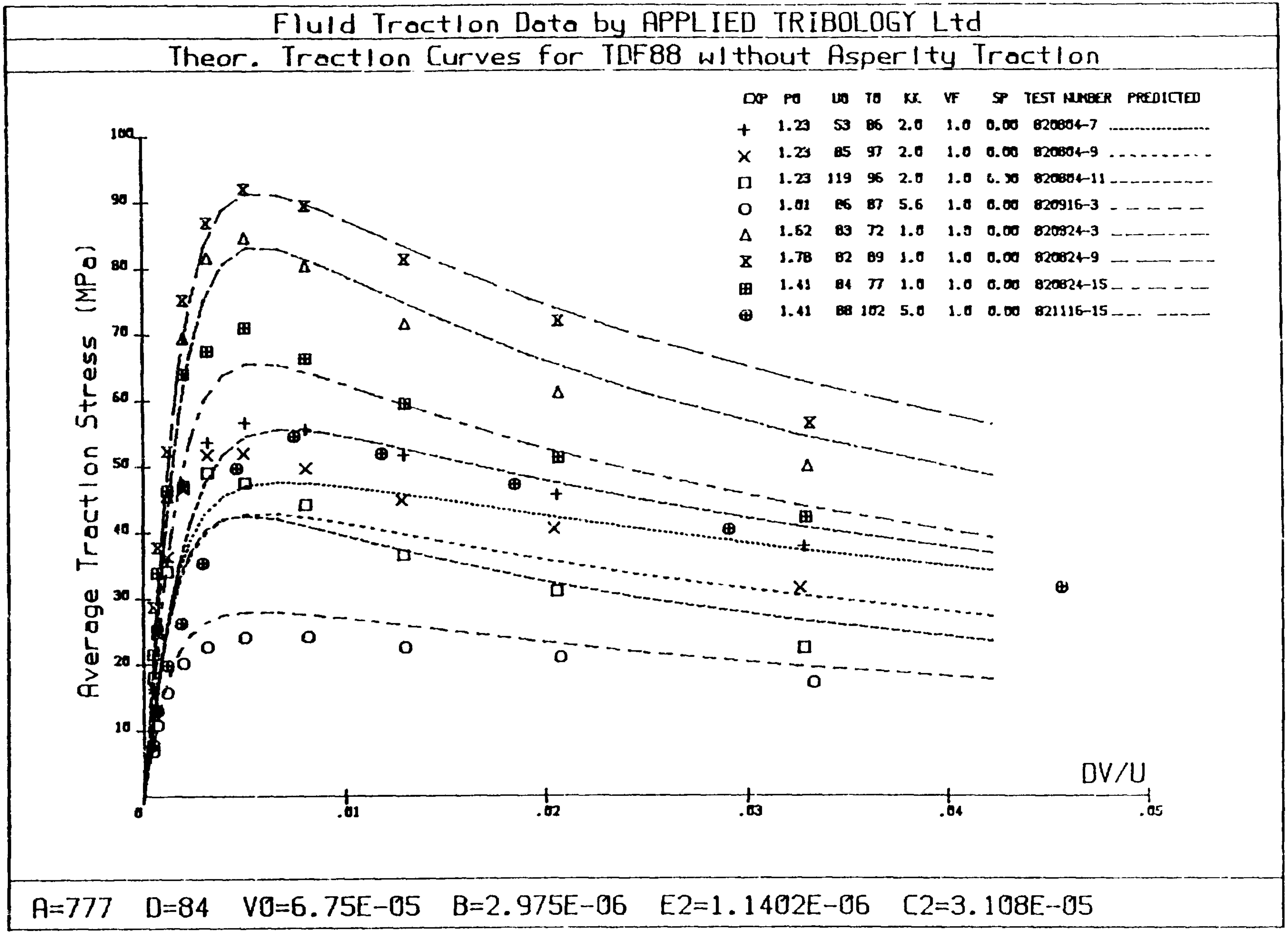

Fig. 6-7 Comparison of experimental with theoretically predicted traction curves for TDF88 based upon multiple curve fitted thermal constants and shear modulus at various pressures, temperatures, rolling velocities and aspect ratios.

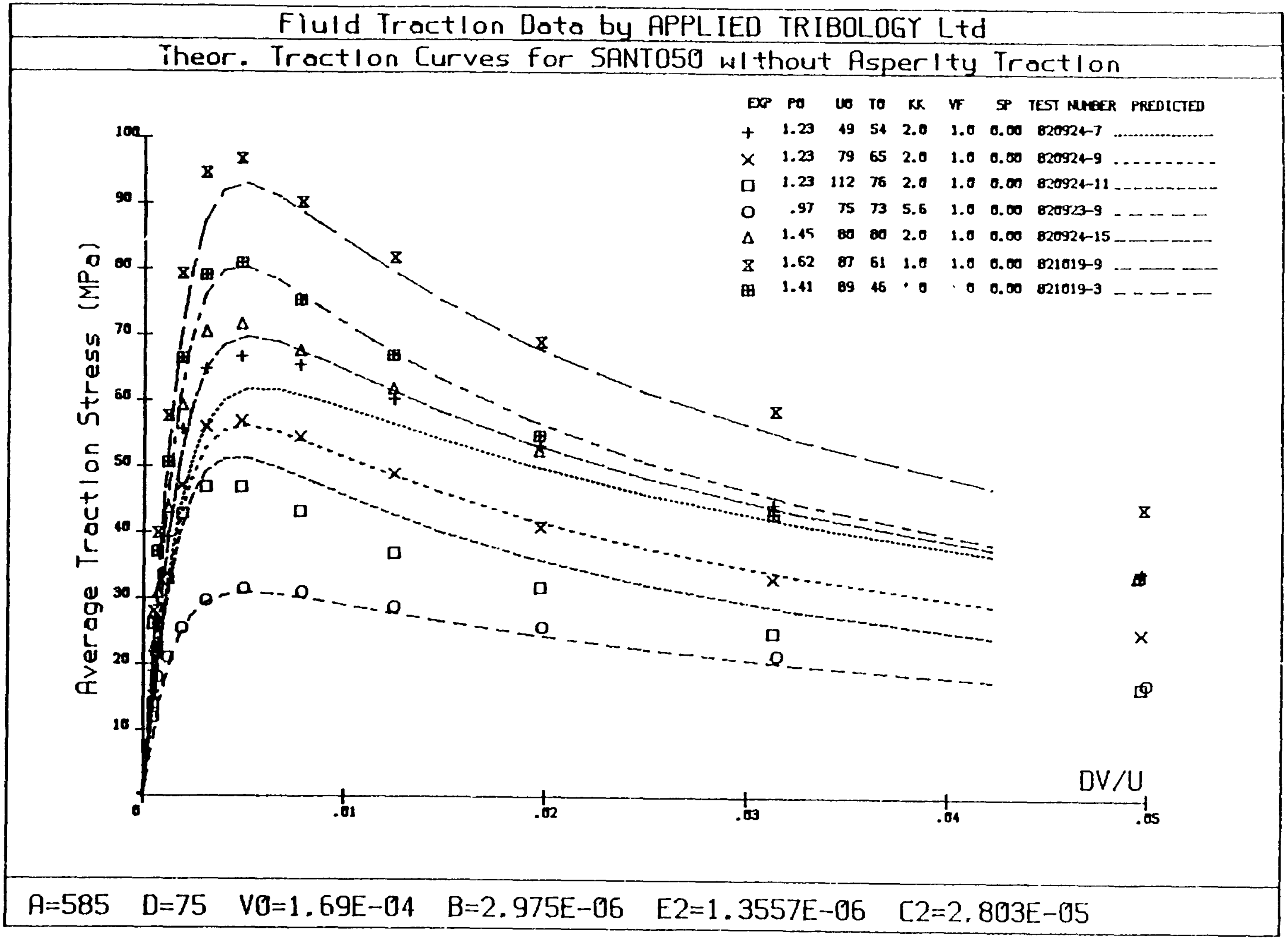

Fig. 6-8 Comparison of experimental with theoretically predicted traction curves for SANTO50 based upon multiple curve fitted thermal constants and shear modulus at various pressures, temperatures, rolling velocities and aspect ratios.

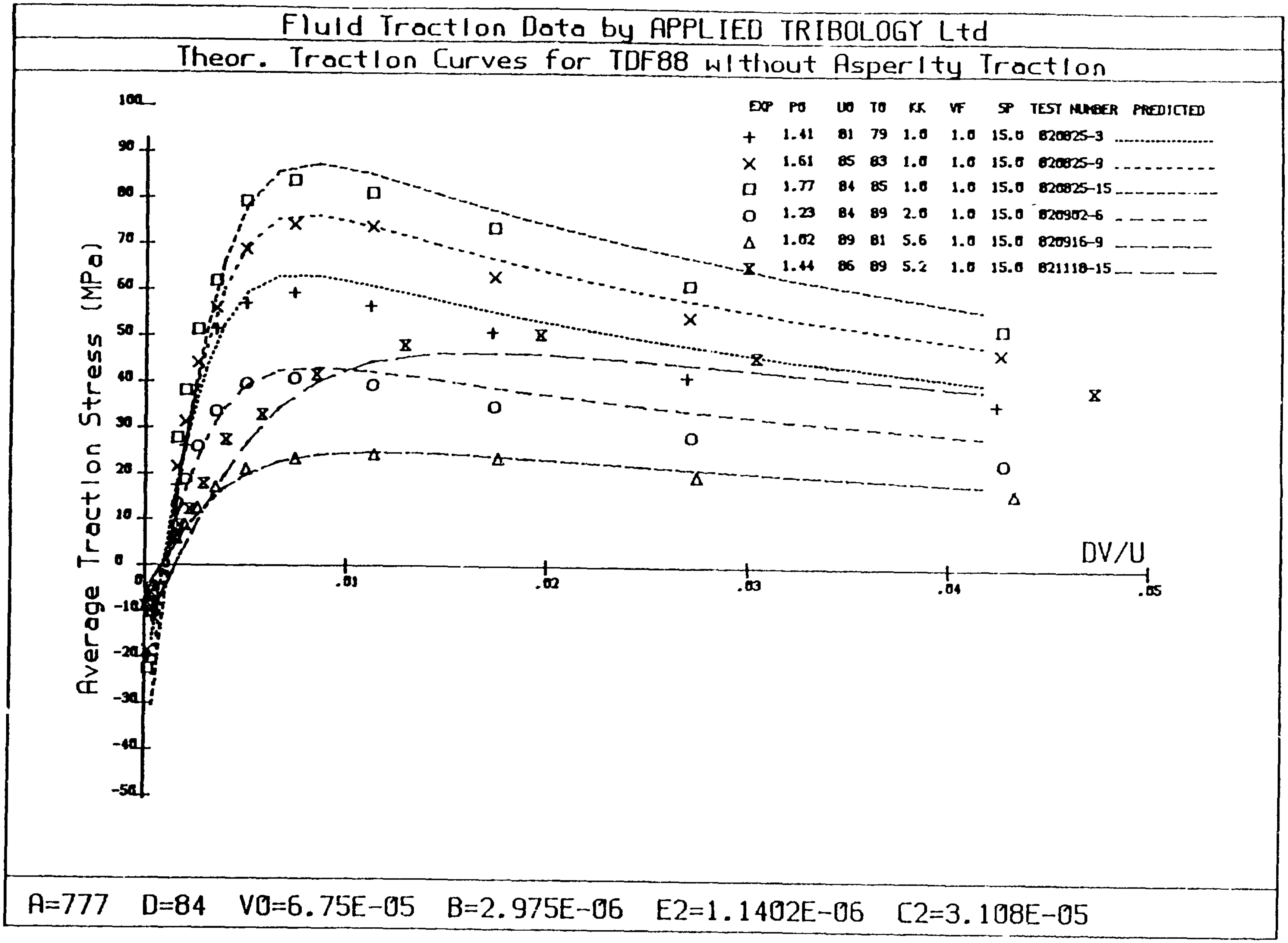

Fig. 6-9 Comparison of experimental with theoretically predicted traction curves for TDF88 based upon multiple curve fitted thermal constants and shear modulus at various pressures, temperatures, rolling velocities, spin and aspect ratios.

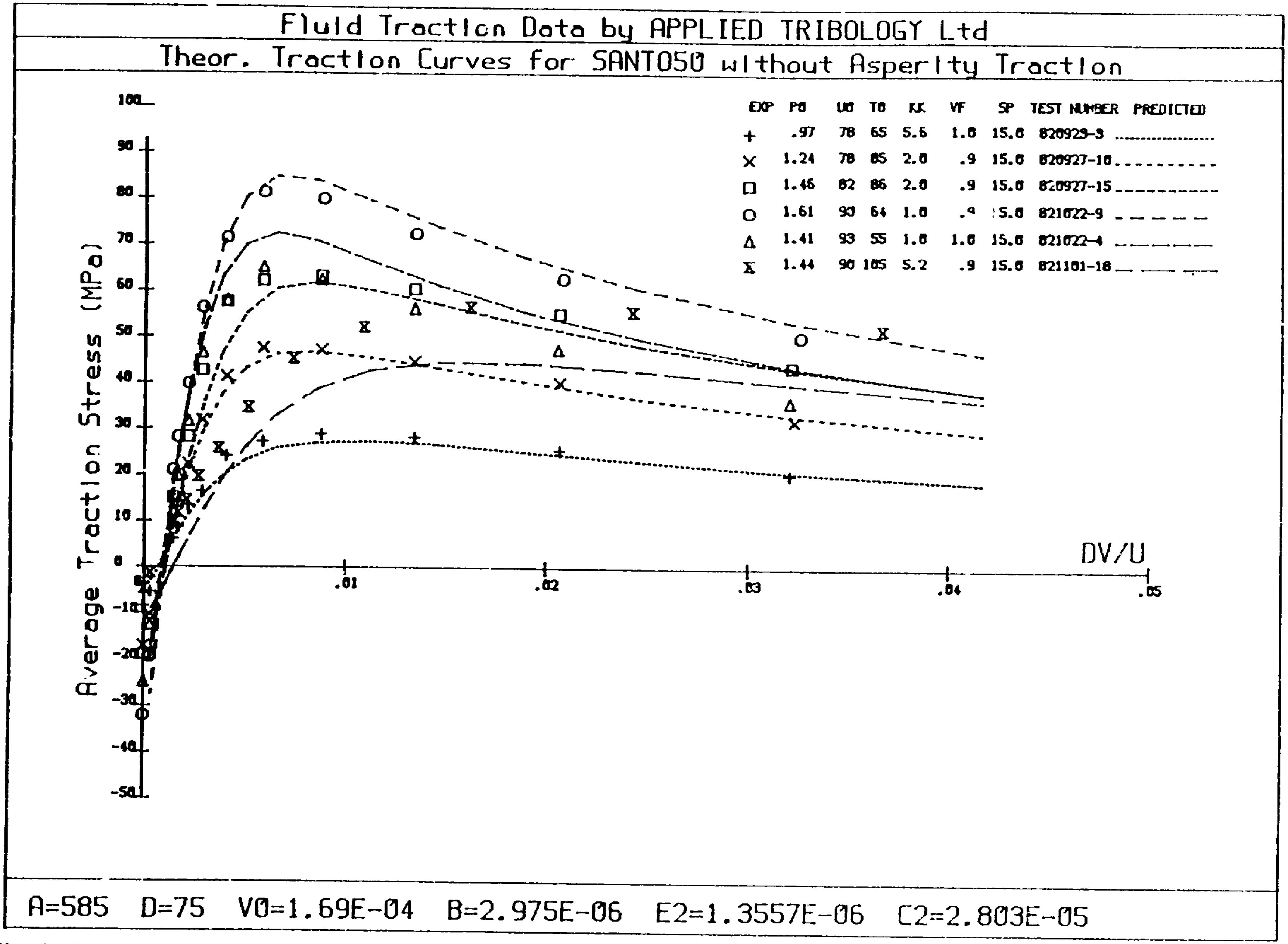

Fig. 6-10 Comparison of experimental with theoretically predicted traction curves for SANTO50 based upon multiple curve fitted thermal constants and shear modulus at various pressures, temperatures, rolling velocities, spin and aspect ratios.

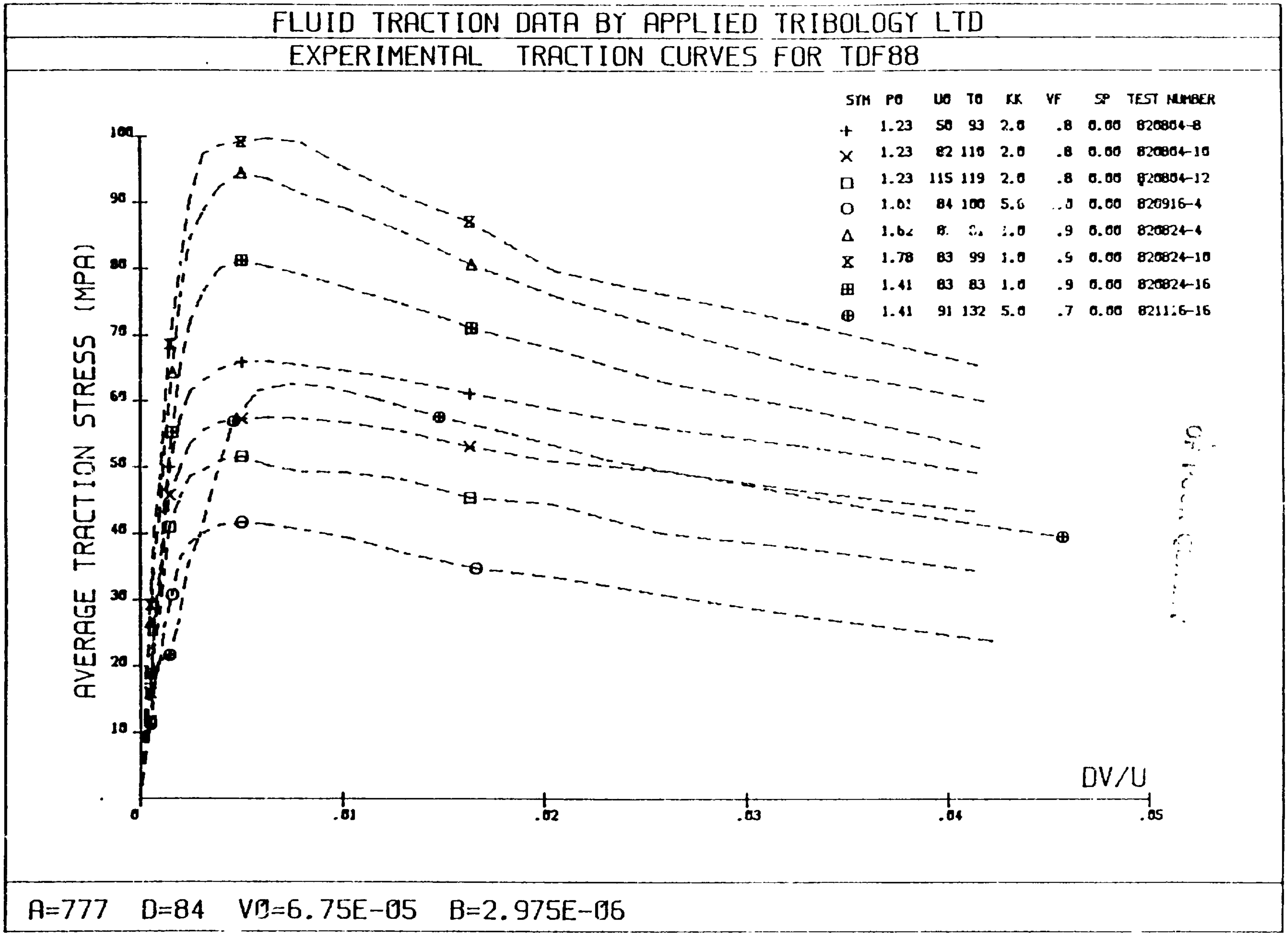

Fig. 6-11 Experimental traction curves for TDF88 under starved conditions at various pressures, temperatures, rolling velocities and aspect ratios.

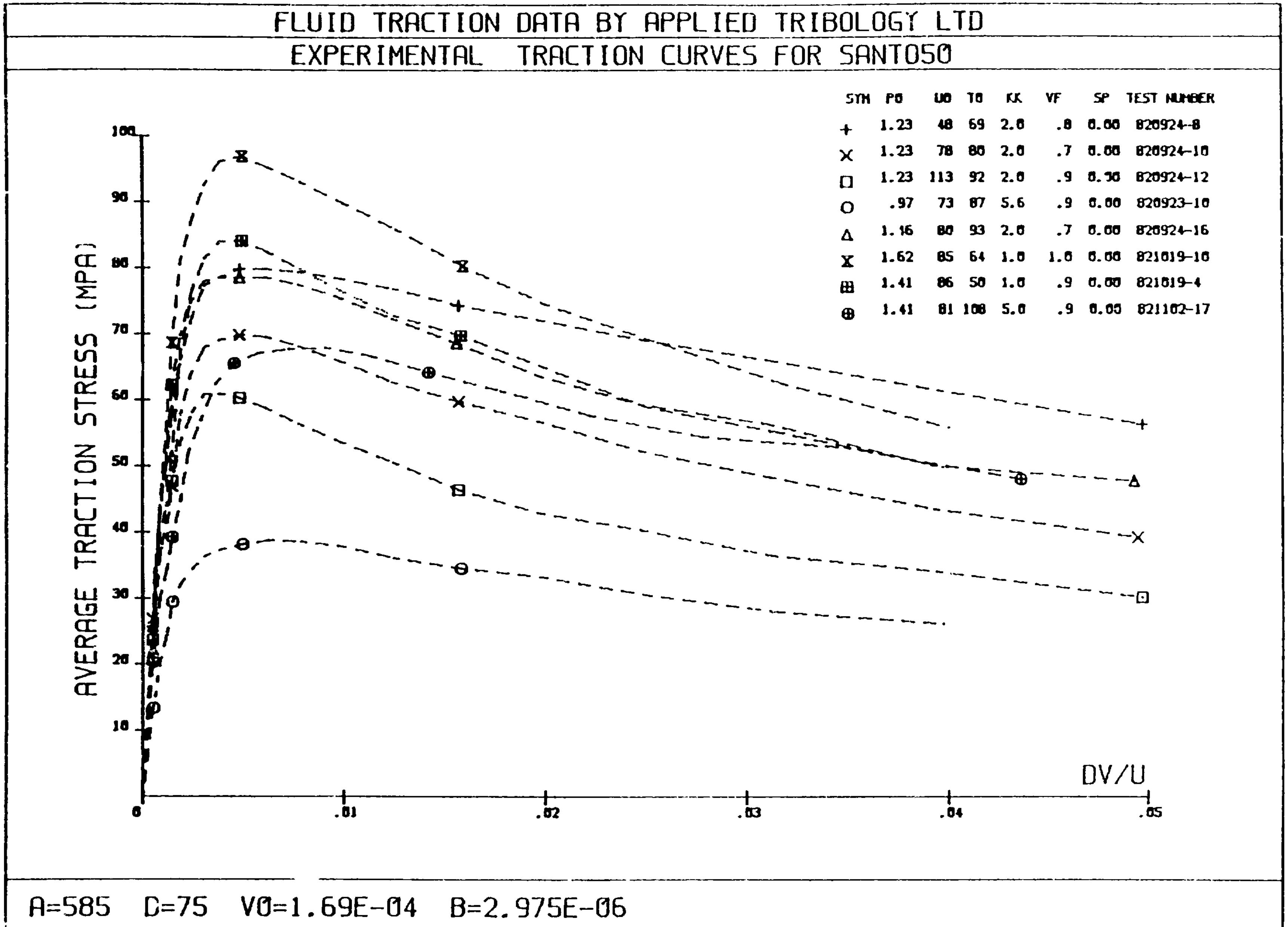

Fig. 6-12 Experimental traction curves for SANTO50 under starved conditions at various pressures, temperatures, rolling velccities and aspect ratic..

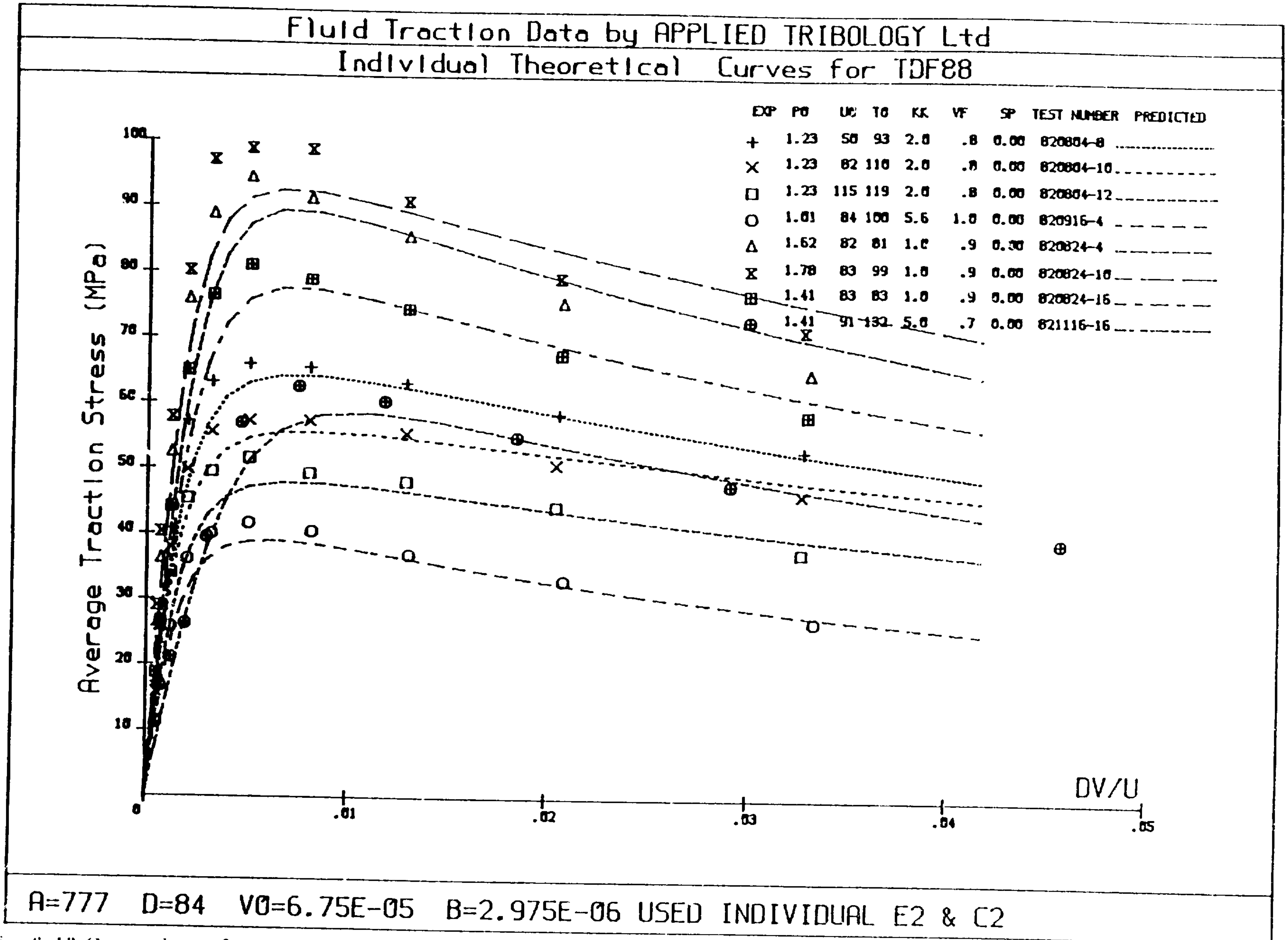

Fig. 6-13 Comparison of experimental with theoretically predicted traction curves for TDF88 under starved conditions based upon individually fitted thermal constants and shear modulus at various pressures, temperatures, rolling velocities and aspect ratios.

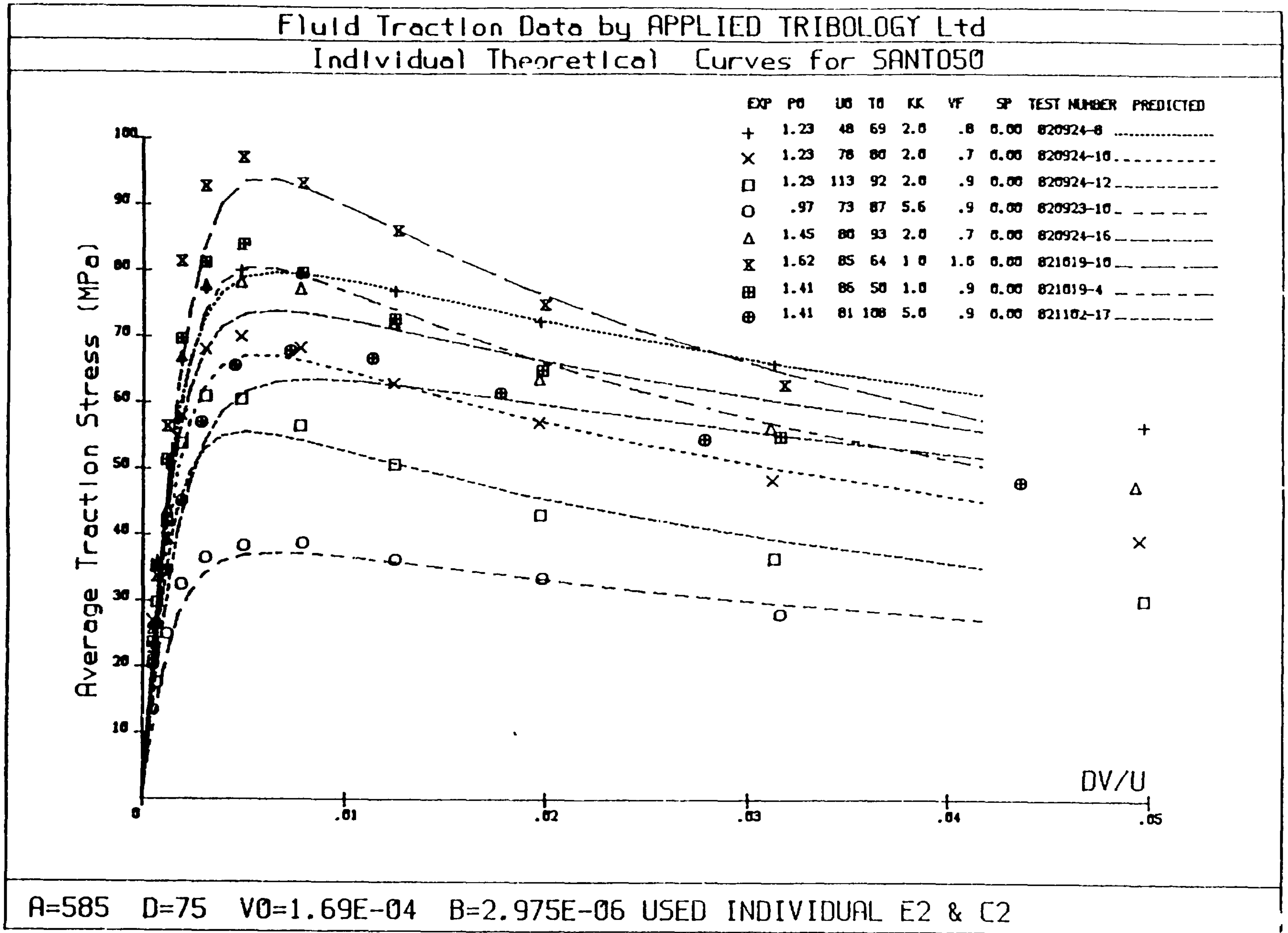

Fig. 6-14 Comparison of experimental with theoretically predicted traction curves for SANTO50 under starved conditions based upon individually fitted thermal constants and shear modulus at various pressures, temperatures, rolling velocities and aspect ratios.

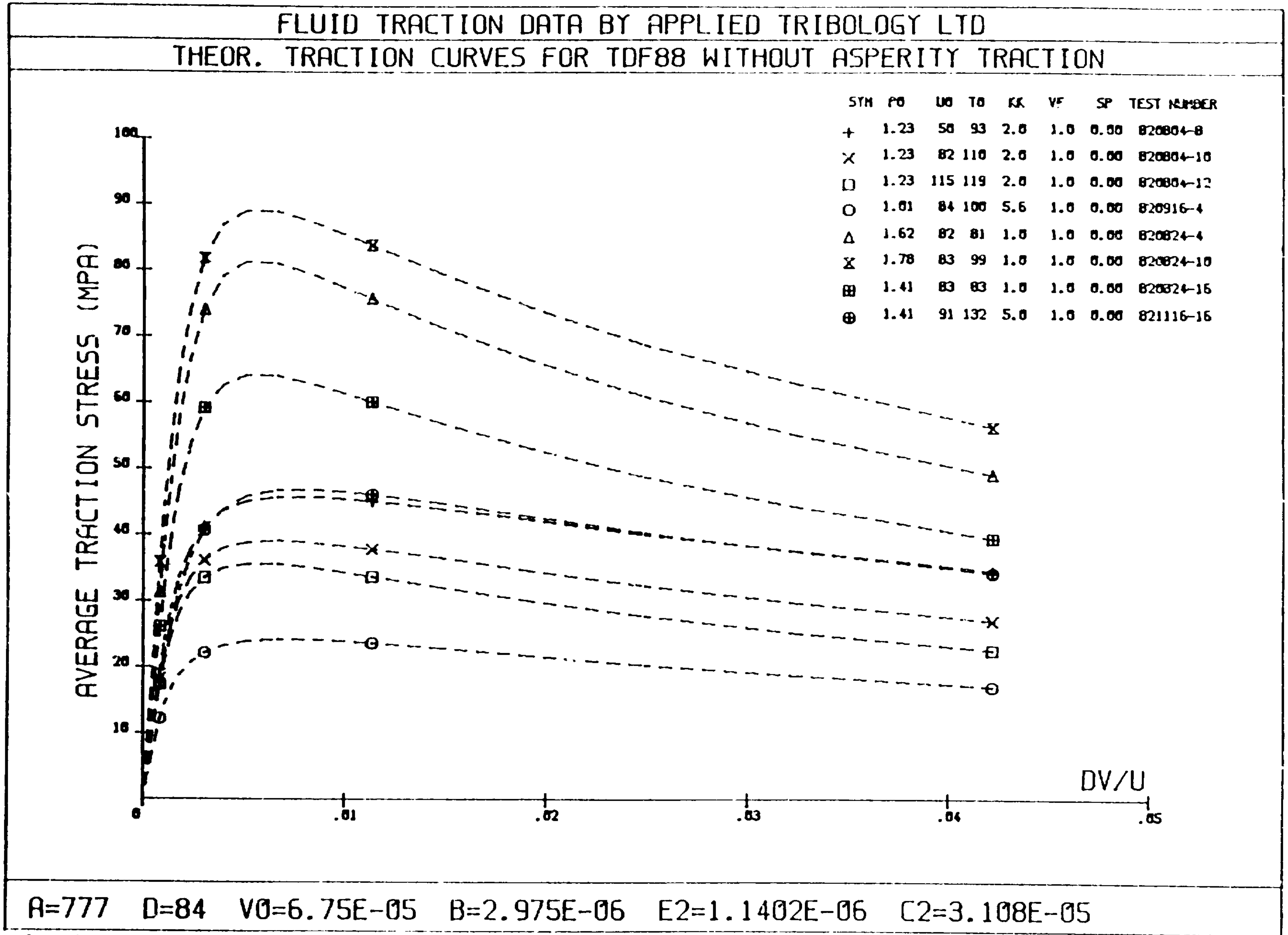

Fig. 6-15 Theoretically predicted traction curves for TDF88 under assumed fully flooded conditions based upon multiple curve fitted thermal constants and shear modulus at various pressures, temperatures, rolling velocities and aspect ratios.

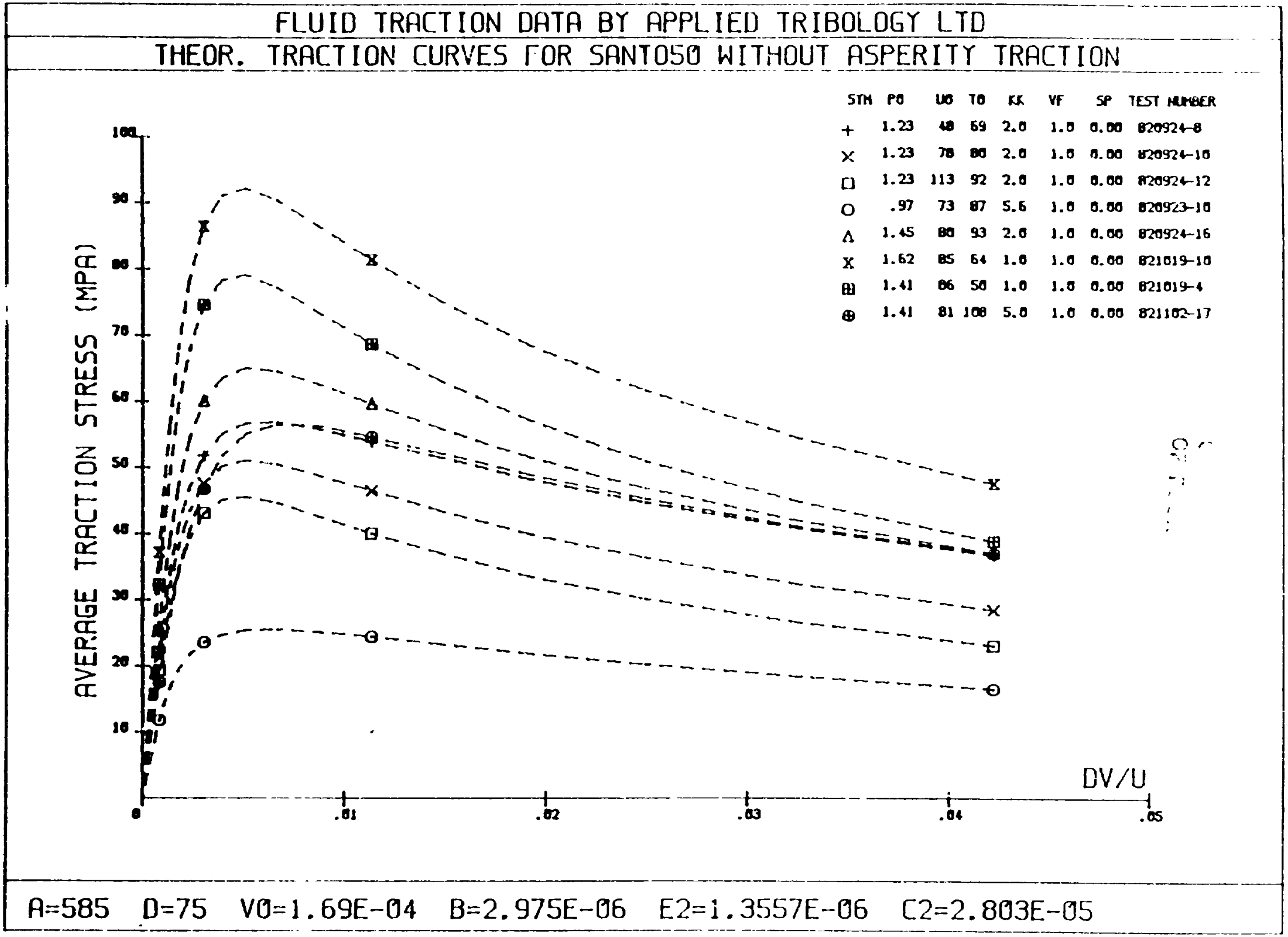

Fig. 6-16 Theoretically predicted traction curves for SANTO50 under assumed fully flooded conditions based upon multiple curve fitted thermal constants and shear modulus at various pressures, temperatures, rolling velocities and aspect ratios.

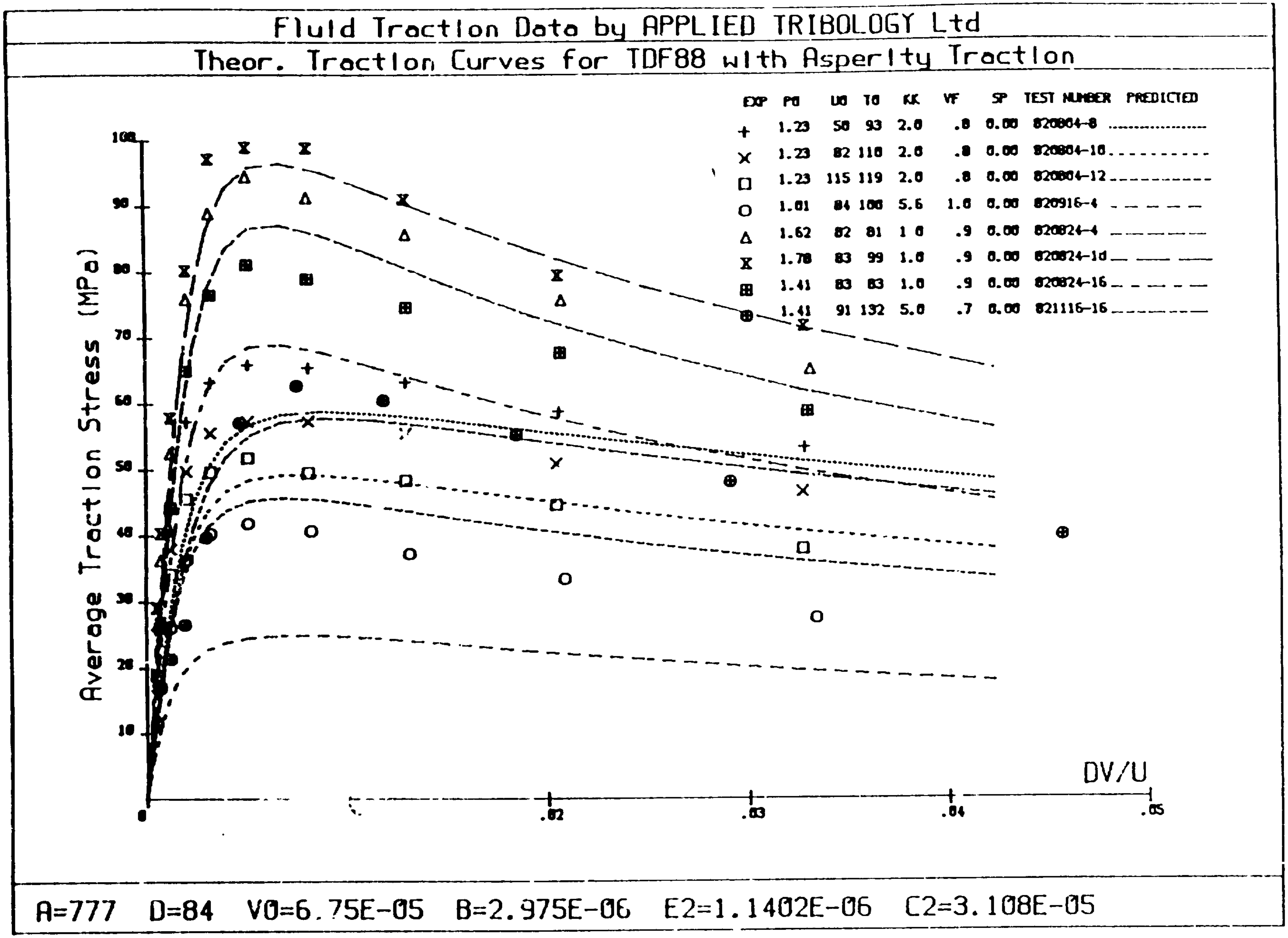

Fig. 6-17 Comparison of experimental with theoretically predicted traction curves for TDF88 including asperity traction due to starved conditions based upon multiple curve fitted thermal constants and shear modulus at various pressures, temperatures, rolling velocities and aspect ratios.

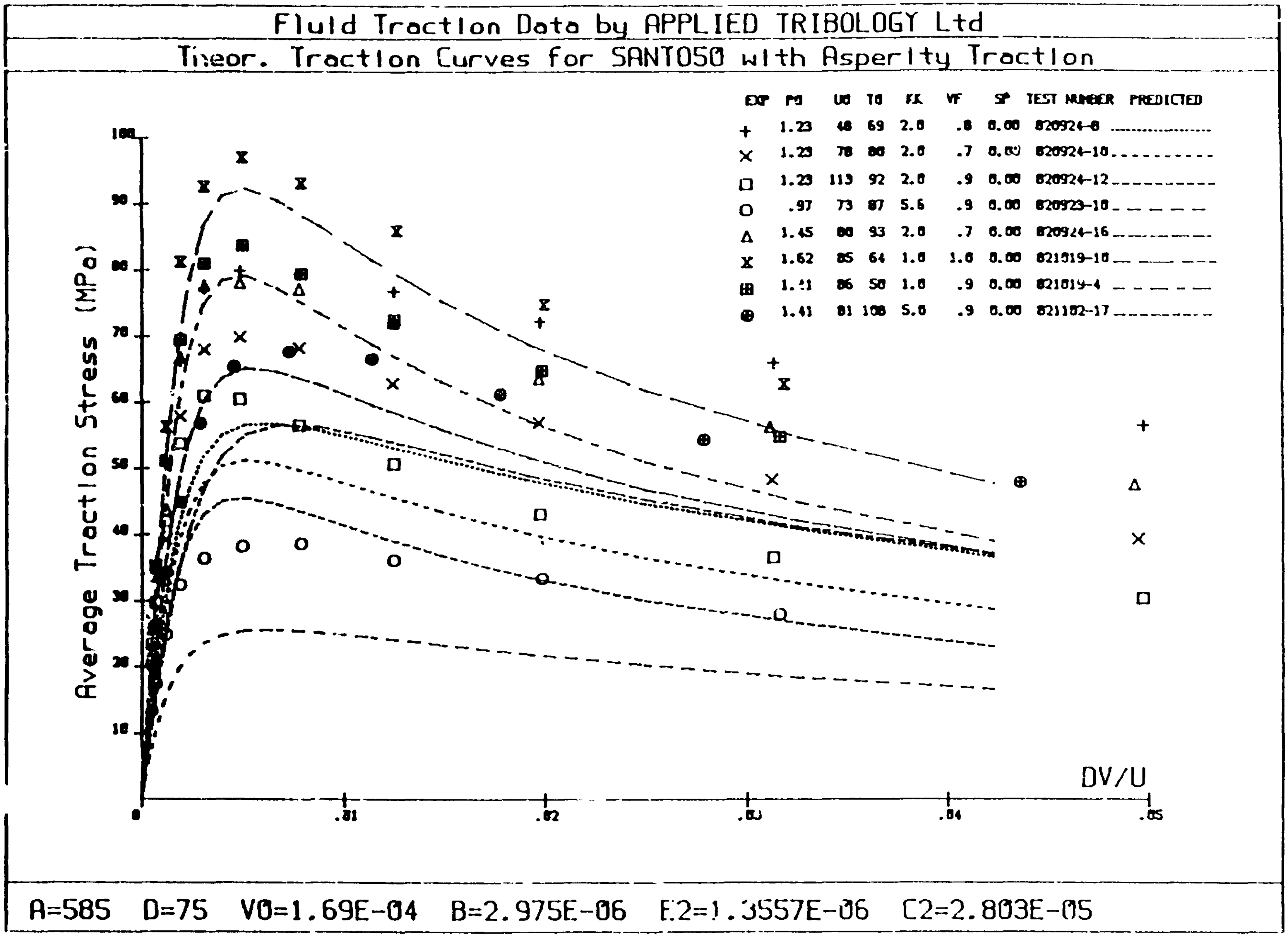

Fig. 6-18 Comparison of experimental with theoretically predicted traction curves for SANTO50 including asperity traction due to starved conditions based upon multiple curve fitted thermal constants and shear modulus at various pressures, temperatures, rolling velocities and aspect ratios.

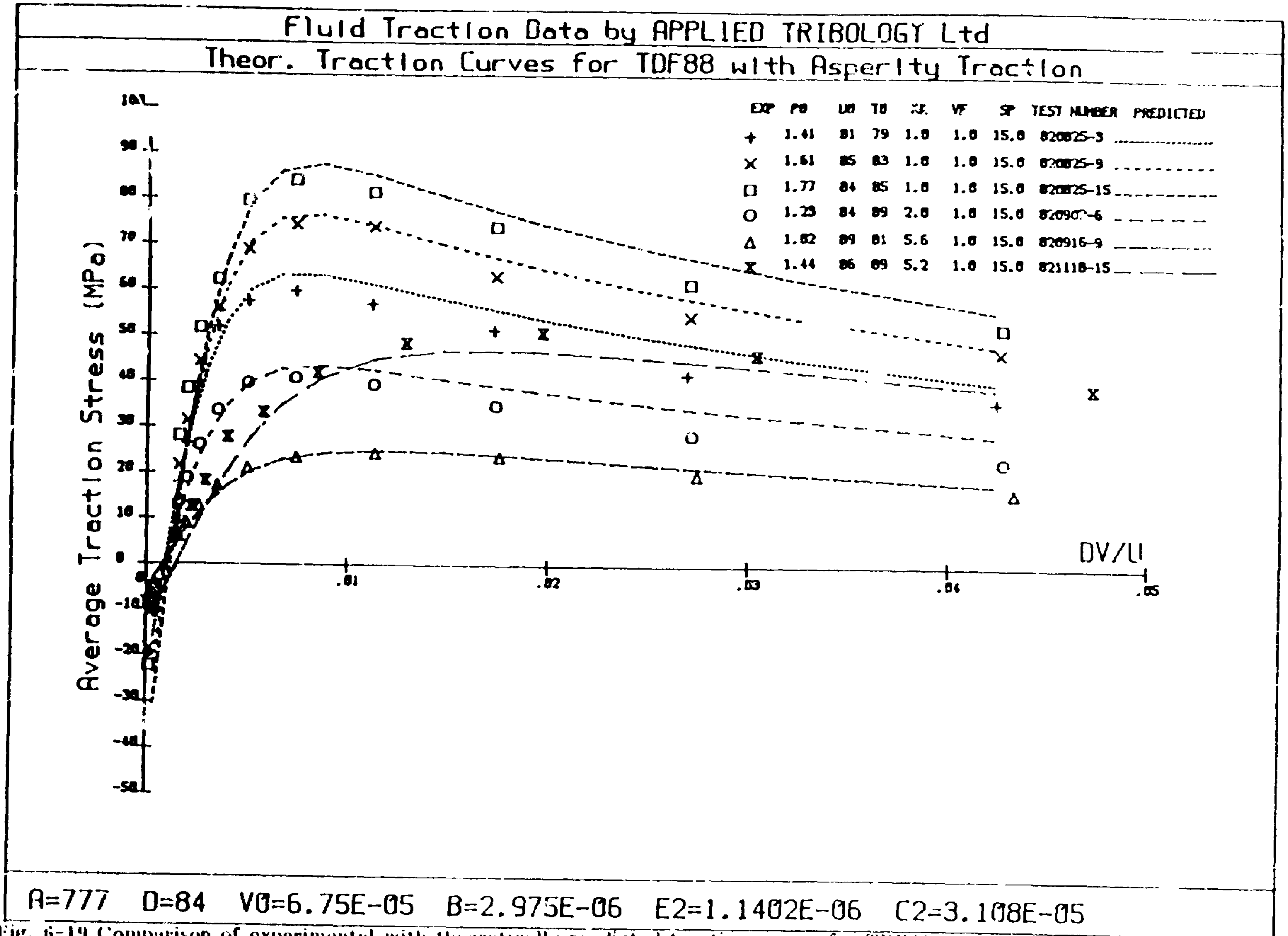

Fig. 6-19 Comparison of experimental with theoretically predicted traction curves for TDF88 including asperity traction due to starved conditions based upon multiple curve fitted thermal constants and shear modulus at various pressures, temperatures, rolling velocities, spin and aspect ratios.

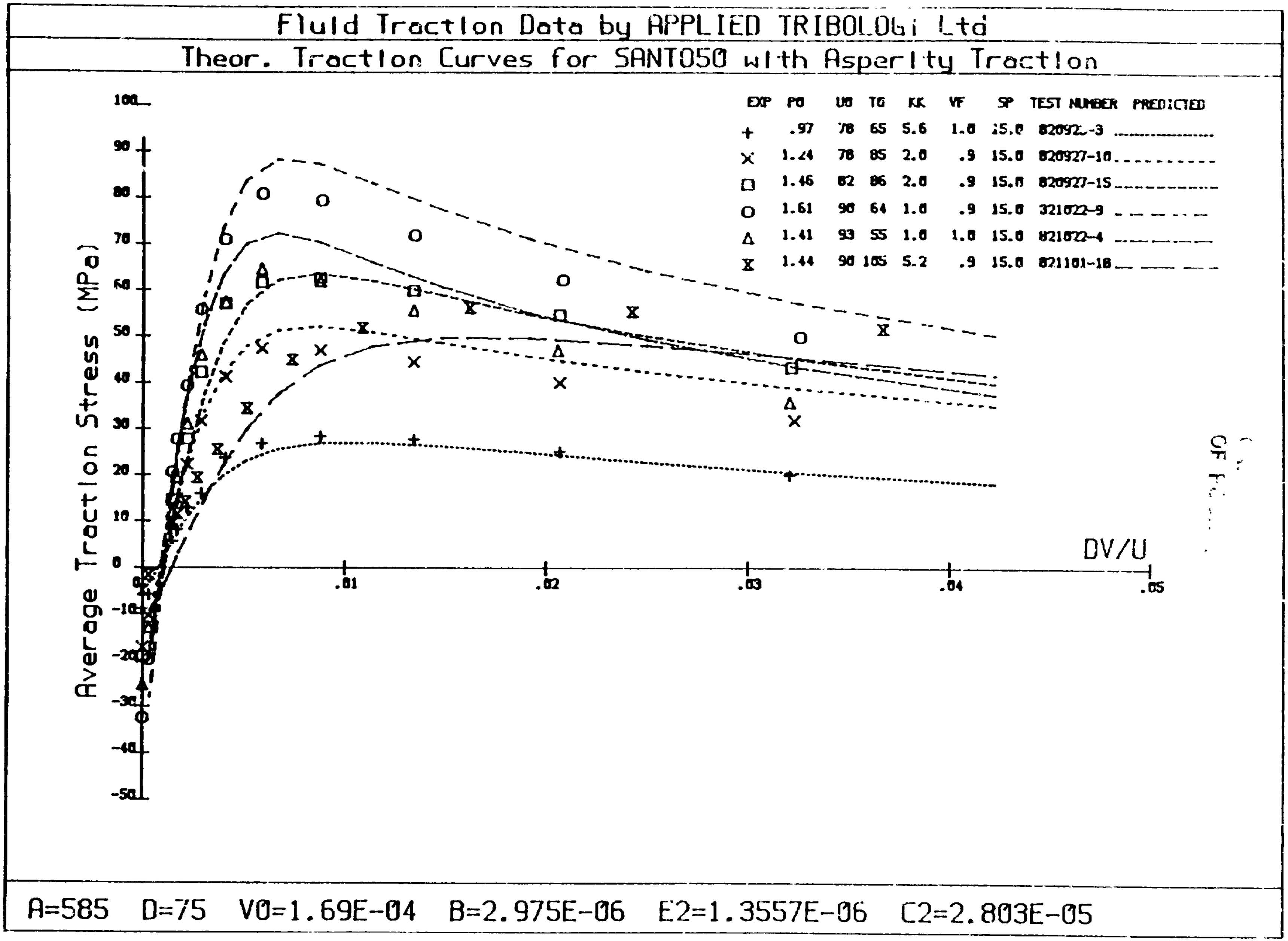

Fig. 6-20 Comparison of experimental with theoretically predicted traction curves for SANTO50 including asperity traction due to starved conditions based upon multiple curve fitted thermal constants and shear modulus at various pressures, temperatures, rolling velocities, spin and aspect ratios.

C-2

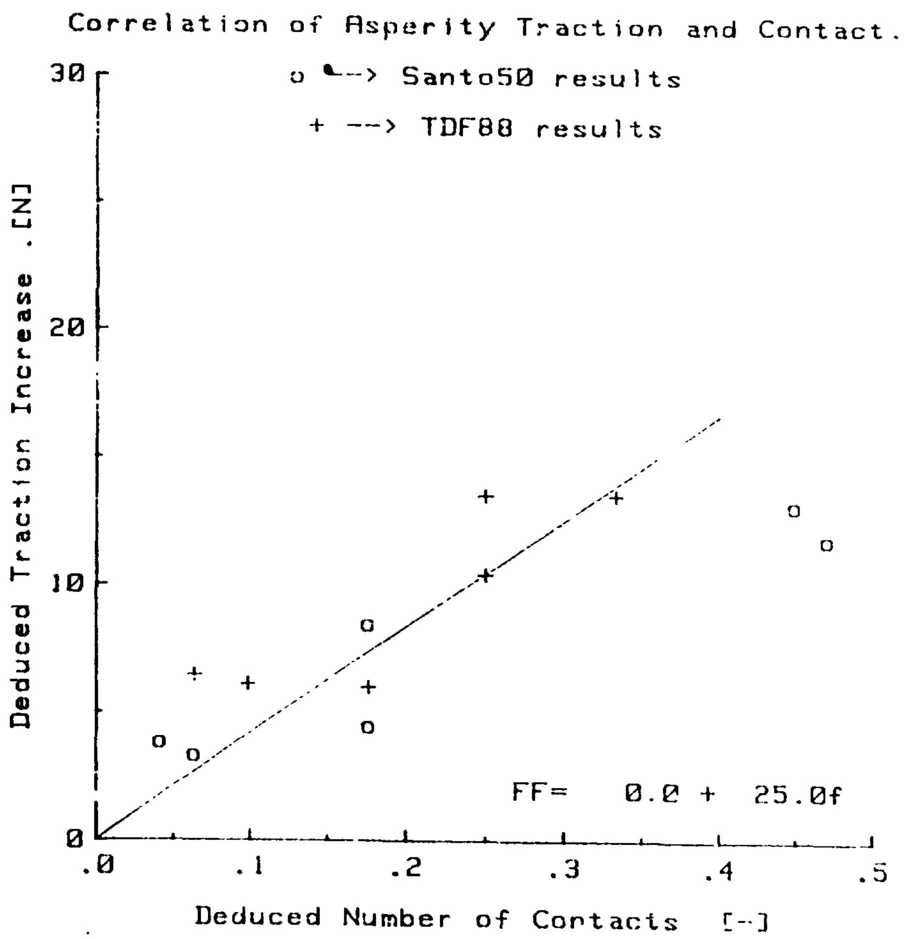

Fig. 6-22 Correlation between the asperity traction and the number of contacts as deduced from the voltage fraction.

APPENDIX I SUMMARY OF THE TRACTION TEST DATA.

The traction tests performed under this contract are summarized in this Appendix. The nomenclature used is as follows;

Test #	Number of the particular test	(YYMMDD-##)
Po	Maximum calculated Hertz contact stress	(GPa)
Uo	Surface rolling velocity in linear region	(m/sec)
To	Disc surface temperature in linear region	('C)
SP	Angle of tilt for spin	(')
VF	No-contact voltage fraction	(-)
RX	Equivalent rolling radius of discs	(mm)
RY	Equivalent transverse radius of discs	(mm)
e	Curvature offset for RY	(mm)
DS	Dimensionless spin (ab/U)	(-)
KK	Contact aspect ratio (b/a)	(-)
A	Semi contact size in rolling direction	(mm)
MS	Slope of curve in linear region	(-)
MU	Peak traction coefficient	(-)

SUMMARY OF TRACTION TEST DATA ON TDF88

TEST #	P0 GPa	U0 m/s	T0 °C	SP	VF	RX mm	RY mm	e mm	DS	KK	A mm	MS	MU
820804-1	1.073	50	71	0.0	1.00	19.1	54.0	-21.0	0.000	2.0	.30	32	.063
820804-2	1.073	52	81	0.0	0.00	19.1	54.0	-21.0	0.000	2.0	.30	46	.079
820804-3	1.073	85	86	0.0	1.00	19.1	54.0	-21.0	0.000	2.0	.30	32	.062
820804-4	1.073	85	98	0.0	0.00	19.1	54.0	-21.0	0.000	2.0	.30	35	.067
820804-5	1.073	113	109	0.0	0.00	19.1	54.0	-21.0	0.000	2.0	.30	40	.060
820804-6	1.073	117	102	0.0	1.00	19.1	54.0	-21.0	0.000	2.0	.30	36	.051
820804-7	1.228	53	86	0.0	1.00	19.1	54.0	-21.0	0.000	2.0	.35	37	.069
820804-8	1.228	50	93	0.0	.75	19.1	54.0	-21.0	0.000	2.0	.35	40	.080
820804-9	1.228	85	97	0.0	1.00	19.1	54.0	-21.0	0.000	2.0	.35	38	.064
820804-10	1.228	82	110	0.0	.80	19.1	54.0	-21.0	0.000	2.0	.35	38	.070
820804-11	1.228	119	96	0.0	1.00	19.1	54.0	-21.0	0.000	2.0	.35	36	.060
820804-12	1.228	115	119	0.0	.80	19.1	54.0	-21.0	0.000	2.0	.35	31	.063
820805-1	1.456	51	116	0.0	1.00	19.1	54.0	-21.0	0.000	2.0	.41	33	.067
820805-2	1.456	51	126	0.0	.69	19.1	54.0	-21.0	0.000	2.0	.41	37	.079
820805-3	1.456	82	118	0.0	1.00	19.1	54.0	-21.0	0.000	2.0	.41	32	.065
820805-4	1.456	82	126	0.0	.80	19.1	54.0	-21.0	0.000	2.0	.41	38	.069
820805-5	1.456	106	103	0.0	1.00	19.1	54.0	-21.0	0.000	2.0	.41	30	.055
820805-6	1.456	100	118	0.0	.80	19.1	54.0	-21.0	0.000	2.0	.41	40	.068
820824-1	1.618	49	61	0.0	1.00	19.1	19.1	14.0	0.000	1.0	.42	38	.084
820824-2	1.618	49	68	0.0	.91	19.1	19.1	14.0	0.000	1.0	.42	38	.095
820824-3	1.618	83	72	0.0	1.00	19.1	19.1	14.0	0.000	1.0	.42	30	.078
820824-4	1.618	82	81	0.0	.91	19.1	19.1	14.0	0.000	1.0	.42	39	.088
820824-5	1.618	118	88	0.0	1.00	19.1	19.1	14.0	0.000	1.0	.42	32	.072
820824-6	1.618	116	101	0.0	.75	19.1	19.1	14.0	0.000	1.0	.42	40	.077
820824-7	1.781	48	83	0.0	1.00	19.1	19.1	14.0	0.000	1.0	.46	38	.085
820824-8	1.781	45	89	0.0	.81	19.1	19.1	14.0	0.000	1.0	.46	42	.090
820824-9	1.781	82	89	0.0	1.00	19.1	19.1	14.0	0.000	1.0	.46	40	.077
820824-10	1.781	83	99	0.0	.85	19.1	19.1	14.0	0.000	1.0	.46	38	.083
820824-11	1.781	119	78	0.0	1.00	19.1	19.1	14.0	0.000	1.0	.46	38	.075
820824-12	1.781	117	95	0.0	.88	19.1	19.1	14.0	0.000	1.0	.46	35	.080
820824-13	1.414	49	74	0.0	1.00	19.1	19.1	14.0	0.000	1.0	.37	37	.082

SUMMARY OF TRACTION TEST DATA ON TDF88

TEST #	PO	UO	TO	SP	VF	RX	RY	e	DS	KK	A	MS	MU
----	GPa	m/s	'C	'	--	mm	mm	mm	--	--	mm	--	--
820824-13	1.414	49	74	0.0	1.00	19.1	19.1	14.0	0.000	1.0	.37	37	.082
820824-14	1.414	49	77	0.0	.94	19.1	19.1	14.0	0.000	1.0	.37	42	.091
820824-15	1.414	84	77	0.0	1.00	19.1	19.1	14.0	0.000	1.0	.37	39	.074
820824-16	1.414	83	83	0.0	.94	19.1	19.1	14.0	0.000	1.0	.37	35	.085
820824-17	1.414	115	88	0.0	1.00	19.1	19.1	14.0	0.000	1.0	.37	36	.069
820824-18	1.414	114	98	0.0	.78	19.1	19.1	14.0	0.000	1.0	.37	39	.077
820825-1	1.409	49	72	15.0	1.00	19.3	19.1	14.0	.0029	1.0	.37	0	.077
820825-2	1.409	49	77	15.0	.96	19.3	19.1	14.0	.0029	1.0	.37	0	.081
820825-3	1.409	81	79	15.0	1.00	19.3	19.1	14.0	.0029	1.0	.37	0	.063
820825-4	1.409	83	89	15.0	.97	19.3	19.1	14.0	.0029	1.0	.37	0	.075
820825-5	1.409	120	97	15.0	1.00	19.3	19.1	14.0	.0029	1.0	.37	0	.058
820825-6	1.409	116	109	15.0	.60	19.3	19.1	14.0	.0029	1.0	.37	0	.065
820825-7	1.613	50	74	15.0	1.00	19.3	19.1	14.0	.0034	1.0	.42	0	.080
820825-8	1.613	49	81	15.0	0.00	19.3	19.1	14.0	.0034	1.0	.42	0	.083
820825-9	1.613	85	83	15.0	1.00	19.3	19.1	14.0	.0034	1.0	.42	0	.068
820825-10	1.613	87	94	15.0	.94	19.3	19.1	14.0	.0034	1.0	.42	0	.076
820825-11	1.613	117	100	15.0	1.00	19.3	19.1	14.0	.0034	1.0	.42	0	.063
820825-12	1.613	120	114	15.0	.60	19.3	19.1	14.0	.0034	1.0	.42	0	.070
820825-13	1.775	49	70	15.0	1.00	19.3	19.1	14.0	.0037	1.0	.47	0	.081
820825-14	1.775	48	79	15.0	.96	19.3	19.1	14.0	.0037	1.0	.47	0	.085
820825-15	1.775	84	85	15.0	1.00	19.3	19.1	14.0	.0037	1.0	.47	0	.070
820825-16	1.775	84	98	15.0	.85	19.3	19.1	14.0	.0037	1.0	.47	0	.077
820825-17	1.775	120	105	15.0	1.00	19.3	19.1	14.0	.0037	1.0	.47	0	.065
820825-18	1.775	118	120	15.0	.64	19.3	19.1	14.0	.0037	1.0	.47	0	.071
820826-1	1.780	50	53	7.5	1.00	19.2	19.1	14.0	.0018	1.0	.46	0	.085
820826-2	1.780	50	66	7.5	0.00	19.2	19.1	14.0	.0018	1.0	.46	0	.096
820826-3	1.780	91	83	7.5	.96	19.2	19.1	14.0	.0018	1.0	.46	0	.085
820826-4	1.780	92	82	7.5	1.00	19.2	19.1	14.0	.0018	1.0	.46	0	.074
820826-5	1.780	118	96	7.5	.89	19.2	19.1	14.0	.0018	1.0	.46	0	.073
820826-6	1.780	119	110	7.5	.64	19.2	19.1	14.0	.0018	1.0	.46	0	.076
820826-7	1.617	50	59	7.5	1.00	19.2	19.1	14.0	.0017	1.0	.42	0	.082

SUMMARY OF TRACTION TEST DATA ON TDF88

TEST #	PO GPa	UO m/s	TO °C	SP °	VF --	RX mm	RY mm	e mm	DS --	KK --	A mm	MS --	MU --
820826-7	1.617	50	59	7.5	1.00	19.2	19.1	14.0	.0017	1.0	.42	0	.082
820826-8	1.617	51	68	7.5	.91	19.2	19.1	14.0	.0017	1.0	.42	0	.093
820826-9	1.617	83	79	7.5	.91	19.2	19.1	14.0	.0017	1.0	.42	0	.086
820826-10	1.617	80	79	7.5	1.00	19.2	19.1	14.0	.0017	1.0	.42	0	.074
820826-11	1.617	124	91	7.5	1.00	19.2	19.1	14.0	.0017	1.0	.42	0	.068
820826-12	1.617	127	105	7.5	.64	19.2	19.1	14.0	.0017	1.0	.42	0	.075
820826-13	1.412	48	65	7.5	1.00	19.2	19.1	14.0	.0015	1.0	.37	0	.081
820826-14	1.412	52	73	7.5	.96	19.2	19.1	14.0	.0015	1.0	.37	0	.092
820826-15	1.412	86	80	7.5	.91	19.2	19.1	14.0	.0015	1.0	.37	0	.084
820826-16	1.412	86	79	7.5	1.00	19.2	19.1	14.0	.0015	1.0	.37	0	.067
820826-17	1.412	125	91	7.5	.93	19.2	19.1	14.0	.0015	1.0	.37	0	.065
820826-18	1.412	125	102	7.5	.81	19.2	19.1	14.0	.0015	1.0	.37	0	.072
820831-1	1.456	29	68	0.0	1.00	19.1	54.0	-21.0	0.000	2.0	.41	36	.078
820831-2	1.458	27	68	7.5	1.00	19.0	54.0	-21.0	.0023	2.0	.41	0	.073
820831-3	1.458	31	83	7.5	0.00	19.0	54.0	-21.0	.0023	2.0	.41	0	.081
820831-4	1.458	58	78	7.5	1.00	19.0	54.0	-21.0	.0023	2.0	.41	0	.062
820831-5	1.458	63	99	7.5	0.00	19.0	54.0	-21.0	.0023	2.0	.41	0	.072
820831-6	1.458	91	99	7.5	1.00	19.0	54.0	-21.0	.0023	2.0	.41	0	.054
820831-7	1.458	91	113	7.5	.96	19.0	54.0	-21.0	.0023	2.0	.41	0	.064
820831-8	1.230	49	62	7.5	1.00	19.0	54.0	-21.0	.0019	2.0	.34	0	.055
820831-9	1.230	46	77	7.5	.94	19.0	54.0	-21.0	.0019	2.0	.34	0	.076
820831-10	1.230	79	81	7.5	1.00	19.0	54.0	-21.0	.0019	2.0	.34	0	.048
820831-11	1.230	78	95	7.5	0.00	19.0	54.0	-21.0	.0019	2.0	.34	0	.066
820831-12	1.230	98	95	7.5	1.00	19.0	54.0	-21.0	.0019	2.0	.34	0	.046
820831-13	1.230	99	105	7.5	.85	19.0	54.0	-21.0	.0019	2.0	.34	0	.059
820831-14	1.074	46	66	7.5	1.00	19.0	54.0	-21.0	.0017	2.0	.30	0	.047
820831-15	1.074	50	82	7.5	0.00	19.0	54.0	-21.0	.0017	2.0	.30	0	.069
820831-16	1.074	82	82	7.5	1.00	19.0	54.0	-21.0	.0017	2.0	.30	0	.038
820831-17	1.074	85	99	7.5	.96	19.0	54.0	-21.0	.0017	2.0	.30	0	.059
820831-18	1.074	114	98	7.5	1.00	19.0	54.0	-21.0	.0017	2.0	.30	0	.035
820831-19	1.074	115	110	7.5	.89	19.0	54.0	-21.0	.0017	2.0	.30	0	.051

SUMMARY OF TRACTION TEST DATA ON TDF88

TEST #	PO	UO	TO	SP	VF	RX	RY	e	DS	KK	A	MS	MU
----	GPa	m/s	°C	°	--	mm	mm	mm	--	--	mm	--	--
820902-1	1.228	48	72	0.0	1.00	19.1	54.0	-21.0	0.000	2.0	.35	34	.060
820902-2	1.228	83	83	0.0	1.00	19.1	54.0	-21.0	0.000	2.0	.35	23	.051
820902-3	1.228	117	96	0.0	1.00	19.1	54.0	-21.0	0.000	2.0	.35	28	.050
820902-4	1.235	46	78	15.0	1.00	18.8	54.0	-21.0	.0040	2.0	.34	0	.059
820902-5	1.235	47	86	15.0	0.00	18.8	54.0	-21.0	.0040	2.0	.34	0	.065
820902-6	1.235	84	89	15.0	1.00	18.8	54.0	-21.0	.0040	2.0	.34	0	.050
820902-7	1.235	83	103	15.0	.97	18.8	54.0	-21.0	.0040	2.0	.34	0	.056
820902-8	1.235	107	80	15.0	1.00	18.8	54.0	-21.0	.0040	2.0	.34	0	.047
820902-9	1.235	99	97	15.0	0.00	18.8	54.0	-21.0	.0040	2.0	.34	0	.057
820903-1	1.073	49	56	0.0	1.00	19.1	54.0	-21.0	0.000	2.0	.30	27	.051
820903-2	1.073	85	69	0.0	1.00	19.1	54.0	-21.0	0.000	2.0	.30	21	.045
820903-3	1.073	115	81	0.0	1.00	19.1	54.0	-21.0	0.000	2.0	.30	35	.051
820903-4	1.078	47	60	15.0	1.00	18.8	54.0	-21.0	.0035	2.0	.30	0	.050
820903-5	1.078	84	77	15.0	1.00	18.8	54.0	-21.0	.0035	2.0	.30	0	.043
820903-6	1.078	84	95	15.0	0.00	18.8	54.0	-21.0	.0035	2.0	.30	0	.056
820903-7	1.078	48	91	15.0	.94	18.8	54.0	-21.0	.0035	2.0	.30	0	.061
820903-8	1.078	113	95	15.0	1.00	18.8	54.0	-21.0	.0035	2.0	.30	0	.042
820903-9	1.078	113	87	15.0	0.00	18.8	54.0	-21.0	.0035	2.0	.30	0	.052
820904-1	1.456	31	66	0.0	1.00	19.1	54.0	-21.0	0.000	2.0	.41	43	.077
820904-2	1.456	29	78	0.0	.94	19.1	54.0	-21.0	0.000	2.0	.41	42	.090
820904-3	1.456	59	80	0.0	1.00	19.1	54.0	-21.0	0.000	2.0	.41	31	.066
820904-4	1.456	58	91	0.0	.89	19.1	54.0	-21.0	0.000	2.0	.41	42	.081
820904-5	1.456	89	87	0.0	1.00	19.1	54.0	-21.0	0.000	2.0	.41	30	.060
820904-6	1.456	86	101	0.0	.85	19.1	54.0	-21.0	0.000	2.0	.41	45	.073
820904-7	1.464	27	67	15.0	1.00	18.8	54.0	-21.0	.0047	2.0	.41	0	.069
820904-8	1.464	30	83	15.0	.98	18.8	54.0	-21.0	.0047	2.0	.41	0	.072
820904-9	1.464	61	84	15.0	1.00	18.8	54.0	-21.0	.0047	2.0	.41	0	.059
820904-10	1.464	61	99	15.0	.89	18.8	54.0	-21.0	.0047	2.0	.41	0	.064
820904-11	1.464	90	101	15.0	1.00	18.8	54.0	-21.0	.0047	2.0	.41	0	.052
820904-12	1.464	89	114	15.0	.91	18.8	54.0	-21.0	.0047	2.0	.41	0	.057
820916-1	1.008	50	71	0.0	1.00	19.1	270.0	-237.0	0.000	5.6	.32	26	.054

SUMMARY OF TRACTION TEST DATA ON TDF88

TEST #	PO	UO	TO	SP	VF	RX	RY	e	DS	KK	A	MS	MU
----	GPa	m/s	'C	'	--	mm	mm	mm	--	--	mm	--	--
820916-2	1.008	48	88	0.0	0.00	19.1	270.0	-237.0	0.000	5.6	.32	45	.081
820916-3	1.008	86	87	0.0	1.00	19.1	270.0	-237.0	0.000	5.6	.32	18	.037
820916-4	1.008	84	100	0.0	.96	19.1	270.0	-237.0	0.000	5.6	.32	35	.061
820916-5	1.008	106	102	0.0	.94	19.1	270.0	-237.0	0.000	5.6	.32	15	.033
820916-6	1.008	113	112	0.0	.80	19.1	270.0	-237.0	0.000	5.6	.32	31	.050
820916-7	1.016	48	65	15.0	1.00	18.7	270.0	-230.0	.0063	5.6	.32	0	.051
820916-8	1.016	46	78	15.0	.98	18.7	270.0	-230.0	.0063	5.6	.32	0	.060
820916-9	1.016	89	81	15.0	1.00	18.7	270.0	-230.0	.0063	5.6	.32	0	.036
820916-10	1.016	89	101	15.0	.96	18.7	270.0	-230.0	.0063	5.6	.32	0	.044
820916-11	1.016	100	97	15.0	.97	18.7	270.0	-230.0	.0063	5.6	.32	0	.032
820916-12	1.016	113	115	15.0	.89	18.7	270.0	-230.0	.0063	5.6	.32	0	.040
820916-13	1.016	31	96	15.0	.89	18.7	270.0	-230.0	.0063	5.6	.32	0	.058
820916-14	1.016	32	87	15.0	1.00	18.7	270.0	-230.0	.0063	5.6	.32	0	.060
821116-1	1.036	48	60	0.0	1.00	11.3	136.0	-121.0	0.000	5.0	.19	19	.055
821116-2	1.036	51	72	0.0	0.00	11.3	136.0	-121.0	0.000	5.0	.19	21	.067
821116-3	1.036	84	87	0.0	.94	11.3	136.0	-121.0	0.000	5.0	.19	31	.068
821116-4	1.036	84	87	0.0	1.00	11.3	136.0	-121.0	0.000	5.0	.19	18	.043
821116-5	1.036	118	94	0.0	.75	11.3	136.0	-121.0	0.000	5.0	.19	19	.042
821116-6	1.036	117	114	0.0	.50	11.3	136.0	-121.0	0.000	5.0	.19	22	.054
821116-7	1.186	51	64	0.0	1.00	11.3	136.0	-121.0	0.000	5.0	.22	24	.065
821116-8	1.186	51	76	0.0	0.00	11.3	136.0	-121.0	0.000	5.0	.22	29	.073
821116-9	1.186	84	87	0.0	.94	11.3	136.0	-121.0	0.000	5.0	.22	23	.052
821116-10	1.186	84	101	0.0	0.00	11.3	136.0	-121.0	0.000	5.0	.22	29	.071
821116-11	1.186	118	106	0.0	.80	11.3	136.0	-121.0	0.000	5.0	.22	19	.045
821116-12	1.186	118	103	0.0	0.00	11.3	136.0	-121.0	0.000	5.0	.22	28	.064
821116-13	1.406	51	71	0.0	1.00	11.3	136.0	-121.0	0.000	5.0	.26	28	.073
821116-14	1.406	51	93	0.0	0.00	11.3	136.0	-121.0	0.000	5.0	.26	32	.081
821116-15	1.406	88	102	0.0	1.00	11.3	136.0	-121.0	0.000	5.0	.26	14	.058
821116-16	1.406	91	132	0.0	.69	11.3	136.0	-121.0	0.000	5.0	.26	16	.066
821116-17	1.406	107	102	0.0	.89	11.3	136.0	-121.0	0.000	5.0	.26	26	.054
821116-18	1.406	116	133	0.0	.60	11.3	136.0	-121.0	0.000	5.0	.26	32	.064

SUMMARY OF TRACTION TEST DATA ON TDF88

TEST #	PO GPa	UO m/s	TO 'C	SP '	VF --	RX mm	RY mm	e mm	DS --	KK --	A mm	MS --	MU --
821118-1	1.062	51	64	15.0	1.00	10.6	136.0	-118.0	.0082	5.2	.19	0	.068
821118-2	1.062	51	76	15.0	.80	10.6	136.0	-118.0	.0082	5.2	.19	0	.080
821118-3	1.062	83	76	15.0	1.00	10.6	136.0	-118.0	.0082	5.2	.19	0	.053
821118-4	1.062	84	91	15.0	.80	10.6	136.0	-118.0	.0082	5.2	.19	0	.073
821118-5	1.062	111	87	15.0	1.00	10.6	136.0	-118.0	.0082	5.2	.19	0	.045
821118-6	1.062	118	103	15.0	.69	10.6	136.0	-118.0	.0082	5.2	.19	0	.072
821118-7	1.216	51	90	15.0	.80	10.6	136.0	-118.0	.0094	5.2	.21	0	.075
821118-8	1.216	51	79	15.0	1.00	10.6	136.0	-118.0	.0094	5.2	.21	0	.065
821118-9	1.216	83	83	15.0	1.00	10.6	136.0	-118.0	.0094	5.2	.21	0	.052
821118-10	1.216	85	105	15.0	.80	10.6	136.0	-118.0	.0094	5.2	.21	0	.060
821118-11	1.216	111	96	15.0	1.00	10.6	136.0	-118.0	.0094	5.2	.21	0	.045
821118-12	1.216	121	109	15.0	.75	10.6	136.0	-118.0	.0094	5.2	.21	0	.058
821118-13	1.441	51	83	15.0	.89	10.6	136.0	-118.0	.0111	5.2	.25	0	.067
821118-14	1.441	51	98	15.0	.60	10.6	136.0	-118.0	.0111	5.2	.25	0	.069
821118-15	1.441	86	89	15.0	1.00	10.6	136.0	-118.0	.0111	5.2	.25	0	.052
821118-16	1.441	87	114	15.0	.69	10.6	136.0	-118.0	.0111	5.2	.25	0	.058
821118-17	1.441	103	100	15.0	1.00	10.6	136.0	-118.0	.0111	5.2	.25	0	.048
821118-18	1.441	110	113	15.0	.75	10.6	136.0	-118.0	.0111	5.2	.25	0	.061

]

SUMMARY OF TRACTION TEST DATA ON SANTO50

TEST #	PO GPa	UO m/s	TO '	SP '	VF --	RX mm	RY mm	e mm	DS --	KK --	A mm	MS --	MU --
820923-1	.975	48	53	15.0	1.00	18.7	270.0	-230.0	.0061	5.6	.30	0	.057
820923-2	.975	48	64	15.0	.96	18.7	270.0	-230.0	.0061	5.6	.30	0	.064
820923-3	.975	78	65	15.0	1.00	18.7	270.0	-230.0	.0061	5.6	.30	0	.044
820923-4	.975	77	83	15.0	.93	18.7	270.0	-230.0	.0061	5.6	.30	0	.050
820923-5	.975	106	84	15.0	.96	18.7	270.0	-230.0	.0061	5.6	.30	0	.033
820923-6	.975	111	103	15.0	.80	18.7	270.0	-230.0	.0061	5.6	.30	0	.040
820923-7	.967	49	61	0.0	1.00	19.1	270.0	-237.0	0.000	5.6	.31	34	.062
820923-8	.967	50	72	0.0	.96	19.1	270.0	-237.0	0.000	5.6	.31	49	.082
820923-9	.967	75	73	0.0	1.00	19.1	270.0	-237.0	0.000	5.6	.31	28	.049
820923-10	.967	73	87	0.0	.86	19.1	270.0	-237.0	0.000	5.6	.31	33	.060
820923-11	.967	113	98	0.0	.94	19.1	270.0	-237.0	0.000	5.6	.31	18	.031
820923-12	.967	113	99	0.0	.69	19.1	270.0	-237.0	0.000	5.6	.31	23	.044
820924-1	1.073	44	46	0.0	1.00	19.1	54.0	-21.0	0.000	2.0	.30	33	.081
820924-2	1.073	47	59	0.0	.69	19.1	54.0	-21.0	0.000	2.0	.30	51	.096
820924-3	1.073	79	58	0.0	1.00	19.1	54.0	-21.0	0.000	2.0	.30	29	.059
820924-4	1.073	81	74	0.0	.69	19.1	54.0	-21.0	0.000	2.0	.30	41	.081
820924-5	1.073	113	75	0.0	1.00	19.1	54.0	-21.0	0.000	2.0	.30	32	.051
820924-6	1.073	113	90	0.0	.75	19.1	54.0	-21.0	0.000	2.0	.30	46	.069
820924-7	1.228	49	54	0.0	1.00	19.1	54.0	-21.0	0.000	2.0	.35	39	.081
820924-8	1.228	48	69	0.0	.78	19.1	54.0	-21.0	0.000	2.0	.35	53	.098
820924-9	1.228	79	65	0.0	1.00	19.1	54.0	-21.0	0.000	2.0	.35	33	.069
820924-10	1.228	78	80	0.0	.68	19.1	54.0	-21.0	0.000	2.0	.35	45	.085
820924-11	1.228	112	76	0.0	1.00	19.1	54.0	-21.0	0.000	2.0	.35	33	.058
820924-12	1.228	113	92	0.0	.85	19.1	54.0	-21.0	0.000	2.0	.35	42	.073
820924-13	1.456	48	71	0.0	1.00	19.1	54.0	-21.0	0.000	2.0	.41	40	.085
820924-14	1.456	47	83	0.0	.60	19.1	54.0	-21.0	0.000	2.0	.41	51	.094
820924-15	1.456	80	80	0.0	1.00	19.1	54.0	-21.0	0.000	2.0	.41	38	.074
820924-16	1.456	80	94	0.0	.69	19.1	54.0	-21.0	0.000	2.0	.41	42	.081
820924-17	1.456	109	91	0.0	1.00	19.1	54.0	-21.0	0.000	2.0	.41	38	.067
820924-18	1.456	113	97	0.0	.60	19.1	54.0	-21.0	0.000	2.0	.41	37	.063
820925-1	1.074	51	60	7.5	1.00	19.0	54.0	-21.0	.0017	2.0	.30	0	.068

SUMMARY OF TRACTION TEST DATA ON SANTO50

TEST #	PO	UO	TO	SP	VF	RX	RY	e	DS	KK	A	MS	MU
----	GPa	m/s	°C	°	--	mm	mm	mm	--	--	mm	--	--
820925-2	1.074	49	63	7.5	0.00	19.0	54.0	-21.0	.0017	2.0	.30	0	.070
820925-3	1.074	85	69	7.5	1.00	19.0	54.0	-21.0	.0017	2.0	.30	0	.051
820925-4	1.074	84	76	7.5	.94	19.0	54.0	-21.0	.0017	2.0	.30	0	.058
820925-5	1.074	112	76	7.5	1.00	19.0	54.0	-21.0	.0017	2.0	.30	0	.044
820925-6	1.074	112	83	7.5	.94	19.0	54.0	-21.0	.0017	2.0	.30	0	.058
820925-7	1.230	52	75	7.5	1.00	19.0	54.0	-21.0	.0019	2.0	.34	0	.072
820925-8	1.230	49	78	7.5	.89	19.0	54.0	-21.0	.0019	2.0	.34	0	.079
820925-9	1.230	80	79	7.5	1.00	19.0	54.0	-21.0	.0019	2.0	.34	0	.062
820925-10	1.230	81	84	7.5	.89	19.0	54.0	-21.0	.0019	2.0	.34	0	.075
820925-11	1.230	109	90	7.5	.89	19.0	54.0	-21.0	.0019	2.0	.34	0	.067
820925-12	1.230	109	92	7.5	.97	19.0	54.0	-21.0	.0019	2.0	.34	0	.055
820925-13	1.458	49	76	7.5	1.00	19.0	54.0	-21.0	.0023	2.0	.41	0	.077
820925-14	1.458	48	82	7.5	.91	19.0	54.0	-21.0	.0023	2.0	.41	0	.077
820925-15	1.458	78	88	7.5	1.00	19.0	54.0	-21.0	.0023	2.0	.41	0	.066
820925-16	1.458	82	94	7.5	.94	19.0	54.0	-21.0	.0023	2.0	.41	0	.066
820925-17	1.458	108	99	7.5	.94	19.0	54.0	-21.0	.0023	2.0	.41	0	.059
820925-18	1.458	110	107	7.5	.80	19.0	54.0	-21.0	.0023	2.0	.41	0	.062
820927-1	1.078	48	65	15.0	1.00	18.8	54.0	-21.0	.0035	2.0	.30	0	.067
820927-2	1.078	49	70	15.0	.96	18.8	54.0	-21.0	.0035	2.0	.30	0	.075
820927-3	1.078	82	77	15.0	1.00	18.8	54.0	-21.0	.0035	2.0	.30	0	.056
820927-4	1.078	83	83	15.0	.94	18.8	54.0	-21.0	.0035	2.0	.30	0	.061
820927-5	1.078	108	91	15.0	1.00	18.8	54.0	-21.0	.0035	2.0	.30	0	.052
820927-6	1.078	113	104	15.0	.85	18.8	54.0	-21.0	.0035	2.0	.30	0	.056
820927-7	1.235	49	72	15.0	1.00	18.8	54.0	-21.0	.0040	2.0	.34	0	.069
820927-8	1.235	48	76	15.0	.97	18.8	54.0	-21.0	.0040	2.0	.34	0	.076
820927-9	1.235	80	85	15.0	.94	18.8	54.0	-21.0	.0040	2.0	[illegible]	0	.065
820927-10	1.235	78	85	15.0	1.00	18.8	54.0	-21.0	.0040	2.0	.34	0	.058
820927-11	1.235	113	95	15.0	.97	18.8	54.0	-21.0	.0040	2.0	.34	0	.052
820927-12	1.235	113	102	15.0	.80	18.8	54.0	-21.0	.0040	2.0	.34	0	.054
820927-13	1.464	48	71	15.0	.98	18.8	54.0	-21.0	.0047	2.0	[illegible]	0	.075
820927-14	1.464	48	79	15.0	.89	18.8	54.0	-21.0	.0047	2.0	[illegible]	0	.079

SUMMARY OF TRACTION TEST DATA ON SANTO50

TEST #	PO	UO	TO	SP	VF	RX	RY	e	DS	KK	A	MS	MU
----	GPa	m/s	°C	°	--	mm	mm	mm	--	--	mm	--	--
820927-15	1.464	82	86	15.0	.94	18.8	54.0	-21.0	.0047	2.0	.41	0	.065
820927-16	1.464	81	94	15.0	.80	18.8	54.0	-21.0	.0047	2.0	.41	0	.068
820927-17	1.464	113	106	15.0	.80	18.8	54.0	-21.0	.0047	2.0	.41	0	.060
820927-18	1.464	112	110	15.0	.89	18.8	54.0	-21.0	.0047	2.0	.41	0	.055
820929-1	1.414	47	34	0.0	1.00	19.1	19.1	14.0	0.000	1.0	.37	38	.093
820929-2	1.414	45	44	0.0	.94	19.1	19.1	14.0	0.000	1.0	.37	45	.095
820929-3	1.414	69	51	0.0	.91	19.1	19.1	14.0	0.000	1.0	.37	41	.086
821019-1	1.414	51	38	0.0	1.00	19.1	19.1	14.0	0.000	1.0	.37	44	.096
821019-2	1.414	50	40	0.0	.94	19.1	19.1	14.0	0.000	1.0	.37	46	.097
821019-3	1.414	89	46	0.0	1.00	19.1	19.1	14.0	0.000	1.0	.37	44	.086
821019-4	1.414	86	50	0.0	.94	19.1	19.1	14.0	0.000	1.0	.37	42	.089
821019-5	1.414	120	57	0.0	1.00	19.1	19.1	14.0	0.000	1.0	.37	40	.080
821019-6	1.414	118	64	0.0	.89	19.1	19.1	14.0	0.000	1.0	.37	46	.080
821019-7	1.618	46	58	0.0	1.00	19.1	19.1	14.0	0.000	1.0	.42	46	.094
821019-8	1.618	47	59	0.0	.94	19.1	19.1	14.0	0.000	1.0	.42	40	.095
821019-9	1.618	87	61	0.0	1.00	19.1	19.1	14.0	0.000	1.0	.42	41	.088
821019-10	1.618	85	64	0.0	.96	19.1	19.1	14.0	0.000	1.0	.42	38	.089
821019-11	1.618	122	70	0.0	.96	19.1	19.1	14.0	0.000	1.0	.42	36	.081
821019-12	1.618	117	76	0.0	.69	19.1	19.1	14.0	0.000	1.0	.42	41	.081
821019-13	1.781	46	53	0.0	1.00	19.1	19.1	14.0	0.000	1.0	.46	38	.096
821019-14	1.781	48	58	0.0	.85	19.1	19.1	14.0	0.000	1.0	.46	42	.098
821019-15	1.781	87	66	0.0	.83	19.1	19.1	14.0	0.000	1.0	.46	41	.091
821019-16	1.781	88	71	0.0	.97	19.1	19.1	14.0	0.000	1.0	.46	41	.087
821019-17	1.781	120	76	0.0	.91	19.1	19.1	14.0	0.000	1.0	.46	42	.082
821019-18	1.781	122	84	0.0	[illegible]	[illegible]	19.1	14.0	0.000	1.0	.46	43	.079
821020-1	1.780	52	64	7.5	[illegible]	[illegible]	19.1	14.0	.0018	1.0	.46	0	.090
821020-2	1.780	50	68	7.5	[illegible]	[illegible]	19.1	14.0	.0018	1.0	.46	0	.093
821020-3	1.780	86	74	7.5	.91	[illegible]	19.1	14.0	.0018	1.0	.46	0	.082
821020-4	1.780	89	79	7.5	.85	19.2	19.1	14.0	.0018	1.0	.46	0	.082
821020-5	1.780	119	84	7.5	.85	19.2	19.1	14.0	.0018	1.0	.46	0	.077

SUMMARY OF TRACTION TEST DATA ON SANTO50

TEST #	PO	UO	TO	SP	VF	RX	RY	e	DS	KK	A	MS	MU
----	GPa	m/s	°C	°	--	mm	mm	mm	--	--	mm	--	--
821020-5	1.780	119	84	7.5	.85	19.2	19.1	14.0	.0018	1.0	.46	0	.077
821020-6	1.780	122	90	7.5	.78	19.2	19.1	14.0	.0018	1.0	.46	0	.076
821020-7	1.617	48	80	7.5	.89	19.2	19.1	14.0	.0017	1.0	.42	0	.086
821020-8	1.617	45	77	7.5	.83	19.2	19.1	14.0	.0017	1.0	.42	0	.089
821020-9	1.617	90	67	7.5	.97	19.2	19.1	14.0	.0017	1.0	.42	0	.081
821020-10	1.617	85	73	7.5	.88	19.2	19.1	14.0	.0017	1.0	.42	0	.085
821020-11	1.617	117	80	7.5	.85	19.2	19.1	14.0	.0017	1.0	.42	0	.076
821020-12	1.617	120	88	7.5	.89	19.2	19.1	14.0	.0017	1.0	.42	0	.070
821020-13	1.412	44	57	7.5	1.00	19.2	19.1	14.0	.0015	1.0	.37	0	.086
821020-14	1.412	46	58	7.5	.96	19.2	19.1	14.0	.0015	1.0	.37	0	.092
821020-15	1.412	89	65	7.5	1.00	19.2	19.1	14.0	.0015	1.0	.37	0	.075
821020-16	1.412	91	67	7.5	.94	19.2	19.1	14.0	.0015	1.0	.37	0	.082
821020-17	1.412	119	72	7.5	.89	19.2	19.1	14.0	.0015	1.0	.37	0	.073
821020-18	1.412	122	81	7.5	.94	19.2	19.1	14.0	.0015	1.0	.37	0	.069
821022-1	1.409	49	38	15.0	1.00	19.3	19.1	14.0	.0029	1.0	.37	0	.082
821022-2	1.409	43	42	15.0	0.00	19.3	19.1	14.0	.0029	1.0	.37	0	.092
821022-3	1.409	87	49	15.0	.93	19.3	19.1	14.0	.0029	1.0	.37	0	.082
821022-4	1.409	93	55	15.0	1.00	19.3	19.1	14.0	.0029	1.0	.37	0	.069
821022-5	1.409	117	62	15.0	.96	19.3	19.1	14.0	.0029	1.0	.37	0	.067
821022-6	1.409	114	67	15.0	.85	19.3	19.1	14.0	.0029	1.0	.37	0	.074
821022-7	1.613	53	62	15.0	.94	19.3	19.1	14.0	.0034	1.0	.42	0	.087
821022-8	1.613	52	62	15.0	.69	19.3	19.1	14.0	.0034	1.0	.42	0	.091
821022-9	1.613	90	64	15.0	.94	19.3	19.1	14.0	.0034	1.0	.42	0	.075
821022-10	1.613	89	67	15.0	.75	19.3	19.1	14.0	.0034	1.0	.42	0	.082
821022-11	1.613	117	73	15.0	.80	19.3	19.1	14.0	.0034	1.0	.42	0	.075
821022-12	1.613	119	79	15.0	.96	19.3	19.1	14.0	.0034	1.0	.42	0	.070
821022-13	1.775	47	61	15.0	.96	19.3	19.1	14.0	.0037	1.0	.47	0	.087
821022-14	1.775	54	64	15.0	.75	19.3	19.1	14.0	.0037	1.0	.47	0	.090
821022-15	1.775	87	69	15.0	.78	19.3	19.1	14.0	.0037	1.0	.47	0	.083
821022-16	1.775	91	73	15.0	.93	19.3	19.1	14.0	.0037	1.0	.47	0	.076
821022-17	1.775	123	80	15.0	.88	19.3	19.1	14.0	.0037	1.0	.47	0	.070

SUMMARY OF TRACTION TEST DATA ON SANTO50

TEST #	PO GPa	UO m/s	TO °C	SP °	VF --	RX mm	RY mm	e mm	DS --	KK -	A mm	MS --	MU --
821022-18	1.775	119	84	15.0	.69	19.3	19.1	14.0	.0037	1.0	.47	0	.073
821101-1	1.062	50	65	15.0	.85	10.6	136.0	-118.0	.0082	5.2	.19	0	.082
821101-2	1.062	50	75	15.0	.69	10.6	136.0	-118.0	.0082	5.2	.19	0	.088
821101-3	1.062	80	75	15.0	.85	10.6	136.0	-118.0	.0082	5.2	.19	0	.076
821101-4	1.062	81	81	15.0	.75	10.6	136.0	-118.0	.0082	5.2	.19	0	.078
821101-5	1.062	111	95	15.0	.60	10.6	136.0	-118.0	.0082	5.2	.19	0	.076
821101-6	1.062	114	91	15.0	.89	10.6	136.0	-118.0	.0082	5.2	.19	0	.071
821101-7	1.062	112	88	15.0	.96	10.6	136.0	-118.0	.0082	5.2	.19	0	.046
821101-8	1.062	119	109	15.0	.80	10.6	136.0	-118.0	.0082	5.2	.19	0	[illegible]
821101-9	1.216	50	69	15.0	1.00	10.6	136.0	-118.0	.0094	5.2	.21	0	.064
821101-10	1.216	50	79	15.0	.89	10.6	136.0	-118.0	.0094	5.2	.21	0	.065
821101-11	1.216	83	90	15.0	.69	10.6	136.0	-118.0	.0094	5.2	.21	0	.064
821101-12	1.216	81	86	15.0	.97	10.6	136.0	-118.0	.0094	5.2	.21	0	.056
821101-13	1.216	103	97	15.0	.94	10.6	136.0	-118.0	.0094	5.2	.21	0	.050
821101-14	1.216	107	119	15.0	.75	10.6	136.0	-118.0	.0094	5.2	.21	0	.061
821101-15	1.441	51	84	15.0	.89	10.6	136.0	-118.0	.0111	5.2	.25	0	.065
821101-16	1.441	52	92	15.0	.80	10.6	136.0	-118.0	.0111	5.2	.25	0	.066
821101-17	1.441	89	109	15.0	.64	10.6	136.0	-118.0	.0111	5.2	.25	0	.062
821101-18	1.441	90	105	15.0	.85	10.6	136.0	-118.0	.0111	5.2	.25	0	.059
821101-19	1.441	94	99	15.0	.94	10.6	136.0	-118.0	.0111	5.2	.25	0	.056
821101-20	1.441	96	122	15.0	.60	10.6	136.0	-118.0	.0111	5.2	.25	0	.061
821102-1	1.036	55	52	0.0	1.00	11.3	136.0	-121.0	0.000	5.0	.19	27	.076
821102-2	1.036	52	63	0.0	0.00	11.3	136.0	-121.0	0.000	5.0	.19	30	.084
821102-3	1.036	93	68	0.0	1.00	11.3	136.0	-121.0	0.000	5.0	.19	30	.070
821102-4	1.036	92	79	0.0	.94	11.3	136.0	-121.0	0.000	5.0	.19	33	.073
821102-5	1.036	114	83	0.0	1.00	11.3	136.0	-121.0	0.000	5.0	.19	28	.063
821102-6	1.036	119	88	0.0	.89	11.3	136.0	-121.0	0.000	5.0	.19	27	.064
821102-7	1.186	47	61	0.0	1.00	11.3	136.0	-121.0	0.000	5.0	.22	29	.082
821102-8	1.186	48	76	0.0	.89	11.3	136.0	-121.0	0.000	5.0	.22	33	.084
821102-9	1.186	85	87	0.0	.94	11.3	136.0	-121.0	0.000	5.0	.22	35	.075
821102-10	1.186	85	85	0.0	.98	11.3	136.0	-121.0	0.000	5.0	.22	27	.068

SUMMARY OF TRACTION TEST DATA ON SANTO50

TEST #	PO	UO	TO	SP	VF	RX	RY	e	DS	KK	A	MS	MU
----	GPa	m/s	°C	'	--	mm	mm	mm	--	--	mm	--	--
821102-11	1.186	116	94	0.0	.89	11.3	136.0	-121.0	0.000	5.0	.22	26	.064
821102-12	1.186	119	102	0.0	.80	11.3	136.0	-121.0	0.000	5.0	.22	30	.063
821102-13	1.406	50	69	0.0	1.00	11.3	136.0	-121.0	0.000	5.0	.26	29	.087
821102-14	1.406	51	83	0.0	.93	11.3	136.0	-121.0	0.000	5.0	.26	30	.088
821102-15	1.406	113	97	0.0	.97	11.3	136.0	-121.0	0.000	5.0	.26	30	.069
821102-16	1.406	123	111	0.0	.80	11.3	136.0	-121.0	0.000	5.0	.26	31	.066
821102-17	1.406	81	108	0.0	.85	11.3	136.0	-121.0	0.000	5.0	.26	30	.071
821102-18	1.406	81	84	0.0	.93	11.3	136.0	-121.0	0.000	5.0	.26	24	.071
821103-1	1.338	51	82	15.0	1.00	10.6	136.0	-118.0	.0103	5.2	.23	0	.065
821103-2	1.338	51	91	15.0	.89	10.6	136.0	-118.0	.0103	5.2	.23	0	.066
821103-3	1.338	80	102	15.0	.80	10.6	136.0	-118.0	.0103	5.2	.23	0	.066

]

APPENDIX II SUMMARY OF THE MODULUS ANALYSIS DATA.

The various shear moduli calculated from the experimental results are summarized in this Appendix. The nomenclature used is as follows;

Test #	Number of the particular test	(YYMMDD-##)
Po	Maximum calculated Hertz contact stress	(GPa)
Uo	Surface rolling velocity in linear region	(m/sec)
To	Disc surface temperature in linear region	('C)
VF	No-contact voltage fraction	(-)
KK	Contact aspect ratio (b/a)	(-)
MS	Slope of curve in linear region	(-)
RG	Regression coefficient on the slope	(-)
MR	Wet to dry slope ratio	(-)
Ho	Isothermal film thickness	(um)
YI	Inlet shear heating factor	(-)
GB	Fluid shear modulus without corrections	(GPa)
GC	Modulus with simple compliance corrections	(GPa)
C'	Effective dimensionless contact radius	(-)
GJ	Modulus with complex compliance corrections	(GPa)
PR	Reduced pressure ratio	(-)
CP	As C above but with reduced pressure	(-)
GP	As GJ above but with inlet shear heating and reduced pressure taken into account	(GPa)

SUMMARY OF MODULUS ANALYSIS ON TDF88

TEST #	P0	U0	T0	VF	KK	MS	RG	MR	H0	YI	GB	GC	C'	GJ	PR	CP	GP
----	GPa	m/s	°C	--	--	--	--	--	um	--	GPa	GPa	-	GPa	--	--	GPa
820804-1	1.07	50	71	1.00	2.0	32	.99	.29	1.90	.45	.17	.24	.62	.95	.974	.60	.50
820804-2	1.07	52	81	0.00	2.0	46	1.00	.43	1.54	.50	.20	.35	.53	19.	.976	.50	0.0
820804-3	1.07	85	86	1.00	2.0	32	.99	.30	1.92	.39	.17	.24	.47	3.7	.976	.42	4.3
820804-4	1.07	85	98	0.00	2.0	35	.99	.32	1.52	.45	.15	.22	.28	0.0	.977	.19	0.0
820804-5	1.07	113	109	0.00	2.0	40	1.00	.37	1.50	.42	.17	.26	0.0	0.0	.978	0.0	0.0
820804-6	1.07	117	102	1.00	2.0	36	1.00	.33	1.76	.38	.17	.26	.17	0.0	.977	0.0	0.0
820804-7	1.23	53	86	1.00	2.0	37	1.00	.40	1.38	.51	.14	.24	.64	1.2	.982	.62	.69
820804-8	1.23	50	93	.75	2.0	40	1.00	.42	1.13	.57	.12	.22	.59	2.2	.983	.56	1.7
820804-9	1.23	85	97	1.00	2.0	38	1.00	.41	1.50	.44	.16	.27	.55	4.3	.982	.53	3.6
820804-10	1.23	82	110	.80	2.0	38	1.00	.41	1.17	.51	.13	.21	.42	0.0	.983	.38	0.0
820804-11	1.23	119	96	1.00	2.0	36	.99	.38	1.92	.35	.19	.31	.56	2.9	.982	.54	1.4
820804-12	1.23	115	119	.80	2.0	31	.99	.33	1.27	.45	.11	.17	.28	0.0	.983	.21	0.0
820805-1	1.46	51	116	1.00	2.0	33	1.00	.42	.75	.66	.07	.12	.61	.93	.989	.60	.70
820805-2	1.46	51	126	.69	2.0	37	1.00	.47	.64	.69	.07	.13	.54	0.0	.990	.53	0.0
820805-3	1.46	82	118	1.00	2.0	32	1.00	.41	.99	.54	.09	.15	.59	1.2	.989	.58	.78
820805-4	1.46	82	126	.80	2.0	38	.99	.48	.88	.57	.09	.18	.54	0.0	.989	.52	0.0
820805-5	1.46	106	103	1.00	2.0	30	.99	.38	1.52	.41	.13	.21	.68	.75	.988	.67	.33
820805-6	1.46	100	118	.80	2.0	40	.99	.51	1.14	.49	.13	.26	.60	16.	.988	.58	0.0
820824-1	1.62	49	61	1.00	1.0	38	1.00	.43	2.00	.39	.23	.40	.88	.72	.993	.88	.28
820824-2	1.62	49	68	.91	1.0	38	1.00	.43	1.65	.44	.19	.34	.86	.66	.994	.86	.29
820824-3	1.62	83	72	1.00	1.0	30	.99	.35	2.12	.32	.19	.30	.85	.55	.994	.85	.18
820824-4	1.62	82	81	.91	1.0	39	1.00	.45	1.70	.37	.20	.37	.83	.87	.994	.82	.33
820824-5	1.62	118	88	1.00	1.0	32	.98	.37	1.86	.32	.18	.29	.81	.67	.994	.80	.21
820824-6	1.62	116	101	.75	1.0	40	1.00	.46	1.43	.38	.17	.32	.76	1.2	.994	.76	.45
820824-7	1.78	48	83	1.00	1.0	38	1.00	.48	1.10	.53	.13	.24	.85	.53	.995	.85	.28
820824-8	1.78	45	89	.81	1.0	42	1.00	.52	.94	.58	.12	.25	.84	.63	.995	.84	.37
820824-9	1.78	82	89	1.00	1.0	40	.99	.50	1.42	.41	.17	.34	.84	.82	.995	.84	.34
820824-10	1.78	83	99	.85	1.0	38	1.00	.48	1.15	.46	.13	.25	.81	.68	.995	.81	.32
820824-11	1.78	119	78	1.00	1.0	38	1.00	.47	2.30	.27	.26	.49	.87	.98	.995	.87	.27
820824-12	1.78	117	95	.88	1.0	35	.99	.44	1.59	.35	.17	.30	.82	.72	.995	.82	.25
820824-13	1.41	49	74	1.00	1.0	37	.99	.37	1.45	.47	.16	.25	.79	.62	.992	.79	.30

SUMMARY OF MODULUS ANALYSIS ON TDF88

TEST #	PO	UO	TO	VF	KK	MS	RG	MR	HO	YI	GB	GC	C'	GJ	PR	CP	GP
----	GPa	m/s	°C	--	--	--	--	--	um	--	GPa	GPa	-	GPa	--	--	GPa
820824-14	1.41	49	77	.94	1.0	42	1.00	.42	1.34	.49	.17	.30	.78	.84	.992	.78	.42
820824-15	1.41	84	77	1.00	1.0	39	1.00	.39	1.95	.35	.23	.37	.78	1.0	.992	.78	.35
820824-16	1.41	83	83	.94	1.0	35	.99	.35	1.67	.38	.17	.27	.76	.76	.992	.75	.30
820824-17	1.41	115	88	1.00	1.0	36	1.00	.36	1.87	.32	.20	.32	.73	1.0	.992	.73	.34
820824-18	1.41	114	98	.78	1.0	39	1.00	.39	1.55	.37	.18	.30	.69	1.5	.993	.68	.57
820831-1	1.46	29	68	1.00	2.0	36	.99	.45	1.36	.58	.14	.25	.83	.50	.986	.82	.30
820902-1	1.23	48	72	1.00	2.0	34	.99	.37	1.78	.46	.17	.27	.73	.76	.981	.71	.38
820902-2	1.23	83	83	1.00	2.0	23	.79	.24	1.97	.38	.13	.17	.66	.52	.981	.64	.21
820902-3	1.23	117	96	1.00	2.0	28	.98	.30	1.92	.35	.15	.21	.57	1.2	.982	.54	.51
820903-1	1.07	49	56	1.00	2.0	27	.99	.25	2.83	.36	.21	.28	.73	.68	.972	.71	.26
820903-2	1.07	85	69	1.00	2.0	21	.97	.20	2.85	.31	.17	.21	.64	.66	.974	.61	.22
820903-3	1.07	115	81	1.00	2.0	35	.98	.32	2.66	.29	.26	.38	.53	3.2	.976	.50	1.4
820904-1	1.46	31	66	1.00	2.0	43	.99	.54	1.51	.54	.18	.39	.84	.88	.986	.83	.49
820904-2	1.46	29	78	.94	2.0	42	.98	.53	1.05	.64	.12	.26	.79	.75	.988	.79	.49
820904-3	1.46	59	80	1.00	2.0	31	.92	.38	1.64	.45	.14	.23	.79	.51	.987	.78	.24
820904-4	1.46	58	91	.89	2.0	42	1.00	.54	1.26	.52	.15	.32	.74	1.4	.987	.73	.77
820904-5	1.46	89	87	1.00	2.0	30	.99	.38	1.86	.38	.16	.26	.76	.64	.987	.75	.25
820904-6	1.46	86	101	.85	2.0	45	.99	.56	1.36	.46	.17	.39	.69	3.8	.988	.68	2.2
820916-1	1.01	50	71	1.00	5.6	26	.99	.26	2.06	.45	.13	.18	.55	.78	.974	.51	.42
820916-2	1.01	48	88	0.00	5.6	45	.99	.45	1.36	.55	.15	.27	.30	0.0	.976	.22	0.0
820916-3	1.01	86	87	1.00	5.6	18	1.00	.18	2.08	.39	.09	.11	.34	1.4	.975	.26	1.8
820916-4	1.01	84	100	.96	5.6	35	.99	.35	1.57	.46	.13	.21	0.0	0.0	.977	0.0	0.0
820916-5	1.01	106	102	.94	5.6	15	1.00	.15	1.76	.41	.06	.07	0.0	0.0	.977	0.0	0.0
820916-6	1.01	113	112	.80	5.6	31	.99	.32	1.56	.43	.12	.18	0.0	0.0	.977	0.0	0.0
821116-1	1.04	48	60	1.00	5.0	19	1.00	.19	2.28	.39	.18	.22	.68	.55	.964	.65	.24
821116-2	1.04	51	72	0.00	5.0	21	.99	.22	1.69	.46	.15	.20	.57	.73	.966	.53	.40
821116-3	1.04	84	87	.94	5.0	31	1.00	.32	1.69	.40	.22	.33	.39	17.	.968	.30	0.0
821116-4	1.04	84	87	1.00	5.0	18	1.00	.18	1.70	.40	.13	.16	.39	1.3	.968	.31	1.2
821116-5	1.04	118	94	.75	5.0	19	.99	.19	1.85	.35	.15	.18	.24	70.	.969	0.0	0.0
821116-6	1.04	117	114	.50	5.0	22	1.00	.23	1.29	.43	.12	.16	0.0	0.0	.971	0.0	0.0
821116-7	1.19	51	64	1.00	5.0	24	.99	.29	2.04	.40	.21	.30	.74	.65	.973	.73	.28

SUMMARY OF MODULUS ANALYSIS ON TDF88

TEST #	PO	UO	TO	VF	KK	MS	RG	MR	HO	YI	GB	GC	C'	GJ	PR	CP	GP
----	GPa	m/s	'C	--	--	--	--	--	um	--	GPa	GPa	-	GPa	--	--	GPa
821116-8	1.19	51	76	0.00	5.0	29	.99	.35	1.53	.47	.19	.29	.68	.86	.975	.66	.45
821116-9	1.19	84	87	.94	5.0	23	.97	.27	1.69	.39	.16	.22	.60	.81	.976	.57	.36
821116-10	1.19	84	101	0.00	5.0	29	.99	.35	1.27	.46	.16	.24	.46	3.5	.977	.42	4.1
821116-11	1.19	118	106	.80	5.0	19	.99	.22	1.47	.39	.12	.15	.40	1.4	.977	.35	.98
821116-12	1.19	118	103	0.00	5.0	28	.98	.33	1.53	.38	.18	.27	.44	4.7	.977	.39	7.7
821116-13	1.41	51	71	1.00	5.0	28	1.00	.39	1.67	.44	.20	.32	.80	.63	.982	.79	.29
821116-14	1.41	51	93	0.00	5.0	32	1.00	.45	1.02	.56	.14	.25	.71	.82	.984	.69	.49
821116-15	1.41	88	102	1.00	5.0	14	.98	.21	1.23	.46	.08	.10	.66	.25	.984	.64	.12
821116-16	1.41	91	132	.69	5.0	16	.97	.23	.79	.57	.05	.07	.43	.56	.986	.40	.40
821116-17	1.41	107	102	.89	5.0	26	1.00	.36	1.42	.40	.15	.24	.66	.81	.984	.64	.35
821116-18	1.41	116	133	.60	5.0	32	.99	.46	.92	.50	.13	.23	.41	0.0	.985	.38	0.0

]

SUMMARY OF MODULUS ANALYSIS ON SANTO50

TEST #	PO	UO	TO	VF	KK	MS	RG	MR	HO	YI	GB	GC	C'	GJ	PR	CP	GP
----	GPa	m/s	'C	--	--	--	--	--	um	--	GPa	GPa	-	GPa	--	--	GPa
820923-7	.97	49	61	1.00	5.6	34	1.00	.33	2.52	.43	.21	.31	.66	.96	.969	.63	.47
820923-8	.97	50	72	.96	5.6	49	.99	.47	1.96	.49	.24	.45	.56	6.9	.971	.52	15.
820923-9	.97	75	73	1.00	5.6	28	1.00	.27	2.53	.39	.17	.24	.55	1.1	.971	.50	.53
820923-10	.97	73	87	.86	5.6	33	1.00	.32	1.91	.46	.15	.23	.37	21.	.972	.29	0.0
820923-11	.97	113	98	.94	5.6	18	1.00	.17	2.10	.39	.09	.11	0.0	0.0	.973	0.0	0.0
820923-12	.97	113	99	.69	5.6	23	1.00	.23	2.07	.40	.12	.15	0.0	0.0	.973	0.0	0.0
820924-1	1.07	44	46	1.00	2.0	33	.99	.31	3.33	.36	.31	.45	.81	.84	.970	.80	.32
820924-2	1.07	47	59	.69	2.0	51	1.00	.47	2.35	.43	.33	.63	.74	2.0	.972	.73	.97
820924-3	1.07	79	58	1.00	2.0	29	1.00	.27	3.48	.29	.28	.39	.75	.87	.973	.7[illegible]	.27
820924-4	1.07	81	74	.69	2.0	41	.99	.38	2.43	.37	.28	.45	.65	1.9	.974	.63	.84
820924-5	1.07	113	75	1.00	2.0	32	1.00	.29	2.94	.30	.26	.37	.64	1.3	.974	.62	.45
820924-6	1.07	113	90	.75	2.0	46	1.00	.42	2.20	.36	.28	.49	.51	0.0	.975	.47	0.0
820924-7	1.23	49	54	1.00	2.0	39	1.00	.42	2.76	.38	.30	.52	.83	.99	.978	.83	.39
820924-8	1.23	48	69	.78	2.0	53	1.00	.56	1.85	.48	.27	.62	.77	2.2	.980	.76	1.2
820924-9	1.23	79	65	1.00	2.0	33	1.00	.35	2.87	.33	.26	.41	.79	.86	.980	.78	.29
820924-10	1.23	78	80	.68	2.0	45	.98	.47	2.05	.41	.26	.49	.72	1.9	.980	.71	.83
820924-11	1.23	112	76	1.00	2.0	33	1.00	.35	2.83	.30	.26	.41	.74	1.1	.981	.73	.34
820924-12	1.23	113	92	.85	2.0	42	1.00	.45	2.09	.37	.25	.45	.65	2.7	.981	.63	1.2
820924-13	1.46	48	71	1.00	2.0	40	1.00	.50	1.73	.49	.19	.39	.84	.80	.986	.83	.40
820924-14	1.46	47	83	.60	2.0	51	.99	.65	1.33	.56	.19	.54	.80	2.4	.987	.79	1.4
820924-15	1.46	80	80	1.00	2.0	38	1.00	.49	2.02	.40	.22	.42	.81	.98	.986	.80	.40
820924-16	1.46	80	94	.69	2.0	42	.99	.53	1.56	.47	.18	.39	.76	1.4	.987	.75	.68
820924-17	1.46	109	91	1.00	2.0	38	.99	.48	2.02	.37	.21	.41	.77	1.2	.987	.76	.45
820924-18	1.46	113	97	.60	2.0	37	1.00	.47	1.84	.39	.19	.36	.74	1.2	.987	.74	.48
820929-1	1.41	47	34	1.00	1.0	38	1.00	.37	4.37	.26	.50	.79	.92	1.2	.990	.92	.30
820929-2	1.41	45	44	.94	1.0	45	1.00	.44	3.02	.33	.41	.74	.90	1.2	.990	.90	.41
820929-3	1.41	69	51	.91	1.0	41	.95	.41	3.22	.28	.40	.67	.89	1.1	.991	.88	.33
821019-1	1.41	51	38	1.00	1.0	44	1.00	.43	3.92	.27	.51	.91	.91	1.4	.990	.91	.39
821019-2	1.41	50	40	.94	1.0	46	1.00	.46	3.62	.29	.51	.94	.91	1.5	.990	.91	.44
821019-3	1.41	89	46	1.00	1.0	44	1.00	.44	4.44	.21	.59	1.0	.90	1.8	.991	.90	.36
821019-4	1.41	86	50	.94	1.0	42	1.00	.41	3.77	.23	.47	.81	.89	1.4	.991	.88	.33

SUMMARY OF MODULUS ANALYSIS ON SANTO50

TEST #	PO	UO	TO	VF	KK	MS	RG	MR	HO	YI	GB	GC	C'	GJ	PR	CP	GP
----	GPa	m/s	°C	--	--	--	--	--	um	--	GPa	GPa	-	GPa	--	--	GPa
821019-5	1.41	120	57	1.00	1.0	40	1.00	.40	3.93	.20	.48	.80	.87	1.5	.992	.87	.30
821019-6	1.41	118	64	.89	1.0	46	1.00	.46	3.25	.24	.45	.84	.85	1.8	.992	.85	.43
821019-7	1.62	46	58	1.00	1.0	46	1.00	.52	1.95	.43	.27	.56	.90	1.0	.993	.90	.43
821019-8	1.62	47	59	.94	1.0	40	.98	.46	1.90	.43	.23	.43	.90	.74	.993	.90	.32
821019-9	1.62	87	61	1.00	1.0	41	1.00	.47	2.78	.29	.35	.65	.89	1.1	.993	.89	.33
821019-10	1.62	85	64	.96	1.0	38	.99	.43	2.51	.31	.29	.51	.89	.90	.993	.88	.28
821019-11	1.62	122	70	.96	1.0	36	.99	.41	2.81	.26	.31	.53	.87	.96	.994	.87	.25
821019-12	1.62	117	76	.69	1.0	41	1.00	.47	2.40	.29	.30	.56	.86	1.2	.994	.86	.34
821019-13	1.78	46	53	1.00	1.0	38	.99	.47	2.18	.40	.25	.47	.93	.73	.994	.92	.29
821019-14	1.78	48	58	.85	1.0	42	1.00	.53	1.94	.42	.25	.52	.92	.88	.994	.92	.37
821019-15	1.78	87	66	.83	1.0	41	.99	.52	2.41	.31	.30	.62	.90	1.1	.995	.90	.34
821019-16	1.78	88	71	.97	1.0	41	.99	.51	2.17	.33	.27	.54	.90	.99	.995	.89	.33
821019-17	1.78	120	76	.91	1.0	42	1.00	.52	2.40	.29	.30	.63	.89	1.2	.995	.88	.35
821019-18	1.78	122	84	.69	1.0	43	.99	.54	2.05	.32	.27	.57	.87	1.3	.995	.87	.40
821102-1	1.04	55	52	1.00	5.0	27	.99	.28	2.95	.34	.34	.47	.77	.94	.962	.75	.34
821102-2	1.04	52	63	0.00	5.0	30	.99	.31	2.10	.43	.26	.38	.70	.99	.964	.67	.47
821102-3	1.04	93	68	1.00	5.0	30	1.00	.31	2.78	.31	.35	.51	.67	1.5	.965	.64	.52
821102-4	1.04	92	79	.94	5.0	33	.99	.34	2.14	.37	.30	.45	.57	2.3	.966	.53	1.1
821102-5	1.04	114	83	1.00	5.0	28	1.00	.30	2.33	.33	.28	.40	.54	2.1	.967	.49	.94
821102-6	1.04	119	88	.89	5.0	27	1.00	.29	2.16	.34	.25	.35	.47	2.7	.967	.41	1.7
821102-7	1.19	47	61	1.00	5.0	29	.99	.35	2.00	.44	.25	.39	.79	.76	.973	.78	.35
821102-8	1.19	48	76	.89	5.0	33	1.00	.40	1.44	.52	.20	.34	.72	.93	.975	.70	.53
821102-9	1.19	85	87	.94	5.0	35	1.00	.42	1.69	.42	.25	.44	.65	1.9	.975	.62	.93
821102-10	1.19	85	85	.98	5.0	27	1.00	.33	1.80	.41	.21	.31	.66	.95	.975	.64	.43
821102-11	1.19	116	94	.89	5.0	26	.97	.31	1.86	.37	.21	.30	.60	1.2	.975	.57	.53
821102-12	1.19	119	102	.80	5.0	30	1.00	.36	1.66	.39	.21	.33	.53	2.5	.976	.49	1.4
821102-13	1.41	50	69	1.00	5.0	29	1.00	.41	1.67	.47	.21	.35	.83	.62	.981	.82	.30
821102-14	1.41	51	83	.93	5.0	30	1.00	.43	1.26	.54	.16	.28	.78	.63	.983	.77	.35
821102-15	1.41	113	97	.97	5.0	30	1.00	.43	1.68	.39	.21	.38	.72	1.1	.983	.71	.44
821102-16	1.41	123	111	.80	5.0	31	1.00	.44	1.44	.42	.19	.34	.65	1.5	.983	.64	.68
821102-17	1.41	81	108	.85	5.0	30	.99	.42	1.13	.52	.14	.25	.67	.93	.983	.65	.52

SUMMARY OF MODULUS ANALYSIS ON SANTO50

TEST #	PO	UO	TO	VF	KK	MS	RG	MR	HO	YI	GB	GC	C'	GJ	PR	CP	GP
----	GPa	m/s	'C	--	--	--	--	--	um	--	GPa	GPa	-	GPa	--	--	GPa
821102-18	1.41	81	84	.93	5.0	24	.99	.35	1.68	.42	.17	.27	.78	.54	.982	.77	.24

]

APPENDIX III SUMMARY OF THERMAL HYPERBOLIC SINE ANALYSIS.

The various hyperbolic sine thermal constants calculated from the experimental results are summarized in this Appendix. The nomenclature used is as follows;

Test #	Number of the particular test	(YYMMDD-##)
Po	Maximum calculated Hertz contact stress	(GPa)
Uo	Surface rolling velocity in linear region	(m/sec)
To	Disc surface temperature in linear region	('C)
VF	No-contact voltage fraction	(-)
KK	Contact aspect ratio (b/a)	(-)
SP	Dimensionless spin (ab/U)	(%)
Ho	Isothermal film thickness	(um)
YI	Inlet shear heating factor	(-)
E1	Hyperbolic sine constant for intercept using no inlet shearheating or reduced pressure effects	(Pa.s)
C1	Slope constant for the above	('C/Pa)
R1	Slope regression coefficient for the above	(-)
P1	Pseudo Peclet number for the above	(-)
E2	Hyperbolic sine constant for intercept using inlet shearheating and reduced pressure effects	(Pa.s)
C2	Slope constant for the above	('C/Pa)
R2	Regression coefficient for the above	(-)
P2	Psuedo Peclet number for the above	(-)

SUMMARY OF THERMAL HYPERBOLIC SINE ANALYSIS ON TDF88

TEST #	P0	U0	T0	VF	KK	SP	H0	YI	E1	C1	R1	P1	PR	E2	C2	R2	P2
----	GPa	m/s	'C	--	--	%	um	--	Pa.s	'C/Pa	--	--	--	Pa.s	'C/Pa	--	--
820804-1	1.07	50	71	1.0	2.0	0.00	1.90	.45	.77E-04	.35E-04	.99	3734	.974	.46E-06	.22E-04	.99	726
820804-2	1.07	52	81	0.0	2.0	0.00	1.54	.50	.99E-03	.37E-04	.98	2365	.976	.17E-04	.27E-04	.97	588
820804-3	1.07	85	86	1.0	2.0	0.00	1.92	.39	.98E-03	.44E-04	.99	8320	.976	.22E-05	.24E-04	.99	1057
820804-4	1.07	85	98	0.0	2.0	0.00	1.52	.45	.64E-02	.51E-04	1.0	5769	.977	.66E-04	.36E-04	.99	933
820804-5	1.07	113	109	0.0	2.0	0.00	1.50	.42	.89E-02	.58E-04	.96	7341	.978	.14E-03	.46E-04	.91	1071
820804-6	1.07	117	102	1.0	2.0	0.00	1.76	.38	.16E-03	.43E-04	.98	8361	.977	.66E-06	.19E-04	.93	1092
820804-7	1.23	53	86	1.0	2.0	0.00	1.38	.51	.27E-04	.31E-04	.99	1919	.982	.38E-06	.21E-04	.99	485
820804-8	1.23	50	93	.8	2.0	0.00	1.13	.57	.41E-03	.35E-04	1.0	1150	.983	.15E-04	.28E-04	.99	369
820804-9	1.23	85	97	1.0	2.0	0.00	1.50	.44	.25E-03	.40E-04	.99	4167	.982	.13E-05	.26E-04	.98	729
820804-10	1.23	82	110	.8	2.0	0.00	1.17	.51	.72E-02	.51E-04	1.0	2487	.983	.21E-03	.41E-04	.99	586
820804-11	1.23	119	96	1.0	2.0	0.00	1.92	.35	.69E-03	.47E-04	.97	11050	.982	.63E-06	.26E-04	.93	1073
820804-12	1.23	115	119	.8	2.0	0.00	1.27	.45	.64E-02	.55E-04	.99	3495	.983	.93E-04	.43E-04	.97	715
820805-1	1.46	51	116	1.0	2.0	0.00	.75	.66	.26E-05	.26E-04	1.0	392	.989	.28E-06	.21E-04	1.0	175
820805-2	1.46	51	126	.7	2.0	0.00	.64	.69	.36E-04	.30E-04	.99	358	.990	.45E-05	.25E-04	.99	166
820805-3	1.46	82	118	1.0	2.0	0.00	.99	.54	.41E-04	.37E-04	.99	1333	.989	.95E-06	.27E-04	.97	380
820805-4	1.46	82	126	.8	2.0	0.00	.88	.57	.31E-02	.52E-04	.98	938	.989	.25E-03	.47E-04	.96	321
820805-5	1.46	106	103	1.0	2.0	0.00	1.52	.41	.23E-03	.51E-04	1.0	4507	.988	.36E-06	.33E-04	.99	670
820805-6	1.46	100	118	.8	2.0	0.00	1.14	.49	.19E-02	.48E-04	.98	1014	.988	.27E-04	.37E-04	.98	326
820824-1	1.62	49	61	1.0	1.0	0.00	2.00	.39	.98E-03	.39E-04	1.0	3297	.993	.37E-06	.29E-04	1.0	445
820824-2	1.62	49	68	.9	1.0	0.00	1.65	.44	.68E-02	.37E-04	1.0	2542	.994	.16E-04	.31E-04	1.0	407
820824-3	1.62	83	72	1.0	1.0	0.00	2.12	.32	.01E+00	.47E-04	.99	9809	.994	.21E-05	.35E-04	.98	667
820824-4	1.62	82	81	.9	1.0	0.00	1.70	.37	.04E+00	.45E-04	1.0	5364	.994	.60E-04	.36E-04	.99	564
820824-5	1.62	118	88	1.0	1.0	0.00	1.88	.32	.73E-02	.47E-04	.99	9010	.994	.12E-05	.34E-04	.98	675
820824-6	1.62	116	101	.8	1.0	0.00	1.43	.38	.07E+00	.53E-04	.99	10620	.994	.30E-03	.45E-04	.98	740
820824-7	1.78	48	83	1.0	1.0	0.00	1.10	.53	.97E-04	.35E-04	1.0	688	.995	.11E-05	.30E-04	1.0	203
820824-8	1.78	45	89	.8	1.0	0.00	.94	.58	.23E-03	.35E-04	1.0	479	.995	.58E-05	.31E-04	1.0	166
820824-9	1.78	82	89	1.0	1.0	0.00	1.42	.41	.91E-03	.41E-04	.99	2721	.995	.11E-05	.32E-04	.99	406
820824-10	1.78	83	99	.9	1.0	0.00	1.15	.46	.70E-02	.45E-04	.99	2185	.995	.61E-04	.39E-04	.98	383
820824-11	1.78	119	78	1.0	1.0	0.00	2.30	.27	.08E+00	.53E-04	.99	26950	.995	.44E-05	.40E-04	.98	790
820824-12	1.78	117	95	.9	1.0	0.00	1.59	.35	.14E+00	.51E-04	1.0	10580	.995	.29E-03	.43E-04	1.0	672
820824-13	1.41	49	74	1.0	1.0	0.00	1.45	.47	.25E-03	.35E-04	1.0	1860	.992	.93E-06	.26E-04	1.0	389

SUMMARY OF THERMAL HYPERBOLIC SINE ANALYSIS ON TDF88

TEST #	P0	U0	T0	VF	KK	SP	H0	YI	E1	C1	R1	P1	PR	E2	C2	R2	P2
----	GPa	m/s	'C	--	--	%	um	--	Pa.s	'C/Pa	--	--	--	Pa.s	'C/Pa	--	--
820824-14	1.41	49	77	.9	1.0	0.00	1.34	.49	.23E-02	.36E-04	1.0	1815	.992	.16E-04	.29E-04	1.0	388
820824-15	1.41	84	77	1.0	1.0	0.00	1.95	.35	.59E-02	.47E-04	.99	8789	.992	.23E-05	.34E-04	.98	736
820824-16	1.41	83	83	.9	1.0	0.00	1.67	.38	.04E+00	.45E-04	1.0	7040	.992	.81E-04	.35E-04	.99	695
820824-17	1.41	115	88	1.0	1.0	0.00	1.87	.32	.02E+00	.55E-04	.99	13650	.992	.83E-05	.39E-04	.97	866
820824-18	1.41	114	98	.8	1.0	0.00	1.55	.37	.05E+00	.51F-04	1.0	9055	.993	.12E-03	.39E-04	1.0	784
820825-1	1.41	49	72	1.0	1.0	.294	1.51	.46	.15E-03	.37E-04	1.0	2367	.992	.31E-06	.26E-04	1.0	432
820825-2	1.41	49	77	1.0	1.0	.294	1.34	.49	.86E-04	.32E-04	.99	1689	.992	.35E-06	.23E-04	1.0	371
820825-3	1.41	81	79	1.0	1.0	.294	1.83	.36	.15E-02	.50E-04	1.0	6633	.992	.52E-06	.33E-04	.99	668
820825-4	1.41	83	89	1.0	1.0	.294	1.48	.41	.91E-03	.37E-04	1.0	4493	.992	.10E-05	.25E-04	1.0	588
820825-5	1.41	120	97	1.0	1.0	.294	1.61	.35	.24E-02	.60E-04	.92	10180	.993	.15E-05	.40E-04	.86	803
820825-6	1.41	116	109	.6	1.0	.294	1.28	.41	.25E-03	.35E-04	.89	4057	.993	.44E-06	.21E-04	.81	586
820825-7	1.61	50	74	1.0	1.0	.336	1.43	.47	.47E-03	.39E-04	1.0	1857	.994	.10E-05	.30E-04	1.0	354
820825-8	1.61	49	81	0.0	1.0	.336	1.21	.51	.20E-03	.36E-04	1.0	1212	.994	.10E-05	.28E-04	1.0	289
820825-9	1.61	85	83	1.0	1.0	.336	1.65	.38	.53E-02	.51E-04	.97	6425	.994	.31E-05	.39E-04	.95	595
820825-10	1.61	87	94	.9	1.0	.336	1.35	.42	.21E-02	.40E-04	.99	3873	.994	.26E-05	.29E-04	.99	504
820825-11	1.61	117	100	1.0	1.0	.336	1.47	.37	.38E-02	.59E-04	.94	6698	.994	.37E-05	.45E-04	.91	625
820825-12	1.61	120	114	.6	1.0	.336	1.18	.42	.20E-02	.45E-04	.99	4587	.995	.37E-05	.32E-04	.99	561
820825-13	1.78	49	70	1.0	1.0	.370	1.53	.45	.12E-02	.41E-04	1.0	2105	.995	.15E-05	.33E-04	1.0	347
820825-14	1.78	48	79	1.0	1.0	.370	1.23	.50	.36E-03	.35E-04	1.0	1278	.995	.15E-05	.29E-04	1.0	279
820825-15	1.78	84	85	1.0	1.0	.370	1.57	.39	.35E-02	.48E-04	.99	4717	.995	.18E-C5	.37E-04	.99	494
820825-16	1.78	84	98	.9	1.0	.370	1.20	.45	.98E-03	.40E-04	1.0	2329	.995	.19E-05	.31E-04	1.0	383
820825-17	1.78	120	105	1.0	1.0	.370	1.34	.39	.85E-02	.59E-04	.97	6682	.995	.12E-04	.46E-04	.96	584
820825-18	1.78	118	120	.6	1.0	.370	1.03	.45	.10E-02	.41E-04	.99	2475	.996	.28E-05	.31E-04	.99	411
820826-1	1.78	50	53	1.0	1.0	.184	2.56	.33	.01E+00	.42E-04	1.0	6600	.994	.64E-06	.32E-04	1.0	519
820826-2	1.78	50	66	0.0	1.0	.184	1.72	.42	.01E+00	.38E-04	1.0	3252	.995	.17E-04	.31E-04	1.0	415
820826-3	1.78	91	83	1.0	1.0	.184	1.72	.36	.05E+00	.46E-04	1.0	7930	.995	.36E-04	.37E-04	.99	589
820826-4	1.78	92	82	1.0	1.0	.184	1.75	.35	.92E-02	.48E-04	.99	6396	.995	.37E-05	.38E-04	.98	550
820826-5	1.78	118	96	.9	1.0	.184	1.55	.35	.01E+00	.50E-04	1.0	7457	.995	.49E-05	.38E-04	.99	597
820826-6	1.78	119	110	.6	1.0	.184	1.23	.41	.02E+00	.51E-04	.99	6015	.995	.81E-04	.4[illegible]E-04	.97	579
820826-7	1.62	50	59	1.0	1.0	.167	2.14	.37	.29E-02	.42E-04	1.0	4417	.993	.73E-06	.32E-04	.99	497
820826-8	1.62	51	68	.9	1.0	.167	1.67	.43	.62E-02	.37E-04	1.0	2751	.994	.92E-05	.30E-04	1.0	419

SUMMARY OF THERMAL HYPERBOLIC SINE ANALYSIS ON TDF88

TEST #	PO	UO	TO	VF	KK	SP	HO	YI	E1	C1	R1	P1	PR	E2	C2	R2	P2
----	GPa	m/s	'C	--	--	%	um	--	Pa.s	'C/Pa	--	--	--	Pa.s	'C/Pa	--	--
820826-9	1.62	83	79	.9	1.0	.167	1.78	.36	.04E+00	.45E-04	1.0	7993	.994	.30E-04	.35E-04	1.0	637
820826-10	1.62	80	79	1.0	1.0	.167	1.75	.37	.90E-03	.41E-04	.99	4945	.994	.28E-06	.30E-04	.99	538
820826-11	1.62	124	91	1.0	1.0	.167	1.80	.32	.61E-02	.51E-04	.96	12940	.994	.10E-05	.36E-04	.93	754
820826-12	1.62	127	105	.6	1.0	.167	1.42	.37	.03E+00	.51E-04	.99	8700	.994	.47E-04	.40E-04	.98	696
820826-13	1.41	48	65	1.0	1.0	.146	1.77	.43	.22E-03	.36E-04	1.0	2743	.991	.22E-06	.25E-04	1.0	459
820826-14	1.41	52	73	1.0	1.0	.146	1.57	.45	.42E-02	.37E-04	1.0	3068	.992	.10E-04	.26E-04	1.0	483
820826-15	1.41	86	80	.9	1.0	.146	1.86	.36	.03E+00	.45E-04	1.0	9649	.992	.18E-04	.32E-04	1.0	761
820826-16	1.41	86	79	1.0	1.0	.146	1.86	.36	.13E-02	.46E-04	.99	6714	.992	.35E-06	.29E-04	.99	674
820826-17	1.41	125	91	.9	1.0	.146	1.88	.32	.29E-02	.49E-04	.98	13560	.992	.49E-06	.30E-04	.97	866
820826-18	1.41	125	102	.8	1.0	.146	1.51	.36	.02E+00	.50E-04	.99	9880	.993	.26E-04	.37E-04	.98	810
820831-1	1.46	29	68	1.0	2.0	0.00	1.36	.58	.37E-06	.26E-04	1.0	563	.986	.10E-07	.20E-04	1.0	210
820831-2	1.46	27	68	1.0	2.0	.230	1.25	.60	.14E-06	.25E-04	.99	536	.987	.47E-08	.19E-04	1.0	203
820831-3	1.46	31	83	0.0	2.0	.230	.98	.65	.10E-05	.24E-04	.99	403	.988	.54E-07	.18E-04	.99	171
820831-4	1.46	58	78	1.0	2.0	.230	1.68	.45	.48E-04	.42E-04	.99	2571	.987	.12E-06	.31E-04	.99	495
820831-5	1.46	63	99	0.0	2.0	.230	1.15	.53	.61E-04	.36E-04	.98	1573	.988	.76E-06	.27E-04	.96	399
820831-6	1.46	91	99	1.0	2.0	.230	1.46	.44	.55E-04	.44E-04	.98	3372	.988	.11E-06	.27E-04	.97	584
820831-7	1.46	91	113	1.0	2.0	.230	1.15	.49	.14E-03	.40E-04	.99	2378	.988	.11E-05	.27E-04	.99	508
820831-8	1.23	49	62	1.0	2.0	.194	2.35	.40	.67E-04	.49E-04	.99	5036	.979	.59E-07	.31E-04	.96	737
820831-9	1.23	46	77	.9	2.0	.194	1.51	.51	.60E-04	.30E-04	1.0	1958	.981	.54E-06	.21E-04	1.0	483
820831-10	1.23	79	81	1.0	2.0	.194	2.00	.38	.51E-04	.48E-04	.98	6335	.981	.70E-0	.27E-04	.95	842
820831-11	1.23	78	95	0.0	2.0	.194	1.46	.46	.20E-03	.37E-04	.99	3796	.982	.11E-05	.23E-04	.99	692
820831-12	1.23	98	95	1.0	2.0	.194	1.74	.39	.18E-04	.46E-04	.52	5533	.982	.82E-07	.32E-04	.24	816
820831-13	1.23	99	105	.9	2.0	.194	1.46	.43	.20E-03	.42E-04	.98	4759	.983	.88E-06	.24E-04	.97	779
820831-14	1.07	46	66	1.0	2.0	.169	2.04	.44	.13E-04	.49E-04	.95	4336	.974	.71E-07	.29E-04	.89	772
820831-15	1.07	50	82	0.0	2.0	.169	1.47	.51	.19E-04	.26E-04	.99	2384	.976	.41E-06	.15E-04	.99	587
820831-16	1.07	82	82	1.0	2.0	.169	2.04	.38	.13E-04	.44E-04	.82	7135	.975	.52E-0[illegible]	.20E-04	.65	988
820831-17	1.07	85	99	1.0	2.0	.169	1.50	.45	.86E-04	.35E-04	.97	4935	.977	.90E-06	.18E-04	.93	865
820831-18	1.07	114	98	1.0	2.0	.169	1.87	.37	.04E+00	.25E-03	.07	10080	.977	.24E+17	.98E-03	.00	1167
820831-19	1.07	115	110	.9	2.0	.169	1.51	.42	.25E-03	.47E-04	.94	7774	.978	.18E-05	.25E-04	.84	1075
820902-1	1.23	48	72	1.0	2.0	0.00	1.78	.46	.42E-05	.33E-04	.99	2241	.981	.31E-07	.21E-04	.99	516
820902-2	1.23	83	83	1.0	2.0	0.00	1.97	.38	.59E-05	.40E-04	.95	5326	.981	.14E-07	.19E-04	.92	790

SUMMARY OF THERMAL HYPERBOLIC SINE ANALYSIS ON TDF88

TEST #	PO	UO	TO	VF	KK	SP	HO	YI	E1	C1	R1	P1	PR	E2	C2	R2	P2
----	GPa	m/s	'C	--	--	%	um	--	Pa.s	'C/Pa	--	--	--	Pa.s	'C/Pa	--	--
820902-3	1.23	117	96	1.0	2.0	0.00	1.92	.35	.60E-04	.43E-04	.88	9014	.982	.81E-07	.21E-04	.79	1000
820902-4	1.24	46	78	1.0	2.0	.400	1.50	.51	.36E-05	.29E-04	.99	1812	.981	.48E-07	.19E-04	.99	463
820902-5	1.24	47	86	0.0	2.0	.400	1.26	.55	.76E-05	.30E-04	.99	1367	.982	.18E-06	.20E-04	.99	401
820902-6	1.24	84	89	1.0	2.0	.400	1.76	.41	.47E-04	.41E-04	.95	4241	.982	.17E-06	.26E-04	.95	724
820902-7	1.24	83	103	1.0	2.0	.400	1.32	.48	.36E-04	.35E-04	.93	2984	.983	.39E-06	.21E-04	.86	622
820902-8	1.24	107	80	1.0	2.0	.400	2.47	.31	.28E-03	.61E-04	.57	11320	.981	.59E-07	.32E-04	.43	1053
820902-9	1.24	99	97	0.0	2.0	.400	1.67	.40	.24E-03	.43E-04	.99	6908	.982	.47E-06	.23E-04	.97	894
820903-1	1.07	49	56	1.0	2.0	0.00	2.83	.36	.37E-04	.46E-04	.94	6982	.972	.31E-07	.23E-04	.98	936
820903-2	1.07	85	69	1.0	2.0	0.00	2.85	.31	.77E-03	.66E-04	.96	15890	.974	.18E-06	.32E-04	.95	1294
820903-3	1.07	115	81	1.0	2.0	0.00	2.66	.29	.39E-03	.49E-04	.85	24580	.976	.17E-06	.25E-04	.66	1514
820903-4	1.08	47	60	1.0	2.0	.350	2.45	.40	.47E-05	.33E-04	.80	5269	.972	.13E-07	.16E-04	.70	832
820903-6	1.08	84	95	0.0	2.0	.350	1.61	.43	.46E-04	.27E-04	.93	4723	.977	.47E-06	.14E-04	.86	844
820903-7	1.08	48	91	.9	2.0	.350	1.18	.57	.77E-05	.26E-04	.98	1520	.977	.40E-06	.15E-04	.98	463
820903-8	1.08	113	95	1.0	2.0	.350	1.94	.36	-.7E-10	-.1E-03	.08	8359	.977	-.4E-09	-.4E-04	.31	1080
820903-9	1.08	113	87	0.0	2.0	.350	2.29	.32	.73E-03	.44E-04	.76	16450	.976	.55E-06	.23E-04	.64	1352
820904-1	1.46	31	66	1.0	2.0	0.00	1.51	.54	.33E-06	.26E-04	.99	779	.986	.56E-08	.20E-04	.99	256
820904-2	1.46	29	78	.9	2.0	0.00	1.05	.64	.19E-05	.24E-04	.99	302	.988	.15E-06	.20E-04	1.0	141
820904-3	1.46	59	80	1.0	2.0	0.00	1.64	.45	.21E-04	.40E-04	.98	2253	.987	.75E-07	.29E-04	.96	469
820904-4	1.46	58	91	.9	2.0	0.00	1.26	.52	.35E-04	.31E-04	.98	1196	.987	.47E-06	.24E-04	.97	343
820904-5	1.46	89	87	1.0	2.0	0.00	1.86	.38	.11E-03	.44E-04	.97	4865	.987	.96E-07	.30E-04	.92	671
820904-6	1.46	86	101	.9	2.0	0.00	1.36	.46	.18E-02	.46E-04	.99	3684	.988	.88E-05	.34E-04	.98	613
820904-7	1.46	27	67	1.0	2.0	.474	1.31	.59	.15E-06	.26E-04	.99	619	.987	.38E-08	.20E-04	1.0	222
820904-8	1.46	30	83	1.0	2.0	.474	.96	.65	.14E-06	.22E-04	.99	415	.988	.96E-08	.17E-04	1.0	174
820904-9	1.46	61	84	1.0	2.0	.474	1.50	.47	.18E-04	.38E-04	.99	2228	.987	.65E-07	.26E-04	.99	467
820904-10	1.46	61	99	.9	2.0	.474	1.12	.54	.15E-04	.35E-04	.97	1437	.988	.19E-06	.24E-04	.95	378
820904-11	1.46	90	101	1.0	2.0	.474	1.39	.45	.41E-04	.42E-04	.95	2552	.988	.18E-06	.29E-04	.96	519
820904-12	1.46	89	114	.9	2.0	.474	1.11	.50	.74E-04	.41E-04	.99	2187	.988	.61E-06	.28E-04	.99	485
820916-1	1.01	50	71	1.0	5.6	0.00	2.06	.45	.13E-03	.43E-04	1.0	3558	.974	.12E-05	[illegible]	.99	749
820916-2	1.01	48	88	0.0	5.6	0.00	1.36	.55	.45E-03	.30E-04	1.0	1593	.976	.22E-04	.23E-04	1.0	498
820916-3	1.01	86	87	1.0	5.6	0.00	2.08	.39	.36E-03	.76E-04	.98	7349	.975	.18E-05	.47E-04	.95	1075
820916-4	1.01	84	100	1.0	5.6	0.00	1.57	.46	.63E-03	.41E-04	.99	4599	.977	.94E-05	.26E-04	.97	890

SUMMARY OF THERMAL HYPERBOLIC SINE ANALYSIS ON TDF88

TEST #	P0	U0	T0	VF	KK	SP	H0	YI	E1	C1	R1	F1	PR	E2	C2	R2	P2
----	GPa	m/s	'C	--	--	%	um	--	Pa.s	'C/Pa	--	--	--	Pa.s	'C/Pa	--	--
820916-5	1.01	106	102	.9	5.6	0.00	1.76	.41	.51E-04	.57E-04	.97	5059	.977	.75E-06	.33E-04	.96	941
820916-6	1.01	113	112	.8	5.6	0.00	1.56	.43	.18E-02	.59E-04	.99	5939	.977	.25E-04	.40E-04	.97	1028
820916-7	1.02	48	65	1.0	5.6	.631	2.31	.43	.28E-03	.47E-04	.99	5411	.973	.94E-06	.28E-04	.99	892
820916-8	1.02	46	78	1.0	5.6	.631	1.65	.51	.90E-04	.34E-04	.97	2580	.975	.16E-05	.21E-04	.97	635
820916-9	1.02	89	81	1.0	5.6	.631	2.37	.35	.26E-03	.58E-04	.96	10100	.975	.49E-06	.31E-04	.96	1194
820916-10	1.02	89	101	1.0	5.6	.631	1.59	.45	.22E-03	.47E-04	.97	5492	.977	.22E-05	.24E-04	.94	956
820916-11	1.02	100	97	1.0	5.6	.631	1.84	.40	.65E-04	.55E-04	.96	6398	.976	.54E-06	.28E-04	.97	1027
820916-12	1.02	113	115	.9	5.6	.631	1.46	.44	.20E-03	.51E-04	.96	5878	.978	.29E-05	.26E-04	.90	1012
820916-13	1.02	31	96	.9	5.6	.631	.84	.70	.65E-05	.24E-04	.99	447	.980	.14E-05	.17E-04	.99	216
820916-14	1.02	32	87	1.0	5.6	.631	1.04	.66	.12E-04	.28E-04	.99	677	.978	.16E-05	.21E-04	1.0	287
821116-1	1.04	48	60	1.0	5.0	0.00	2.28	.39	.16E-03	.46E-04	.98	6880	.964	.38E-06	.28E-04	.99	1094
821116-2	1.04	51	72	0.0	5.0	0.00	1.69	.46	.27E-03	.37E-04	.98	4675	.966	.20E-05	.24E-04	.99	929
821116-3	1.04	84	87	.9	5.0	0.00	1.69	.40	.15E-02	.41E-04	.99	8579	.968	.61E-05	.24E-04	.99	1260
821116-4	1.04	84	87	1.0	5.0	0.00	1.70	.40	.10E-03	.52E-04	.99	10300	.968	.36E-06	.24E-04	.98	1341
821116-5	1.04	118	94	.8	5.0	0.00	1.85	.35	.61E-04	.45E-04	.79	13070	.969	.21E-06	.18E-04	.54	1511
821116-6	1.04	117	114	.5	5.0	0.00	1.29	.43	.13E-03	.35E-04	.96	7370	.971	.18E-05	.16E-04	.91	1234
821116-7	1.19	51	64	1.0	5.0	0.00	2.04	.40	.12E-03	.37E-04	.97	5004	.973	.24E-06	.25E-04	.98	862
821116-8	1.19	51	76	0.0	5.0	0.00	1.53	.47	.46E-03	.38E-04	1.0	3744	.975	.30E-05	.27E-04	1.0	762
821116-9	1.19	84	87	.9	5.0	0.00	1.69	.39	.15E-03	.45E-04	.99	7153	.976	.31E-06	.26E-04	.99	1047
821116-10	1.19	84	101	0.0	5.0	0.00	1.27	.46	.91E-03	.40E-04	.99	6153	.977	.62E-05	.26E-04	1.0	994
821116-11	1.19	118	106	.8	5.0	0.00	1.47	.39	.71E-04	.48E-04	.99	9721	.977	.22E-06	.27E-04	.98	1218
821116-12	1.19	118	103	0.0	5.0	0.00	1.53	.38	.13E-02	.44E-04	.99	11180	.977	.27E-05	.25E-04	.99	1289
821116-13	1.41	51	71	1.0	5.0	0.00	1.67	.44	.13E-03	.37E-04	.98	2837	.982	.41E-06	.28E-04	.99	593
821116-14	1.41	51	93	0.0	5.0	0.00	1.02	.56	.12E-03	.33E-04	.99	1273	.984	.31E-05	.27E-04	1.0	396
821116-15	1.41	88	102	1.0	5.0	0.00	1.23	.46	.11E-03	.43E-04	.99	4209	.984	.52E-06	.29E-04	.99	746
821116-16	1.41	91	132	.7	5.0	0.00	.79	.57	.11E-03	.36E-04	.99	1638	.986	.39E-05	.27E-04	.99	485
821116-17	1.41	107	102	.9	5.0	0.00	1.42	.40	.20E-03	.48E-04	.98	6026	.984	.31E 06	.30E-04	.99	875
821116-18	1.41	116	133	.6	5.0	0.00	.92	.50	.64E-03	.43E-04	1.0	3256	.985	.70E-05	.30E-04	.98	696
821118-1	1.06	51	64	1.0	5.2	.821	2.06	.40	.01E+00	.50E-04	1.0	10320	.966	.26E-04	.34E-04	.99	1271
821118-2	1.06	51	76	.8	5.2	.821	1.54	.47	.01E+00	.43E-04	.99	4958	.968	.12E-03	.31E-04	1.0	951
821118-3	1.06	83	76	1.0	5.2	.821	2.10	.35	.47E-02	.52E-04	.99	18080	.968	.34E-05	.30E-04	.99	1599

SUMMARY OF THERMAL HYPERBOLIC SINE ANALYSIS ON TDF88

TEST #	P0	U0	T0	VF	KK	SP	H0	YI	E1	C1	R1	P1	PR	E2	C2	R2	P2
----	GPa	m/s	'C	--	--	%	um	--	Pa.s	'C/Pa	--	--	--	Pa.s	'C/Pa	--	--
821118-4	1.06	84	91	.8	5.2	.821	1.52	.42	.04E+00	.50E-04	1.0	11910	.970	.17E-03	.33E-04	1.0	1413
821118-5	1.06	111	87	1.0	5.2	.821	2.01	.33	.26E-02	.56E-04	.98	20160	.970	.23E-05	.31E-04	.98	1710
821118-6	1.06	118	103	.7	5.2	.821	1.53	.38	.27E+00	.67E-04	.98	21600	.971	.37E-02	.52E-04	.97	1789
821118-7	1.22	51	90	.8	5.2	.940	1.09	.55	.89E-02	.46E-04	.99	2570	.978	.30E-03	.38E-04	1.0	637
821118-8	1.22	51	79	1.0	5.2	.940	1.37	.49	.51E-03	.38E-04	.98	3193	.976	.38E-05	.27E-04	.97	701
821118-9	1.22	83	83	1.0	5.2	.940	1.74	.38	.25E-02	.52E-04	1.0	10370	.976	.28E-05	.33E-04	1.0	1183
821118-10	1.22	85	105	.8	5.2	.940	1.16	.48	.33E-02	.48E-04	.99	4227	.978	.35E-04	.34E-04	.99	843
821118-11	1.22	111	96	1.0	5.2	.940	1.65	.37	.41E-02	.66E-04	.98	12600	.977	.53E-05	.42E-04	.98	1309
821118-12	1.22	121	109	.8	5.2	.940	1.36	.40	.03E+00	.61E-04	.99	10070	.978	.17E-03	.45E-04	.99	1234
821118-13	1.44	51	83	.9	5.2	1.11	1.21	.52	.12E-02	.44E-04	.99	2110	.984	.15E-04	.36E-04	.99	512
821118-14	1.44	51	98	.6	5.2	1.11	.90	.59	.68E-03	.41E-04	.97	784	.985	.48E-04	.37E-04	.99	299
821118-15	1.44	86	89	1.0	5.2	1.11	1.53	.40	.32E-02	.56E-04	1.0	7278	.984	.47E-05	.41E-04	.99	908
821118-16	1.44	87	114	.7	5.2	1.11	.97	.51	.21E-02	.52E-04	.99	2394	.985	.32E-04	.42E-04	1.0	576
821118-17	1.44	103	100	1.0	5.2	1.11	1.39	.41	.32E-02	.61E-04	1.0	6779	.984	.70E-05	.43E-04	1.0	905
821118-18	1.44	110	113	.8	5.2	1.11	1.17	.44	.09E+00	.67E-04	1.0	6182	.985	.22E-02	.58E-04	.99	893

]

SUMMARY OF THERMAL HYPERBOLIC SINE ANALYSIS ON SANTO50

TEST #	PO	UO	TO	VF	KK	SP	HO	YI	E1	C1	P1	P1	PR	E2	C2	R2	P2
----	GPa	m/s	'C	--	--	%	um	--	Pa.s	'C/Pa	--	--	--	Pa.s	'C/Pa	--	--
820923-1	.98	48	53	1.0	5.6	.605	3.06	.39	.92E-03	.40E-04	.98	10450	.969	.11E-05	.24E-04	.97	1347
820923-2	.98	48	64	1.0	5.6	.605	2.30	.46	.74E-03	.33E-04	.99	5293	.970	.50E-05	.22E-04	.98	1032
820923-3	.98	78	65	1.0	5.6	.605	3.11	.33	.19E-02	.56E-04	.98	18650	.970	.15E-05	.33E-04	.97	1736
820923-4	.98	77	83	.9	5.6	.605	2.10	.43	.20E-02	.51E-04	.99	9373	.972	.87E-05	.29E-04	.98	1388
820923-5	.98	106	84	1.0	5.6	.605	2.55	.35	.33E-03	.58E-04	.87	14110	.972	.69E-06	.27E-04	.85	1666
820923-6	.98	111	103	.8	5.6	.605	1.90	.42	.40E-03	.46E-04	.97	7826	.973	.39E-05	.23E-04	.98	1366
820923-7	.97	49	61	1.0	5.6	0.00	2.52	.43	.51E-03	.41E-04	.99	5276	.969	.30E-05	.27E-04	1.0	1036
820923-8	.97	50	72	1.0	5.6	0.00	1.96	.49	.49E-02	.35E-04	.96	3889	.971	.99E-04	.27E-04	.95	909
820923-9	.97	75	73	1.0	5.6	0.00	2.53	.39	.14E-02	.58E-04	1.0	10680	.971	.36E-05	.34E-04	.99	1451
820923-10	.97	73	87	.9	5.6	0.00	1.91	.46	.37E-02	.50E-04	.98	6090	.972	.49E-04	.35E-04	.96	1176
820923-11	.97	113	98	.9	5.6	0.00	2.10	.39	.38E-03	.82E-04	.91	11180	.973	.23E-05	.44E-04	.80	1577
820923-12	.97	113	99	.7	5.6	0.00	2.07	.40	.03E+00	.98E-04	.87	19810	.973	.92E-03	.85E-04	.72	1968
820924-1	1.07	44	46	1.0	2.0	0.00	3.33	.36	.20E-02	.34E-04	.99	9715	.970	.90E-06	.23E-04	1.0	1186
820924-2	1.07	47	59	.7	2.0	0.00	2.35	.43	.05E+00	.39E-04	1.0	7774	.972	.27E-03	.30E-04	1.0	1114
820924-3	1.07	79	58	1.0	2.0	0.00	3.48	.29	.49E-02	.52E-04	.99	24060	.973	.56E-06	.30E-04	.96	1679
820924-4	1.07	81	74	.7	2.0	0.00	2.43	.37	.06E+00	.44E-04	1.0	17960	.974	.12E-03	.31E-04	1.0	1585
820924-5	1.07	113	75	1.0	2.0	0.00	2.94	.30	.87E-03	.47E-04	.83	21580	.974	.21E-06	.22E-04	.69	1715
820924-6	1.07	113	90	.8	2.0	0.00	2.20	.36	.02E+00	.47E-04	.99	19030	.975	.44E-04	.31E-04	.99	1705
820924-7	1.23	49	54	1.0	2.0	0.00	2.76	.38	.47E-02	.39E-04	1.0	9083	.978	.23E-05	.27E-04	1.0	1047
820924-8	1.23	48	69	.8	2.0	0.00	1.85	.48	.04E+00	.38E-04	1.0	4106	.980	.47E-03	.31E-04	1.0	781
820924-9	1.23	79	65	1.0	2.0	0.00	2.87	.33	.68E-02	.44E-04	1.0	16200	.980	.12E-05	.28E-04	1.0	1331
820924-10	1.23	78	80	.7	2.0	0.00	2.05	.41	.04E+00	.43E-04	1.0	10130	.980	.12E-03	.32E-04	1.0	1173
820924-11	1.23	112	76	1.0	2.0	0.00	2.83	.30	.39E-02	.52E-04	.99	25590	.981	.44E-06	.30E-04	.96	1579
820924-12	1.23	113	92	.9	2.0	0.00	2.09	.37	.04E+00	.50E-04	.99	21490	.981	.67E-04	.36E-04	.97	1560
820924-13	1.46	48	71	1.0	2.0	0.00	1.73	.49	.71E-03	.36E-04	1.0	2314	.986	.33E-05	.28E-04	1.0	528
820924-14	1.46	47	83	.6	2.0	0.00	1.33	.56	.01E+00	.37E-04	1.0	1450	.987	.34E-03	.33E-04	1.0	424
820924-15	1.46	80	80	1.0	2.0	0.00	2.02	.40	.27E-02	.42E-04	1.0	6787	.986	.22E-05	.30E-04	1.0	882
820924-16	1.46	80	94	.7	2.0	0.00	1.56	.47	.02E+00	.46E-04	.99	4701	.987	.29E-03	.39E-04	.97	798
820924-17	1.46	109	91	1.0	2.0	0.00	2.02	.37	.58E-02	.49E-04	.99	11810	.987	.45E-05	.35E-04	.97	1112
820924-18	1.46	113	97	.6	2.0	0.00	1.84	.39	.22E-02	.48E-04	.99	8439	.987	.23E-05	.33E-04	.99	1002
820925-1	1.07	51	60	1.0	2.0	.169	2.47	.41	.99E-03	.42E-04	.99	8104	.972	.15E-05	.26E-04	.99	1134

SUMMARY OF THERMAL HYPERBOLIC SINE ANALYSIS ON SANTO50

TEST #	P0	U0	T0	VF	KK	SP	H0	YI	E1	C1	R1	P1	PR	E2	C2	R2	P2
----	GPa	m/s	'C	--	--	%	um	--	Pa.s	'C/Pa	--	--	--	Pa.s	'C/Pa	--	--
820925-2	1.07	49	63	0.0	2.0	.169	2.22	.44	.43E-03	.37E-04	.99	5518	.973	.16E-05	.25E-04	.99	969
820925-3	1.07	85	69	1.0	2.0	.169	2.77	.34	.15E-02	.54E-04	.99	16840	.974	.64E-06	.30E-04	.99	1541
820925-4	1.07	84	76	.9	2.0	.169	2.39	.37	.15E-02	.48E-04	.98	14390	.974	.15E-05	.27E-04	.97	1478
820925-5	1.07	112	76	1.0	2.0	.169	2.85	.30	.68E-03	.54E-04	.93	20730	.974	.20E-06	.26E-04	.84	1690
820925-6	1.07	112	83	.9	2.0	.169	2.50	.33	.29E-02	.46E-04	.99	19920	.975	.16E-05	.24E-04	.98	1687
820925-7	1.23	52	75	1.0	2.0	.194	1.70	.50	.18E-03	.35E-04	1.0	3062	.981	.12E-05	.25E-04	1.0	683
820925-8	1.23	49	78	.9	2.0	.194	1.52	.53	.89E-03	.36E-04	1.0	2773	.981	.10E-04	.27E-04	1.0	654
820925-9	1.23	80	79	1.0	2.0	.194	2.09	.40	.75E-03	.44E-04	.98	8482	.980	.88E-06	.28E-04	.97	1091
820925-10	1.23	81	84	.9	2.0	.194	1.91	.42	.69E-02	.41E-04	1.0	8227	.981	.16E-04	.28E-04	1.0	1091
820925-11	1.23	109	90	.9	2.0	.194	2.12	.37	.02E+00	.49E-04	.99	16310	.981	.14E-04	.32E-04	.99	1421
820925-12	1.23	109	92	1.0	2.0	.194	2.05	.37	.29E-03	.44E-04	.71	8996	.981	.35E-06	.26E-04	.55	1158
820925-13	1.46	49	76	1.0	2.0	.230	1.55	.52	.28E-03	.36E-04	1.0	2171	.986	.15E-05	.28E-04	1.0	514
820925-14	1.46	48	82	.9	2.0	.230	1.35	.55	.19E-03	.36E-04	1.0	1522	.987	.23E-05	.28E-04	1.0	430
820925-15	1.46	78	88	1.0	2.0	.230	1.70	.45	.50E-03	.42E-04	.99	4372	.986	.98E-06	.30E-04	.99	738
820925-16	1.46	82	94	.9	2.0	.230	1.57	.46	.10E-02	.43E-04	.99	4071	.987	.34E-05	.32E-04	.99	728
820925-17	1.46	108	99	.9	2.0	.230	1.74	.41	.39E-03	.40E-04	.99	6860	.987	.44E-06	.26E-04	.99	924
820925-18	1.46	110	107	.8	2.0	.230	1.56	.43	.42E-02	.50E-04	.99	7398	.987	.11E-04	.36E-04	.99	968
820927-1	1.08	48	65	1.0	2.0	.350	2.04	.46	.14E-03	.34E-04	.99	4738	.973	.59E-06	.21E-04	.99	905
820927-2	1.08	49	70	1.0	2.0	.350	1.88	.48	.62E-03	.35E-04	1.0	5054	.974	.31E-05	.22E-04	.99	942
820927-3	1.08	82	77	1.0	2.0	.350	2.25	.39	.11E-02	.48E-04	.96	9758	.974	.19E-05	.29E-04	.93	1282
820927-4	1.08	83	83	.9	2.0	.350	2.04	.41	.13E-02	.42E-04	.99	9218	.975	.28E-05	.23E-04	.98	1270
820927-5	1.08	108	91	1.0	2.0	.350	2.09	.38	.29E-03	.39E-04	.96	11020	.975	.74E-06	.19E-04	.94	1399
820927-6	1.08	113	104	.9	2.0	.350	1.75	.42	.14E-02	.46E-04	.96	11350	.976	.58E-05	.25E-04	.88	1443
820927-7	1.24	49	72	1.0	2.0	.400	1.74	.50	.25E-03	.37E-04	.99	3109	.980	.13E-05	.26E-04	.99	682
820927-8	1.24	48	76	1.0	2.0	.400	1.57	.52	.15E-03	.30E-04	.99	2475	.981	.14E-05	.21E-04	.99	611
820927-9	1.24	80	85	.9	2.0	.400	1.86	.43	.18E-02	.42E-04	1.0	7266	.981	.38E-05	.28E-04	.99	1037
820927-10	1.24	78	85	1.0	2.0	.400	1.84	.43	.25E-03	.40E-04	.97	5568	.981	.62E-06	.25E-04	97	928
820927-11	1.24	113	95	1.0	2.0	.400	1.97	.38	.49E-03	.42E-04	.91	9857	.981	.67E-06	.24E-04	.86	1209
820927-12	1.24	113	102	.8	2.0	.400	1.75	.41	.57E-03	.42E-04	.99	8586	.982	.14E-05	.24E-04	.98	1162
820927-13	1.46	48	71	1.0	2.0	.474	1.68	.50	.52E-03	.39E-04	1.0	2880	.986	.17E-05	.29E-04	1.0	583
820927-14	1.46	48	79	.9	2.0	.474	1.42	.54	.37E-03	.34E-04	1.0	1961	.987	.26E-05	.26E-04	1.0	488

SUMMARY OF THERMAL HYPERBOLIC SINE ANALYSIS ON SANTO50

TEST #	P0	U0	T0	VF	KK	SP	H0	YI	E1	C1	R1	P1	PR	E2	C2	R2	P2
----	GPa	m/s	'C	--	--	%	um	--	Pa.s	'C/Pa	--	--	--	Pa.s	'C/Pa	--	--
820927-15	1.46	82	86	.9	2.0	.474	1.81	.42	.27E-02	.46E-04	.99	5343	.986	.37E-05	.33E-04	.99	804
820927-16	1.46	81	94	.8	2.0	.474	1.54	.47	.31E-02	.44E-04	1.0	5082	.987	.10E-04	.32E-04	.99	801
820927-17	1.46	113	106	.8	2.0	.474	1.59	.42	.40E-02	.50E-04	.99	8204	.987	.79E-05	.34E-04	.99	999
820927-18	1.46	112	110	.9	2.0	.474	1.50	.44	.16E-02	.51E-04	.99	6101	.987	.41E-05	.35E-04	.99	899
820929-1	1.41	47	34	1.0	1.0	0.00	4.37	.26	.27E+00	.42E-04	.99	30350	.990	.14E-05	.29E-04	.99	1080
820929-2	1.41	45	44	.9	1.0	0.00	3.02	.33	.07E+00	.39E-04	1.0	11550	.990	.75E-05	.29E-04	.99	856
820929-3	1.41	69	51	.9	1.0	0.00	3.22	.28	.20E+00	.46E-04	1.0	27780	.991	.80E-05	.33E-04	1.0	1105
821019-1	1.41	51	38	1.0	1.0	0.00	3.92	.27	.49E+00	.42E-04	1.0	28260	.990	.12E-04	.30E-04	1.0	1074
821019-2	1.41	50	40	.9	1.0	0.00	3.62	.29	.16E+01	.45E-04	1.0	37500	.990	.32E-03	.35E-04	1.0	1142
821019-3	1.41	89	46	1.0	1.0	0.00	4.44	.21	.90E+00	.46E-04	1.0	118400	.991	.17E-05	.29E-04	1.0	1428
821019-4	1.41	86	50	.9	1.0	0.00	3.77	.23	.22E+01	.51E-04	1.0	149200	.991	.71E-04	.35E-04	1.0	1472
821019-5	1.41	120	57	1.0	1.0	0.00	3.93	.20	.92E+00	.51E-04	.99	250000	.992	.32E-05	.32E-04	.98	1616
821019-6	1.41	118	64	.9	1.0	0.00	3.25	.24	.14E+01	.56E-04	1.0	184100	.992	.59E-04	.38E-04	1.0	1582
821019-7	1.62	46	58	1.0	1.0	0.00	1.95	.43	.42E-02	.37E-04	1.0	3334	.993	.31E-05	.29E-04	1.0	505
821019-8	1.62	47	59	.9	1.0	0.00	1.90	.43	.01E+00	.38E-04	1.0	3901	.993	.14E-04	.30E-04	1.0	541
821019-9	1.62	87	61	1.0	1.0	0.00	2.78	.29	.19E+00	.44E-04	1.0	29050	.993	.52E-05	.31E-04	1.0	1002
821019-10	1.62	85	64	1.0	1.0	0.00	2.51	.31	.23E+00	.44E-04	1.0	25430	.993	.21E-04	.32E-04	1.0	981
821019-11	1.62	122	70	1.0	1.0	0.00	2.81	.26	.33E+00	.49E-04	1.0	51110	.994	.58E-05	.33E-04	1.0	1165
821019-12	1.62	117	76	.7	1.0	0.00	2.40	.29	.54E+00	.53E-04	1.0	51460	.994	.79E-04	.39E-04	1.0	1180
821019-13	1.78	46	53	1.0	1.0	0.00	2.18	.40	.01E+00	.37E-04	1.0	4147	.994	.49E-05	.30E-04	1.0	506
821019-14	1.78	48	58	.9	1.0	0.00	1.94	.42	.05E+00	.39E-04	1.0	4277	.994	.63E-04	.33E-04	1.0	522
821019-15	1.78	87	66	.8	1.0	0.00	2.41	.31	.60E+00	.47E-04	1.0	35580	.995	.11E-03	.36E-04	1.0	960
821019-16	1.78	88	71	1.0	1.0	0.00	2.17	.33	.13E+00	.45E-04	1.0	18[illegible]00	.995	.22E-04	.35E-04	1.0	846
821019-17	1.78	120	76	.9	1.0	0.00	2.40	.29	.29E+00	.49E-04	.99	37[illegible]30	.995	.17E-04	.36E-04	.99	1008
821019-18	1.78	122	84	.7	1.0	0.00	2.05	.32	.57E+00	.55E-04	.99	71040	.995	.24E-03	.43E-04	.99	1151
821020-1	1.78	52	64	1.0	1.0	.184	1.77	.43	.52E-02	.37E-04	1.0	3045	.995	.56E-05	.31E-04	1.0	461
821020-2	1.78	50	68	.9	1.0	.184	1.57	.47	.40E-02	.36E-04	1.0	2302	.995	.97E-05	.30E-04	1.0	413
821020-3	1.78	86	74	.9	1.0	.184	2.02	.35	.02E+00	.44E-04	1.0	10470	.995	.33E-05	.33E-04	1.0	732
821020-4	1.78	89	79	.9	1.0	.184	1.86	.37	.11E+00	.47E-04	1.0	11270	.995	.67E-04	.37E-04	1.0	763
821020-5	1.78	119	84	.9	1.0	.184	2.03	.32	.13E+00	.50E-04	.99	26130	.995	.28E-04	.38E-04	.99	963
821020-6	1.78	122	90	.8	1.0	.184	1.85	.34	.10E+00	.51E-04	.99	20700	.995	.41E-04	.39E-04	.99	931

SUMMARY OF THERMAL HYPERBOLIC SINE ANALYSIS ON SANTO50

TEST #	P0	U0	T0	VF	KK	SP	H0	YI	E1	C1	R1	P1	PR	E2	C2	R2	P2
----	GPa	m/s	'C	--	--	%	um	--	Pa.s	'C/Pa	--	--	--	Pa.s	'C/Pa	--	--
821020-7	1.62	48	80	.9	1.0	.167	1.20	.54	.32E-03	.34E-04	1.0	1298	.994	.28E-05	.28E-04	1.0	337
821020-8	1.62	45	77	.8	1.0	.167	1.23	.54	.23E-03	.33E-04	1.0	1230	.994	.15E-05	.27E-04	1.0	326
821020-9	1.62	90	67	1.0	1.0	.167	2.44	.31	.07E+00	.48E-04	.99	25750	.994	.55E-05	.35E-04	.98	996
821020-10	1.62	85	73	.9	1.0	.167	2.08	.35	.08E+00	.45E-04	.99	15580	.994	.29E-04	.34E-04	.99	896
821020-11	1.62	117	80	.9	1.0	.167	2.21	.31	.09E+00	.49E-04	.99	25470	.994	.14E-04	.36E-04	.99	1041
821020-12	1.62	120	88	.9	1.0	.167	1.92	.34	.01E+00	.47E-04	.98	13830	.994	.14E-05	.31E-04	.97	910
821020-13	1.41	44	57	1.0	1.0	.146	1.97	.44	.37E-03	.33E-04	1.0	3467	.991	.33E-06	.25E-04	1.0	565
821020-14	1.41	46	58	1.0	1.0	.146	1.96	.43	.41E-02	.35E-04	.98	3499	.991	.47E-05	.27E-04	.98	573
821020-15	1.41	89	65	1.0	1.0	.146	2.64	.30	.03E+00	.47E-04	.98	27710	.991	.14E-05	.32E-04	.97	1154
821020-16	1.41	91	67	.9	1.0	.146	2.51	.31	.09E+00	.45E-04	1.0	25830	.991	.12E-04	.32E-04	.99	1147
821020-17	1.41	119	72	.9	1.0	.146	2.68	.27	.12E+00	.51E-04	.99	47230	.992	.57E-05	.34E-04	.99	1336
821020-18	1.41	122	81	.9	1.0	.146	2.30	.30	.51E-02	.45E-04	.94	18220	.992	.23E-06	.26E-04	.89	1099
821022-1	1.41	49	38	1.0	1.0	.294	3.82	.28	.05E+00	.42E-04	1.0	20070	.990	.39E-06	.28E-04	1.0	987
821022-2	1.41	43	42	0.0	1.0	.294	3.04	.34	.29E+00	.44E-04	1.0	14470	.990	.14E-03	.35E-04	1.0	912
821022-3	1.41	87	49	.9	1.0	.294	4.03	.22	.17E+01	.48E-04	.99	99210	.991	.28E-04	.33E-04	.98	1406
821022-4	1.41	93	55	1.0	1.0	.294	3.53	.24	.08E+00	.52E-04	.97	56410	.991	.61E-06	.35E-04	.95	1307
821022-5	1.41	117	62	1.0	1.0	.294	3.42	.23	.09E+00	.50E-04	.99	48660	.992	.37E-06	.30E-04	.98	1310
821022-6	1.41	114	67	.9	1.0	.294	2.96	.26	.17E+00	.47E-04	.99	48990	.992	.46E-05	.31E-04	.99	1328
821022-7	1.61	53	62	.9	1.0	.336	1.94	.41	.01E+00	.40E-04	1.0	4677	.993	.11E-04	.32E-04	1.0	585
821022-8	1.61	52	62	.7	1.0	.336	1.91	.42	.01E+00	.36E-04	.99	4086	.993	.94E-05	.28E-04	.99	556
821022-9	1.61	90	64	.9	1.0	.336	2.60	.30	.03E+00	.42E-04	.99	16980	.993	.46E-06	.28E-04	.99	897
821022-10	1.61	89	67	.8	1.0	.336	2.41	.32	.11E+00	.44E-04	1.0	16820	.994	.12E-04	.32E-04	.99	904
821022-11	1.61	117	73	.8	1.0	.336	2.54	.28	.21E+00	.49E-04	1.0	37130	.994	.11E-04	.35E-04	.99	1109
821022-12	1.61	119	79	1.0	1.0	.336	2.28	.30	.02E+00	.45E-04	.97	16610	.994	.97E-06	.30E-04	.96	936
821022-13	1.78	47	61	1.0	1.0	.370	1.77	.45	.42E-02	.40E-04	1.0	2867	.995	.43E-05	.33E-04	1.0	444
821022-14	1.78	54	64	.8	1.0	.370	1.80	.43	.01E+00	.38E-04	1.0	3836	.995	.99E-05	.30E-04	1.0	505
821022-15	1.78	87	69	.8	1.0	.370	2.27	.33	.16E+00	.45E-04	1.0	16210	.995	.26E-04	.35E-04	1.0	818
821022-16	1.78	91	73	.9	1.0	.370	2.11	.34	.04E+00	.46E-04	1.0	11880	.995	.51E-05	.34E-04	1.0	762
821022-17	1.78	123	80	.9	1.0	.370	2.25	.30	.04E+00	.45E-04	.97	16050	.995	.14E-05	.31E-04	.97	848
821022-18	1.78	119	84	.7	1.0	.370	2.02	.32	.08E+00	.49E-04	.99	15330	.995	.10E-04	.35E-04	.99	850
821101-1	1.06	50	65	.9	5.2	.821	1.92	.45	.06E+00	.41E-04	.99	7498	.966	.63E-03	.33E-04	.99	1285

SUMMARY OF THERMAL HYPERBOLIC SINE ANALYSIS ON SANTO50

TEST #	P0	U0	T0	VF	KK	SP	H0	YI	E1	C1	R1	P1	PR	E2	C2	R2	P2
----	GPa	m/s	'C	--	--	%	um	--	Pa.s	'C/Pa	--	--	--	Pa.s	'C/Pa	--	--
821101-2	1.06	50	75	.7	5.2	.821	1.51	.51	.08E+00	.40E-04	1.0	4963	.968	.27E-02	.34E-04	1.0	1083
821101-3	1.06	80	75	.9	5.2	.821	2.06	.38	.29E+00	.51E-04	.99	23430	.967	.24E-02	.40E-04	.99	2048
821101-4	1.06	81	81	.8	5.2	.821	1.87	.40	.86E+00	.58E-04	1.0	17260	.967	.03E+00	.50E-04	1.0	1875
821101-5	1.06	111	95	.6	5.2	.821	1.77	.39	.27E+01	.75E-04	.93	24120	.969	.28E+00	.66E-04	.85	2180
821101-6	1.06	114	91	.9	5.2	.821	1.96	.36	.83E+00	.68E-04	.90	28460	.968	.03E+00	.61E-04	.81	2289
821101-7	1.06	112	88	1.0	5.2	.821	2.04	.35	.01E+00	.62E-04	.95	20360	.968	.15E-04	.39E-04	.93	2034
821101-8	1.06	119	109	.8	5.2	.821	1.56	.42	.32E+00	.60E-04	1.0	22370	.970	.64E-02	.46E-04	.99	2199
821101-9	1.22	50	69	1.0	5.2	.940	1.70	.47	.51E-02	.46E-04	1.0	5167	.974	.37E-04	.36E-04	1.0	985
821101-10	1.22	50	79	.9	5.2	.940	1.36	.53	.46E-02	.47E-04	1.0	2992	.976	.90E-04	.38E-04	1.0	769
821101-11	1.22	83	90	.7	5.2	.940	1.56	.44	.08E+00	.58E-04	1.0	10270	.976	.72E-03	.45E-04	1.0	1394
821101-12	1.22	81	86	1.0	5.2	.940	1.66	.43	.75E-02	.53E-04	1.0	9591	.976	.25E-04	.37E-04	1.0	1346
821101-13	1.22	103	97	.9	5.2	.940	1.59	.41	.36E-02	.53E-04	.98	9861	.976	.11E-04	.36E-04	.97	1410
821101-14	1.22	107	119	.8	5.2	.940	1.19	.48	.09E+00	.66E-04	.99	8667	.977	.31E-02	.55E-04	.99	1391
821101-15	1.44	51	84	.9	5.2	1.11	1.22	.54	.46E-02	.48E-04	1.0	2214	.983	.10E-03	.41E-04	1.0	595
821101-16	1.44	52	92	.8	5.2	1.11	1.06	.58	.76E-02	.51E-04	.99	1749	.984	.31E-03	.44E-04	1.0	529
821101-17	1.44	89	109	.6	5.2	1.11	1.16	.50	.04E+00	.56E-04	.97	4931	.984	.96E-03	.48E-04	.99	935
821101-18	1.44	90	105	.9	5.2	1.11	1.24	.48	.01E+00	.54E-04	.99	4739	.984	.20E-03	.45E-04	1.0	918
821101-19	1.44	94	99	.9	5.2	1.11	1.41	.44	.64E-02	.48E-04	.99	5468	.983	.50E-04	.41E-04	.99	973
821101-20	1.44	96	122	.6	5.2	1.11	1.03	.52	.08E+00	.64E-04	1.0	3791	.984	.29E-02	.54E-04	1.0	845
821102-1	1.04	55	52	1.0	5.0	0.00	2.95	.34	.01E+00	.40E-04	.99	17740	.962	.51E-05	.26E-04	.99	1777
821102-2	1.04	52	63	0.0	5.0	0.00	2.10	.43	.48E-02	.36E-04	1.0	8086	.964	.22E-04	.26E-04	1.0	1336
821102-3	1.04	93	68	1.0	5.0	0.00	2.78	.31	.01E+00	.41E-04	.98	26400	.965	.37E-05	.24E-04	.98	2145
821102-4	1.04	92	79	.9	5.0	0.00	2.14	.37	.01E+00	.41E-04	.99	15780	.966	.18E-04	.26E-04	.99	1848
821102-5	1.04	114	83	1.0	5.0	0.00	2.33	.33	.23E-02	.40E-04	.99	27850	.967	.15E-05	.19E-04	.85	2256
821102-6	1.04	119	88	.9	5.0	0.00	2.16	.34	.24E-02	.41E-04	.82	20860	.967	.25E-05	.20E-04	.65	2087
821102-7	1.19	47	61	1.0	5.0	0.00	2.00	.44	.13E-02	.35E-04	.99	5906	.973	.31E-05	.24E-04	1.0	1043
821102-8	1.19	48	76	.9	5.0	0.00	1.44	.52	.11E-02	.34E-04	.99	2379	.975	.26E-04	.28E-04	1.0	687
821102-9	1.19	85	87	.9	5.0	0.00	1.69	.42	.36E-02	.39E-04	1.0	7621	.975	13E-04	.27E-04	.99	1259
821102-10	1.19	85	85	1.0	5.0	0.00	1.80	.41	.28E-02	.42E-04	.99	10040	.975	.76E-05	.29E-04	1.0	1386
821102-11	1.19	116	94	.9	5.0	0.00	1.86	.37	.36E-02	.43E-04	.99	15370	.975	.53E-05	.27E-04	.99	1678
821102-12	1.19	119	102	.8	5.0	0.00	1.66	.39	.35E-02	.45E-04	.99	11870	.976	.10E-04	.29E-04	.97	1561

SUMMARY OF THERMAL HYPERBOLIC SINE ANALYSIS ON SANTO50

TEST #	P0	U0	T0	VF	KK	SP	H0	YI	E1	C1	R1	P1	PR	E2	C2	R2	P2
----	GPa	m/s	'C	--	--	%	um	--	Pa.s	'C/Pa	--	--	--	Pa.s	'C/Pa	--	--
821102-13	1.41	50	69	1.0	5.0	0.00	1.67	.47	.28E-02	.35E-04	.99	2934	.981	.[illegible]2E-04	.30E-04	1.0	684
821102-14	1.41	51	83	.9	5.0	0.00	1.26	.54	.20E-02	.35E-04	.99	901	.983	.78E-04	.31E-04	1.0	364
821102-15	1.41	113	97	1.0	5.0	0.00	1.68	.39	.77E-02	.46E-04	.99	8129	.983	.13E-04	.34E-04	1.0	1192
821102-16	1.41	123	111	.8	5.0	0.00	1.44	.42	.61E-02	.49E-04	1.0	7777	.983	.30E-04	.36E-04	1.0	1194
821102-17	1.41	81	108	.9	5.0	0.00	1.13	.52	.53E-02	.48E-04	.97	2689	.983	.15E-03	.41E-04	.97	715
821102-18	1.41	81	84	.9	5.0	0.00	1.68	.42	.87E-02	.45E-04	.99	5552	.982	.42E-04	.37E-04	1.0	971
821103-1	1.34	51	82	1.0	5.2	1.03	1.27	.54	.43E-02	.48E-04	1.0	2786	.980	.83E-04	.40E-04	1.0	696
821103-2	1.34	51	91	.9	5.2	1.03	1.08	.58	.37E-02	.48E-04	.99	1745	.981	.15E-03	.41E-04	1.0	551
821103-3	1.34	80	102	.8	5.2	1.03	1.21	.50	.23E+00	.67E-04	1.0	5214	.981	.01E+00	.58E-04	1.0	992

1